A Custom Triflange Acetabular Component (CTAC) Positioning Study

W.M.H. Meurs

Universiteit Leiden

TU Delft Delft University of Technology

Erasmus ERASMUS UNIVERSITEIT ROTTERDAM

Accuracy of Positioning Custom Triflange Acetabular Components in THA Revision and Tumor Resection Surgery – A 3D-CT Assessment Study

Willemijne Maria Helena Meurs
Student number : 4404467
May 10, 2021

Thesis in partial fulfilment of the requirements for the joint degree of Master of Science in

Technical Medicine

Leiden University - Delft University of Technology - Erasmus University Rotterdam

Preface

During the first year of my Bachelor's Degree, I developed an interest for the orthopeadics. One of the first exciting courses was a combination of the musculoskeletal anatomy and biomechanics. During my Master's Degree, I completed four clinical research internships. These internships where at the department of transplantation surgery, the department of orthopaedics, the heart-lung center and the department of oncological surgery. In my opinion, the department of orthopaedics is a perfect environment for a TM intern. Due to the technical possibilities, the complex patient population at the LUMC, and the welcoming multidisciplinary team which made every day exciting, sociable, and educational. During my TM2 internship, I was soon convinced to the department of Orthopaedics to conduct my master thesis research.

I gained technical experience in the field of image processing, and programming throughout the courses and my internships. During my master thesis research, I was eager to combine my orthopaedics interest with image processing and programming. Fortunately, Demien is currently working on a promotion project on custom triflange acetabular components in combination with orthopaedic surgeons in Australia. Therefore, I was lucky to participate as a master thesis student in one of his projects. The combination of orthopaedics with traveling to Sydney to partly execute our project from there was the perfect end of my studies. We started planning and writing our research protocol at the end of 2019. Our proposal got approved and we were ready to start our project.

There were some challenges and difficulties last year caused by the COVID-19 pandemic. It was not possible to travel to Sydney to get all the patient data personally. Instead, we depended on the transfer of all the patient data from Australia. Despite this and some other COVID-19 related setbacks, I had an amazing year at the department of orthopaedics and developed myself clinically, technically, and I learned how to manage a project with stakeholders from different countries. I think we can be very proud of what we achieved as a team, and hopefully, we contributed to the knowledge and improvement of reconstructing severe pelvic defects. I'm very thankful for the support and enthusiasm, throughout this one and a half years, from my supervisors; Demien Broekhuis, Bart Kaptein and Prof. Rob Nelissen.

In the coming months, the results from this masters' thesis will be re-written in the form of a scientific article.

Willemijne Meurs

23-04-2021

Summary

The surgical management of large pelvic bone defects remains technically challenging. Large constructs or major hip altering procedures are needed, if there is gross bone loss, discontinuity of the pelvic ring or tumor resection. Several treatment options for pelvic bone defects are available but these are often insufficient or suboptimal in patients who had multiple THA revision procedures or who need large tumor resections. Options are limited in large bone defects, as they cannot easily be bridged by the off-the-shelf implants. To overcome a possible geometric mismatch between an off-the-shelf implant and the large pelvic bone defects, custom triflange acetabular components (CTAC) are increasingly used. Our aim of this thesis was to assess the 3D positioning of CTACs.

First, a systematic review was conducted to examine the complications, reoperations and failures of CTAC placements over time. We concluded a decreasing trend over time of the number of failures, reoperations, and complications of implanted CTACs. However, due to limited study data and high between-study variation, we were not able to verify the cause of this trend over time. Second, a research protocol was written to obtain ethical approval from the participating institutions ethics committees to execute our study. Last, for the main part of this thesis, a semi-automatic assessment tool was developed to analyze the 3D surgical position of CTACs in THA revision and tumor patients. To our knowledge, this is the largest 3D positioning study assessing CTACs. We concluded that the post-operative implant position showed good agreement to the pre-operative planned position.

Universiteit Leiden

TUDelft Delft University of Technology

ERASMUS UNIVERSITEIT ROTTERDAM

Table of Contents

Universiteit Leiden

TUDelft Delft University of Technology

ERASMUS UNIVERSITEIT ROTTERDAM

List of abbreviations

2D	Two-dimentional
3D	Three-dimentional
AL	Acetabular aseptic loosening
APP	Anterior pelvic plane
AQUILA	Assessment of Quality In Lower Limb Arthroplasty
ASIS	Anterior superior iliac spine
AV	Anteversion
Ax	Axial
BMI	Body mass index
CI	Confidence intervals
Co	Coronal
COR	Center of rotation
CT	Computer tomography
CTAC	Custom triflange acetabular components
DICOM	Digital Imaging and Communications in Medicine
ICP	Iterative closest point
INCL	Inclination
MA	Mean of the absolute value
mm	millimeters
OA	Osteoarthritis
PET	Positron emission tomography
Plan	Pre-operative planning
Post	Post-operative
PRISMA	Preferred reporting items for systematic reviews and meta-analyses
PSI	Patient specific instrumentation
PT	Pubic tubercle
RA	Radiographic anteversion
RI	Radiographic inclination
Sa	Sagittal
SC	Sacral crest
SD	Standard deviation
STL	Standard Triangle Language
SVD	Singular Value Decomposition
THA	Total hip arthroplasty

Universiteit Leiden

TUDelft Delft University of Technology

ERASMUS UNIVERSITEIT ROTTERDAM

Introduction

1. Background

The pelvis is a group of fused bones and connects the axial skeleton, lumbar spinal column, to the lower extremities. The pelvic bone can be subdivided into the pelvic girdle, the sacrum and the coccyx. The pelvic girdle, also known as the os coxae, is formed by three bones: the ilium, ischium and pubis. The pelvic girdle is anterior enclosed by the pubic symphysis and posterior by the sacroiliac joints. The attachment of the three bones of the os coxae forms the acetabulum, Figure 1. The hip joint is a ball and socket joint between the head of the femur and the acetabulum to allow maximal mobility of the joint. The hip joint allows for movements, facilitates weight-bearing and retaining balance.

Figure 1. Anatomy of the pelvis
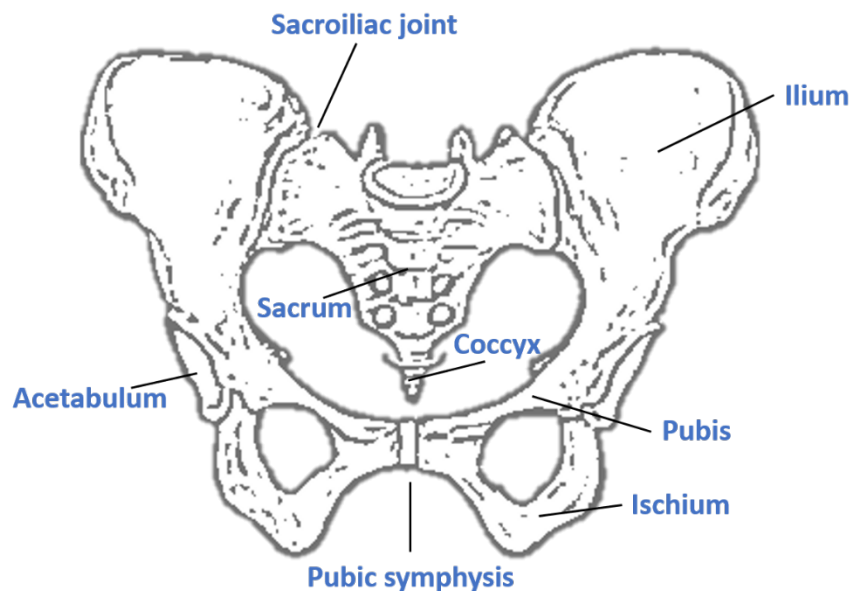
Osteoarthritis (OA) is a type of degenerative joint disease that results from the breakdown of the cartilage and causing friction, damage to the bones and inflammation. Hip pain and stiffness are the most common symptoms of OA of the hip. Total hip arthroplasty (THA) is a cost-effective intervention to reduce pain and improve function in patients suffering from degenerative bone and joint diseases such as OA. The basic principle of THA is to replace the damaged hip joint by an artificial acetabular cup and femoral head. Yearly, more than 33,000 primary total hip replacements are performed in Australia. The Australian joint registry data reveals that approximately 4.1% of hip replacements are revised after 15 years (1). With an expected increasing amount of hip joint replacements performed every year, it is likely that the amount of revisions will increase.

Particle wear disease in artificial joints causes periprosthetic osteolysis, aseptic loosening of the components and ultimately can lead to pelvic bone defects. Other reasons for pelvic bone defects are septic loosening, aseptic lymphocyte- dominated vasculitis-associated lesions (ALVAL) caused by metal on metal articulations, trauma or tumor (2, 3). Currently, several treatment options for pelvic bone defects are available but are often insufficient or suboptimal in patients who had multiple THA revision procedures or who need large tumor resections. Options are limited in large bone defects, as they cannot easily be bridged by the off-the-shelf implants. To overcome a possible geometric mismatch between an off-the-shelf implant and the large pelvic bone defects, custom triflange acetabular components (CTAC) are increasingly used.

A CTAC is designed from the patient's CT scan data. Traditionally, the CTAC consist of three flanges. It achieves fixation on the remaining pubic, ischial and iliac bone with multiple fixation screws, Figure 2. CTACs are designed to fit one exact position. Consequently, correct surgical placement of the CTAC is crucial. More recent attention has focused on the placement and follow-up of CTACs. However, literature on the 3D positioning of CTACs is sparsely available and with limited cohorts. Therefore, we aimed in this thesis to evaluate the surgical positioning of CTACs by developing a 3D-CT positioning assessment tool.

1. Approach and research objectives

This master thesis is divided in different parts. First a literature study was conducted to identify published articles documenting the placement of CTACs, with a focus on the follow-up complications, reoperation and failure rates over time. Second, a research protocol was written to obtain ethical approval from the participating institutions' ethics committees to execute our study. Finally, a semi-automatic assessment tool was developed to analyze the 3D surgical position of the included cases.

Each thesis objective is discussed in the three parts of this thesis, comprising the literature review (TM30003), the master thesis (TM30004) and the research protocol. The overarching aim was to contribute to the knowledge on custom triflange acetabular components.

The three research objectives were as follows:

Systematically review current literature on the follow-up rates of custom triflange acetabular components (CTAC).
*Part I - **Literature review***

Develop a semi-automatic 3D-CT assessment tool and analyze the planned and achieved position of custom triflange acetabular components (CTAC).
*Part II - **Main thesis***

Research protocol to obtain ethical approval from the participating institutions ethics committees.
*Part III - **Research protocol – Appendix B***

Part II includes the main thesis paper on the Accuracy of Positioning Custom Triflange Acetabular Components in THA Revision and Tumor Resection Surgery – A 3D-CT Assessment Study.

Figure 2. CTAC fixated onto the pelvic bone

References

1.   Osteoarthritis Web report. Australian Institute of Health and Welfare 2020 [internet] Available from: https://wwwaihwgovau/reports/chronic-muscles-conditions/osteoarthritis [Accessed 18-04-2021]
2.   Langton DJ, Sidaginamale RP, Joyce TJ, Bowsher JG, Holland JP, Deehan D, et al. Aseptic lymphocyte-dominated vasculitis-associated lesions are related to changes in metal ion handling in the joint capsules of metal-on-metal hip arthroplasties. Bone Joint Res. 2018;7(6):388-96.
3.   Nieminen J, Pakarinen TK, Laitinen M. Orthopaedic Reconstruction of Complex Pelvic Bone Defects. Evaluation of Various Treatment Methods. Scandinavian Journal of Surgery. 2013;102(1):36-41.

Universiteit Leiden

TUDelft Delft University of Technology

ERASMUS UNIVERSITEIT ROTTERDAM

Part I - Systematic review

For the first thesis objective, we performed a systematic review as part of the literature study (TM30003). Research on the available literature on custom triflange acetabular components, resulted in a study on the complication, reoperation and failure rates of CTAC over time. The literature study contributed to the development of the 3D-CT assessment tool.

Trends in Complication, Reoperation, and Failure Rates of Custom Triflange Acetabular Components Over Time; a Systematic Review.

Abstract

Introduction The surgical management of massive acetabular bone defects remains technically challenging in revision total hip arthroplasty surgery. Custom triflange acetabular components (CTAC) have become increasingly popular for the treatment of Paprosky type III defects with the adoption of rapid prototyping and 3-dimentional (3D) additive manufacturing techniques. The aim of this study was to determine trends in the implant survival rate, the complication rate and the re-operation rate, for patients receiving treatment of large pelvic defects by means of patient specific acetabular components. **Method** Studies on the management of massive acetabular bone defects using patient specific acetabular components were identified in accordance to the PRISMA guidelines. Evaluable studies were reviewed for quality and the study start year of each study was chosen to represent the surgery date. Inter-study follow-up and patient number variations were normalized by using both the event rate percentage of total implanted hips and event rate per 100 observed component years. The effect of study date on complication, reoperation and failure over time was computed using mixed-effects meta-regression. **Results** 18 articles met our inclusion criteria. A total of 626 CTACs were implanted. The all-cause failure rate was 17,7%. The overall complication rate was 31,6%. Dislocation and periprosthetic joint infection were the most common complications observed with an incidence of 10,9% and 7,0%, respectively. The overall failure rate was 3,74 per 100 observed component years. For each consecutive study year, the amount of failures per 100 component years decreased by 0,081 units in terms of the average relative risk. However, the between-study variation was large. **Discussion** A decreasing trend of the number of failures, reoperations, and complications of implanted CTACs was seen over time. Although, due to limited study data and high between-study variation, we were not able to verify the cause of this trend over time. To further examine the trend of implant survival and complications over the course of time for custom-made acetabular implants, individual patient data should be reported more frequently in the literature.

1. Introduction

The surgical management of massive acetabular bone defects remains technically challenging in revision total hip arthroplasty surgery (1, 2). The classified Paprosky type IIIA and IIIB, defined as the most severe acetabular defects characterized by destruction of supporting structures, are particularly difficult to repair (3, 4). Multiple reconstructive procedures have been proposed for severe acetabular defects such as jumbo acetabular cups, impaction bone grafting combined with a cemented cup, structural allograft and a hemispherical cup, oblong acetabular cup, antiprotrusio cages, cup-cage constructs, and highly porous augments. (5-11). Although several studies have reported encouraging results using these techniques, the optimal surgical technique for Paprosky type III defects has not been established (1, 10).

Custom triflange acetabular components (CTAC) have become increasingly popular for the treatment of Paprosky type III defects with the adoption of rapid prototyping and 3-dimentional (3D) additive manufacturing techniques, Figure 1 (12). De Martino et al. reported an overall survival rate of 82,7% at a mean follow-up of 4,8 years for CTAC (1). 3D reconstruction using rapid prototyping technology has evolved substantially during the past decade (13). Using pre-operative planning software, the surgeon has the possibility to determine the exact component positioning, and the component shape location and length of the screws (13). Additionally, the current 3D additive manufacturing technique gives the ability

to intraoperatively check the bone and implant positioning with an additional sterile printed model. The continuous improvements of implant materials, rapid prototyping techniques, and pre-/intra-operative planning software could reduce intraoperative time, complications, anesthetic exposure, and improve clinical outcomes. (12, 14, 15).

Figure 1. OSSIS custom triflange acetabular component developed from a patient's pelvic CT scan.

Prior studies investigating the outcomes of CTAC have reported comparable results to alternative techniques used to treat massive acetabular bone defects (1, 16-21). However, there are many factors which may influence the clinical outcomes and complication rates of CTAC that are not reflected in these studies. One of these factors is the inclusion of articles reporting CTAC outcomes of the oldest generation CTAC techniques (17, 19-24). Therefore, the aim of this study was to determine trends in the implant survival rate, the complication rate and the re-operation rate, for patients receiving treatment of large pelvic defects by means of patient specific acetabular components.

2. Method

2.1 Literature search

A systematic review was conducted in accordance to the PRISMA guidelines (25). Journal articles were searched using PubMed, MEDLINE, Embase, Web of Science, COCHRAINE library and Emcare databases utilizing various combinations of the search terms: 'Hip replacement arthroplasty', 'Total tip replacement', 'Triflange', 'Revision', 'Acetabular defects', 'bone loss', 'bone defect' 'Paprosky', 'custom-made', 'patient specific' and 'acetabulum' in combination with the Boolean operators (AND, OR, *), Appendix A Part I. No limit regarding the year of publication was set. All journals were considered.

2.2 Inclusion and Exclusion criteria

All papers investigating custom acetabular implant for acetabular reconstruction in total hip arthroplasty revision, 3D printed or machined implants, bone defects graded as Paprosky type 3A, 3B or AAOS type 3 and 4 acetabular defects, and reported clinical outcomes were included in this study. Exclusion criteria were case reports, surgical technique reports, review articles, expert opinions, letters to editors, biomechanical reports, instructional course lectures, studies on animals, cadaver or in vitro investigations, book chapters, abstracts from scientific meetings, studies with less than 10 hips, studies with a mean follow-up of less than 12 months, studies using the same database, and studies written in a language other than English.

2.3 Study selection

Articles were screened on titles and abstracts for eligibility by the author before proceeding to the full text. If the information required to determine eligibility was not in the title and abstract, a full text screen was performed. Full-text articles were assessed based on inclusion and exclusion criteria for eligibility.

2.4 Data extraction

The following data was extracted in a spreadsheet: study title, year of publication, author, study design, number of patients and hips included, study period, patient demographics (age, gender,

Universiteit Leiden

TUDelft Delft University of Technology

Erasmus ERASMUS UNIVERSITEIT ROTTERDAM

BMI), follow-up in months, acetabular defect type (Paprosky/AAOS), implant related complications, and implant survival/failure.

2.5 Methodological quality

All the included studies were assessed for methodological quality based on the Assessment of Quality In Lower Limb Arthroplasty (AQUILA) checklist, a tool specifically designed to appraise the quality of observational studies concerning total hip (THA) and knee replacement. (26) The author assessed the quality of all the included studies using a predefined data extraction sheet.

2.6 Data analysis

Descriptive statistics were used to present quantitative data. Primary outcomes measures were the number of complications, reoperations and failures as a proportion of the number of implant placements included in each study corresponding to the study year and the visualization of the trend over time of these event rates. To normalize the separate articles with different follow-up and number of implant placements, the outcomes were corrected based on the event rate per 100 observed component years. This is a descriptive epidemiological parameter comparable to pack years in tobacco smoking (27, 28). The component years were calculated as the number of implant placements multiplied by the mean follow-up in years. Secondly, the event rate per 100 observed component years was calculated as number of events measured x 100 divided by component years. A value of 1 revision per 100 observed component years correspond to a revision rate of 1% at 1 year in a linear function (28, 29). Study start year was selected to represent the event rates corresponding to each article (30). Figures of the event rates were created to visualize the event rate trend over time. Mixed-effects meta-regression was used to identify the source of heterogeneity, and to explore the influence of study start year and follow-up on reoperations and failures over time. A meta-regression correction has been performed twice, based on follow-up time as well as per 100 observed component years. P-values lower than 0.05 were considered significant.

3. Results

3.1 Study selection

The search strategy identified 1,531 articles. After removal of duplicates, 473 articles were screened for eligibility based on title and abstract. After screening, 117 potentially eligible articles were included for full-text assessment. After assessing the full text studies, 99 studies were excluded, see Figure 2. 34 articles were reviews or expert opinions, 16 articles described another technique, 33 articles included less than 10 patients or had insufficient data, 14 articles were non-English and 2 articles were unpublished, leaving 18 studies for inclusion in the final analysis (13, 17, 20-23, 31-42). The dates of study inclusion ranged from 1992 to 2018. An overview of study characteristics is shown in Table 1.

3.2 Quality Assessment

The mean AQUILA methodological quality score was 7,1 points out of 11 points (range 4 - 8), showing that the quality of the study was not optimal. The main issue was the limited information provided on how the follow-up was performed, see Table 2.
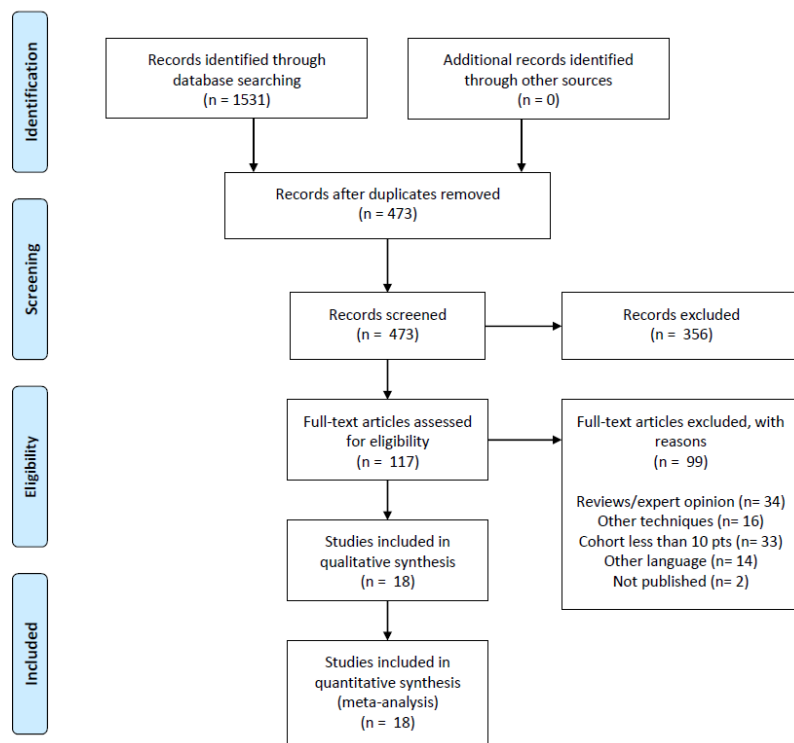
Figure 2. *PRISMA flow diagram outlining the systematic review process*

Table 1. *Study Characteristics and Patient Demographics.*

Article Demographics							
Article	Study Design	Inclusion year*	N patients	N hips	Mean age (range)	Mean follow-up*** (range)	Male/Female
Joshi et al. (2002)	Retrospective	1993	27	27	68 (55-77)	40 (25-56)	9/18
Christie et al. (2001)	Retrospective	1992	76	78	59 (29-87)	53 (24-107)	20/56
DeBoer et al. (2007)	Retrospective	1992	18	20	56 (30-77)	123 (89-157)	3/15
Taunton et al. (2012)	Retrospective	1992	57	57	61 (35-81)	76 (24-215)	6/51
Wind et al. (2013)	Retrospective	2001	19	19	58 (42-79)	31 (16-59)	7/12
Gladnick et al. (2018)	Retrospective	2000	73	73	59 (32-83)	90 (60-144)	21/5
Mao et al. (2015)	Retrospective	2001	22	23	61 (38-80)	82 (N/A)**	N/A**
Berasi et al. (2015)	Retrospective	2003	23	24	67 (47-85)	57 (28-108)	7/17
Li et al. (2016)	Retrospective	2003	24	24	65 (54-79)	67 (24-120)	8/16
Friedrich et al. (2014)	Retrospective	2007	18	18	68 (26-79)	30 (17-62)	7/11
Berend et al. (2018)	Retrospective	2004	94	95	66 (38-85)	43 (4-128)	34/61
Kieser et al. (2018)	Retrospective	2007	20	20	67 (50-89)	38 (34-110)	8/12
Baauw et al. (2017)	Retrospective	2011	12	12	66 (33-79)	25 (18-39)	3/9
Myncke et al. (2017)	Retrospective	2009	21	21	67 (50-83)	25 (N/A)**	6/15
Walter et al. (2020)	Retrospective	2008	54	58	70 (N/A)**	56 (24-120)	14/44
Burastero et al. (2020)	Retrospective	2014	19	20	60 (N/A)**	42 (N/A)**	11/8
Matar et al. (2020)	Retrospective	2013	17	17	72 (61-83)	44 (25-54)	3/14
Durand-Hill et al. (2020)	Retrospective	2016	20	20	66 (49/90)	26 (12-40)	7/13

* Start year of surgery inclusion

** N/A: results not available

*** Mean follow-up in months

3.3 Demographic data

A total of 614 patients (626 implants) underwent revision THA with custom-made acetabular components and were included in this study. The average follow-up of the studies was 53 months (range, 16 - 215). The mean age of the patients at the time of surgery was 64 years (range, 26 - 90), see Table 1.

3.4 Complications

All 18 studies reported complication rates, Table 3. The overall complication rate was 31,6% (198 out of 626 hips). The most common complications reported were dislocation (10,9%), followed by periprosthetic joint infection (7,0%), nerve lesion (2,6%) and loosening of the implant (2,6%), as shown in Table 4.

3.5 Reoperations and failures

The overall reoperation rate was 21,1% (132 out of 626 hips). Dislocation and periprosthetic infection were the most common reasons for reoperation, respectively 6,9% and 6,7%. The overall reoperation rate per 100 observed component years was 4,45 (range, 0 - 12,22). The incidence of overall failures was 17,7% (111 out of 626 hips), resulting in an overall failure rate of 3,74 per 100 observed component years (range, 0 - 8,89).

To visualize the complication, reoperation and failure trend over time, the event rates as percentage of total implanted hips were visualized for each individual study in Figure 3.

AQUILA Methodological Quality Items	Number of Studies
1. Is there a clear primary research question / hypothesis?	Yes: 12 of 18
2. How were the cohorts constructed? A. Consecutively B. Non-consecutively C. Unknown	A: 11 of 18 B: 4 of 18 C: 3 of 18
3. How adequate was the follow-up (FU)? A. Fully completed FU B. 5% or less lost-to-FU or FU quotient is 1 or less C. More than 5% lost-to-FU or FU quotient is more than 1 D. Unknown	A: 10 of 18 B: 5 of 18 C: 3 of 18 D: 0 of 18
4. How was the follow-up performed? A. Predefined (e.g. yearly) B. When patients had complaints or chart review (of non-predefined FU) C. Unknown	A: 4 of 18 B: 13 of 18 C: 1 of 18
5. How many arthroplasties are at risk at the FU of interest? A. 20 or more B. Less than 20 C. Unknown	A: 8 of 18 B: 10 of 18 C: 0 of 18
6. Has a worst-case analysis or competing risk analysis for competing endpoints been performed?	Yes: 0 of 18

Table 2. *AQUILA Methodological quality assessment.*

Universiteit Leiden

TUDelft — Delft University of Technology

Erasmus — ERASMUS UNIVERSITEIT ROTTERDAM

Table 3. *Summary of CTACs in Revision THA: Results showing Complications, Reoperations, and Failures. Obcy = Event rate per 100 observed component years*

				Event rate complications, reoperations and failures						
Article	N Hips	N Complications	Mean Complications *	Obcy Complications **	N Reoperations	Mean Reoperations *	Obcy Reoperations **	N Failures	Mean Failures *	Obcy Failures **
Joshi et al. (2002)	27	6	22%	6,8	3	11%	3,4	2	7%	2,3
Christie et al. (2001)	78	18	23%	5,2	7	9%	2,0	7	9%	2,0
DeBoer et al. (2007)	20	8	40%	3,9	6	30%	2,9	6	30%	2,9
Taunton et al. (2012)	57	33	58%	9,1	26	46%	7,2	26	46%	7,2
Wind et al. (2013)	19	15	79%	30,6	6	32%	12,2	4	21%	8,1
Gladnick et al. (2018)	73	29	40%	5,3	27	37%	4,9	19	26%	3,5
Mao et al. (2015)	23	4	17%	2,6	1	4%	0,6	1	4%	0,6
Berasi et al. (2015)	24	4	17%	3,5	4	17%	3,5	4	17%	3,5
Li et al. (2016)	24	3	13%	2,2	2	8%	1,5	0	0%	0,0
Friedrich et al. (2014)	18	6	33%	13,3	5	28%	11,1	4	22%	8,9
Berend et al. (2018)	95	20	21%	5,8	19	20%	5,6	19	20%	5,6
Kieser et al. (2018)	20	1	5%	1,6	1	5%	1,6	1	5%	1,6
Baauw et al. (2017)	12	4	33%	16,1	0	0%	0,0	0	0%	0,0
Myncke et al. (2017)	21	8	38%	18,3	0	0%	0,0	0	0%	0,0
Walter et al. (2020)	58	29	50%	10,7	21	36%	7,7	14	24%	5,1
Burastero et al. (2020)	20	3	15%	4,3	2	10%	2,8	2	10%	2,8
Matar et al. (2020)	17	6	35%	9,8	1	6%	1,6	1	6%	1,6
Durand-Hill et al. (2020)	20	1	5%	2,4	1	5%	2,4	1	5%	2,4

* Mean event rate is measured as n event devided by n hips
** Event rate per 100 observed component years (event/100 components)

Table 4. *Summary of CTACs in Revision THA: Results showing Complications by reason*

	Complications specified						
Article	Periprostetic joint infection	Dislocation	Nerve leason	Screw failure	Implant loosening	Periprostetic fracture	Other complications
Joshi et al. (2002)	2 (7%)	1 (4%)	2 (7%)	0 (0%)	0 (0%)	0 (0%)	1 (4%)
Christie et al. (2001)	0 (0%)	12 (15%)	5 (6%)	1 (1%)	0 (0%)	0 (0%)	0 (0%)
DeBoer et al. (2007)	0 (0%)	6 (30%)	1 (5%)	0 (0%)	1 (5%)	0 (0%)	0 (0%)
Taunton et al. (2012)	4 (7%)	12 (21%)	2 (4%)	3 (5%)	3 (5%)	3 (5%)	6 (11%)
Wind et al. (2013)	2 (11%)	5 (26%)	1 (5%)	3 (16%)	4 (21%)	0 (0%)	0 (0%)
Gladnick et al. (2018)	8 (11%)	7 (10%)	0 (0%)	1 (1%)	3 (4%)	2 (3%)	8 (11%)
Mao et al. (2015)	0 (0%)	2 (9%)	0 (0%)	0 (0%)	2 (9%)	0 (0%)	0 (0%)
Berasi et al. (2015)	2 (8%)	0 (0%)	0 (0%)	0 (0%)	0 (0%)	2 (8%)	0 (0%)
Li et al. (2016)	2 (8%)	1 (4%)	0 (0%)	0 (0%)	0 (0%)	0 (0%)	0 (0%)
Friedrich et al. (2014)	2 (11%)	3 (17%)	0 (0%)	0 (0%)	0 (0%)	0 (0%)	1 (6%)
Berend et al. (2018)	6 (6%)	6 (6%)	0 (0%)	0 (0%)	1 (1%)	2 (2%)	5 (5%)
Kieser et al. (2018)	1(5%)	0 (0%)	0 (0%)	0 (0%)	0 (0%)	0 (0%)	0 (0%)
Baauw et al. (2017)	0 (0%)	1 (8%)	1 (8%)	0 (0%)	0 (0%)	2 (17%)	0 (0%)
Myncke et al. (2017)	1 (5%)	4 (19%)	1 (5%)	1 (5%)	0 (0%)	0 (0%)	1 (5%)
Walter et al. (2020)	12 (21%)	6 (10%)	3 (5%)	0 (0%)	2 (3%)	2 (3%)	4 (7%)
Burastero et al. (2020)	2 (10%)	1 (5%)	0 (0%)	0 (0%)	0 (0%)	0 (0%)	0 (0%)
Matar et al. (2020)	0 (0%)	1 (6%)	0 (0%)	3 (18%)	0 (0%)	1 (6%)	1 (6%)
Durand-Hill et al. (2020)	0 (0%)	0 (0%)	0 (0%)	0 (0%)	0 (0%)	1 (5%)	0 (0%)
Total	**44 (7%)**	**68 (11%)**	**16 (3%)**	**12 (2%)**	**16 (3%)**	**15 (2%)**	**27 (4%)**

Number of complications measured in study (Percentage of all hips in study)

3.6 Meta-Regression

A more recent start year of the study was associated with a decrease in the risk of failure and reoperation, respectively; 0,75% per year (95%CI 0,02 - 1,47%) and 0,83% (95%CI 0,00 - 1,65%). After correction with follow-up, this association decreased to respectively; 0,44% per year (95%CI -0,44 - 1,32%) and 0,45% (95%CI -0,55 - 1,44%). However, the between-study variation was large

For each consecutive study year, the amount of failures per 100 component years decreased by

0,081 (95% CI: −0,11 - 0,27) units in terms of the average relative risk. Start year of the study had no significant influence on the amount of failures per 100 component years (p = 0,4). The test for residual heterogeneity was significant (p < 0,01), indicating that other moderators, not considered in this model, were influencing the amount of failure per 100 component years. To visualize the normalized complication, reoperation and failure trend over time, the event rates per 100 observed component years were visualized for each individual study in Figure 4.

Universiteit Leiden

TUDelft Delft University of Technology

Erasmus ERASMUS UNIVERSITEIT ROTTERDAM

Figure 3. *Visual representation of event rate in percentage over time, based on study start year.*

Figure 4. *Visual representation of event rate per 100 observed component years over time, based on study start year*

4. Discussion

The overall complication rate for custom-made acetabular implants was high (31,6%). Among the reported complications, dislocation was the most common (10,9%), follow by periprosthetic joint infection (7,0%), nerve lesion (2,6%) and loosening of the implant (2,6%). The overall reoperation rate for any reason (21,1%) is higher compared to other treatment options for severe acetabular defects; jumbo cups (12,1%), reinforces cages and rings (11%), trabecular metal augments (7,3%), and impaction bone grafting (7,3%) (43, 44). Despite the relatively high complications and reoperation rates, Martino et al. (1), showed considerable improvements in a variety of functional scores when implanting custom-made acetabular implants. According to the National Arthroplasty register of New Zealand, deriving revision rates from widely varying follow up times is more accurate when using the observed component years methodology (45). The derived overall failure rate, normalized for follow up and number of placed implants, corresponded to 3,74 failures per 100 observed component years (range, 0 - 8,89).

Focussing on the trend over time, for each consecutive study year, the amount of failures per 100 component years decreases by 0.081 (95% CI: −0.11 - 0.27). Differently formulated, a more recent start of the study was associated with a decrease in the risk of failure and reoperation, respectively; 0.75% per year (95% CI 0.02 - 1.47%) and 0.83% (95%CI 0.00 - 1.65%). However, after correction with follow-up in the meta-regression models, the association with study year decreases. Both corrections with follow-up and failures per 100 component years lead to an effect decrease and a non-significant effect. This was possibly due to a decrease in study power, because an extra modifier was included in the analysis. Secondly, a lot of study heterogeneity was seen, resulting in high between-study variation. This indicated that other moderators, not considered in this model, were possibly influencing the risk of failures and reoperations. A decreasing trend of the number of failures, reoperations, and complications of implanted CTACs was seen over time. Although, we were not able to verify the cause of this trend over time.

To compare the event rates at different implant periods, both the percentage as well as the observed component years for each event rate were calculated and visualized as a trend line. As can be seen from the trend lines in the graphs, Figure 3 and 4, both reoperation and failures trend lines decreases over the course of time. The complication rate trend line differ between both graphs. A plausible explanation could have been that complications mostly occur at an early stage following surgery. As the interstudy follow-up period differs, the complication rate could have been over- or underrated when not taking follow-up period into account. When normalizing the complication rate for follow-up period, we still encountered the same problem. As the chance of suffering from complications is not uniform over the whole follow-up period, the correct calculation of both the percentage of all implants, as well as the observed component years, was not correct with the derived data. Therefore, we included both graphs in this study without drawing hard conclusions.

Recent studies describe custom-made acetabular implants as an efficacious treatment option for severe acetabular defects where standard implants are not sufficient (1, 16). Even though several systematic reviews have previously published multiple treatment options for severe acetabular defects, no clear consensus on the optimal treatment is described (1, 16-21). Most of these previously published systematic reviews describing custom-made acetabular implants include all available articles without any date restriction, as the availability of studies with high quality is limited (1, 16). There are many factors which may influence the clinical outcomes and complication rates that are not reflected in these studies. One of these factors is the inclusion of articles reporting CTAC outcomes of the oldest generation CTAC techniques (17, 19-24). We hypothesized a trend improvement in complication, reoperation and failures rates of articles with a more recent study start year. We showed a decrease of failures and reoperations of implanted CTACs over time. Unfortunately, due to limited study data and high between-study variation, we were not able to draw solid conclusions from our results.

There were a variety of limitations in this study. First, as discussed above, we were limited by the quality of the included studies, the variability in inclusion criteria, the number of patients per study,

the follow-up time per study and the different methods of reporting events across the studies. As a result, the direct comparison of the complication rate, as well as the reoperation rate, over the course of time was not possible due to limited individual patient data provided in the studies. To compare those event rates over time, it is necessary to include individual patient data, such as individual patient surgery date, individual dates of complications etc. Considering only four studies included individual patient data, three reported individual follow-up data and none reported individual event timepoints, we're far from comparing and formulating correct event rates at different time points.

Second, the study surgery dates were not provided in the included studies. Therefore, study start year was selected to represent the event rates corresponding to each article. We assumed the technique used at the start of the study was comparable over the whole period of the study. Unfortunately, the description of the technique was limited in several studies and could have changed during the study without mentioning. Secondly, the studies did not describe any advances of the techniques which were used. Therefore, this could have resulted to an incorrect representation. Larger multicenter studies using similar outcome assessment methodologies would be helpful to better compare results of the custom-made acetabular implants over time.

5. Conclusion

The management of severe acetabular defects remains a challenging problem. Despite the high complication and reoperation rates, custom-made acetabular implants have become a commonly used treatment option in recent years. A decreasing trend of the number of failures, reoperations, and complications of implanted CTACs was seen over time. Although, due to limited study data and high between-study variation, we were not able to verify the cause of this trend over time. To further examine the trend of implant survival and complications over the course of time for custom-made acetabular implants, individual patient data, such as occurred complications per year and surgery year, should be reported more frequently in the literature.

References

1.   De Martino I, Strigelli V, Cacciola G, Gu A, Bostrom MP, Sculco PK. Survivorship and Clinical Outcomes of Custom Triflange Acetabular Components in Revision Total Hip Arthroplasty: A Systematic Review. The Journal of Arthroplasty. 2019;34(10):2511-8.
2.   Di Laura A, Henckel J, Wescott R, Hothi H, Hart AJ. The effect of metal artefact on the design of custom 3D printed acetabular implants. 3D Printing in Medicine. 2020;6(1).
3.   Telleria JJM, Gee AO. Classifications In Brief: Paprosky Classification of Acetabular Bone Loss. Clinical Orthopaedics and Related Research®. 2013;471(11):3725-30.
4.   Paprosky WG, Perona PG, Lawrence JM. Acetabular defect classification and surgical reconstruction in revision arthroplasty. The Journal of Arthroplasty. 1994;9(1):33-44.
5.   Woo S-H, Sung M-J, Park K-S, Yoon T-R. Three-dimensional-printing Technology in Hip and Pelvic Surgery: Current Landscape. Hip & Pelvis. 2020;32(1):1.
6.   Abolghasemian M, Tangsataporn S, Sternheim A, Backstein D, Safir O, Gross AE. Combined trabecular metal acetabular shell and augment for acetabular revision with substantial bone loss: a mid-term review. Bone Joint J. 2013;95-b(2):166-72.
7.   Banerjee S, Issa K, Kapadia BH, Pivec R, Khanuja HS, Mont MA. Systematic review on outcomes of acetabular revisions with highly-porous metals. Int Orthop. 2014;38(4):689-702.

Universiteit Leiden

TUDelft Delft University of Technology

Erasmus Universiteit Rotterdam

8.   Beckmann NA, Weiss S, Klotz MC, Gondan M, Jaeger S, Bitsch RG. Loosening after acetabular revision: comparison of trabecular metal and reinforcement rings. A systematic review. J Arthroplasty. 2014;29(1):229-35.

9.   Sculco PK, Ledford CK, Hanssen AD, Abdel MP, Lewallen DG. The Evolution of the Cup-Cage Technique for Major Acetabular Defects: Full and Half Cup-Cage Reconstruction. J Bone Joint Surg Am. 2017;99(13):1104-10.

10.   Barlow BT, Oi KK, Lee YY, Carli AV, Choi DS, Bostrom MP. Outcomes of Custom Flange Acetabular Components in Revision Total Hip Arthroplasty and Predictors of Failure. J Arthroplasty. 2016;31(5):1057-64.

11.   Berry DJ. Antiprotrusio cages for acetabular revision. Clin Orthop Relat Res. 2004(420):106-12.

12.   Xia RZ, Zhai ZJ, Chang YY, Li HW. Clinical Applications of 3-Dimensional Printing Technology in Hip Joint. Orthopaedic Surgery. 2019;11(4):533-44.

13.   Berasi CC, Berend KR, Adams JB, Ruh EL, Lombardi AV. Are Custom Triflange Acetabular Components Effective for Reconstruction of Catastrophic Bone Loss? Clinical Orthopaedics and Related Research®. 2015;473(2):528-35.

14.   Won SH, Lee YK, Ha YC, Suh YS, Koo KH. Improving pre-operative planning for complex total hip replacement with a Rapid Prototype model enabling surgical simulation. Bone Joint J. 2013;95-b(11):1458-63.

15.   Tserovski S, Georgieva S, Simeonov R, Bigdeli A, Röttinger H, Kinov P. Advantages and disadvantages of 3D printing for pre-operative planning of revision hip surgery. Journal of Surgical Case Reports. 2019;2019(7).

16.   Chiarlone F, Zanirato A, Cavagnaro L, Alessio-Mazzola M, Felli L, Burastero G. Acetabular custom-made implants for severe acetabular bone defect in revision total hip arthroplasty: a systematic review of the literature. Archives of Orthopaedic and Trauma Surgery. 2020;140(3):415-24.

17.   Christie MJ, Barrington SA, Brinson MF, Ruhling ME, Deboer DK. Bridging Massive Acetabular Defects With the Triflange Cup. Clinical Orthopaedics and Related Research. 2001;393:216-27.

18.   Colen S, Harake R, De Haan J, Mulier M. A modified custom-made triflanged acetabular reconstruction ring (MCTARR) for revision hip arthroplasty with severe acetabular defects. Acta Orthop Belg. 2013;79(1):71-5.

19.   Holt GE, Dennis DA. Use of custom triflanged acetabular components in revision total hip arthroplasty. Clin Orthop Relat Res. 2004(429):209-14.

20.   Joshi AB, Lee J, Christensen C. Results for a custom acetabular component for acetabular deficiency. The Journal of Arthroplasty. 2002;17(5):643-8.

21.   Wind MA, Swank ML, Sorger JI. Short-term Results of a Custom Triflange Acetabular Component for Massive Acetabular Bone Loss in Revision THA. Orthopedics. 2013;36(3):e260-e5.

22.   Deboer DK, Christie MJ, Brinson MF, Morrison JC. Revision Total Hip Arthroplasty for Pelvic Discontinuity. The Journal of Bone & Joint Surgery. 2007;89(4):835-40.

23.   Taunton MJ, Fehring TK, Edwards P, Bernasek T, Holt GE, Christie MJ. Pelvic Discontinuity Treated With Custom Triflange Component: A Reliable Option. Clinical Orthopaedics and Related Research®. 2012;470(2):428-34.

24.   Moore KD, McClenny MD, Wills BW. Custom Triflange Acetabular Components for Large Acetabular Defects: Minimum 10-Year Follow-up. Orthopedics. 2018;41(3):e316-e20.

25.   Moher D, Shamseer L, Clarke M, Ghersi D, Liberati A, Petticrew M, et al. Preferred reporting items for systematic review and meta-analysis protocols (PRISMA-P) 2015 statement. Systematic Reviews. 2015;4(1):1.

26.   Pijls BG, Dekkers OM, Middeldorp S, Valstar ER, Van Der Heide HJ, Van Der Linden-Van Der Zwaag HM, et al. AQUILA: assessment of quality in lower limb arthroplasty. An expert Delphi consensus for total knee and total hip arthroplasty. BMC Musculoskeletal Disorders. 2011;12(1):173.

27.   Doll R, Hill AB. Lung cancer and other causes of death in relation to smoking; a second report on the mortality of British doctors. Br Med J. 1956;2(5001):1071-81.

28.   Labek G, Thaler M, Janda W, Agreiter M, Stöckl B. Revision rates after total joint replacement: cumulative results from worldwide joint register datasets. J Bone Joint Surg Br. 2011;93(3):293-7.

Universiteit Leiden

TUDelft Delft University of Technology

Erasmus UNIVERSITEIT ROTTERDAM

29.   Pabinger C, Lumenta DB, Cupak D, Berghold A, Boehler N, Labek G. Quality of outcome data in knee arthroplasty. Acta Orthopaedica. 2015;86(1):58-62.

30.   Nouta K-A, Pijls BG, Nelissen RGHH. All-polyethylene tibial components in TKA in rheumatoid arthritis: a 25-year follow-up study. International Orthopaedics. 2012;36(3):565-70.

31.   Mao Y, Xu C, Xu J, Li H, Liu F, Yu D, et al. The use of customized cages in revision total hip arthroplasty for Paprosky type III acetabular bone defects. International Orthopaedics. 2015;39(10):2023-30.

32.   Li H, Qu X, Mao Y, Dai K, Zhu Z. Custom Acetabular Cages Offer Stable Fixation and Improved Hip Scores for Revision THA With Severe Bone Defects. Clinical Orthopaedics and Related Research®. 2016;474(3):731-40.

33.   Friedrich MJ, Schmolders J, Michel RD, Randau TM, Wimmer MD, Kohlhof H, et al. Management of severe periacetabular bone loss combined with pelvic discontinuity in revision hip arthroplasty. International Orthopaedics. 2014;38(12):2455-61.

34.   Berend ME, Berend KR, Lombardi AV, Cates H, Faris P. The patient-specific Triflange acetabular implant for revision total hip arthroplasty in patients with severe acetabular defects. The Bone & Joint Journal. 2018;100-B(1_Supple_A):50-4.

35.   Kieser DC, Ailabouni R, Kieser SCJ, Wyatt MC, Armour PC, Coates MH, et al. The use of an Ossis custom 3D-printed tri-flanged acetabular implant for major bone loss: minimum 2-year follow-up. HIP International. 2018;28(6):668-74.

36.   Baauw M, Van Hellemondt GG, Spruit M. A Custom-made Acetabular Implant for Paprosky Type 3 Defects. Orthopedics. 2017;40(1):e195-e8.

37.   Walter SG, Randau TM, Gravius N, Gravius S, Fröschen FS. Monoflanged Custom-Made Acetabular Components Promote Biomechanical Restoration of Severe Acetabular Bone Defects by Metallic Defect Reconstruction. The Journal of Arthroplasty. 2020;35(3):831-5.

38.   Burastero G, Cavagnaro L, Chiarlone F, Zanirato A, Mosconi L, Felli L, et al. Clinical study of outcomes after revision surgery using porous titanium custom-made implants for severe acetabular septic bone defects. International Orthopaedics. 2020.

39.   Matar HE, Selvaratnam V, Shah N, Wynn Jones H. Custom triflange revision acetabular components for significant bone defects and pelvic discontinuity: Early UK experience. Journal of Orthopaedics. 2020;21:25-30.

40.   Durand-Hill M, Henckel J, Di Laura A, Hart AJ. Can custom 3D printed implants successfully reconstruct massive acetabular defects? A 3D-CT assessment. Journal of Orthopaedic Research. 2020.

41.   Myncke I, van Schaik D, Scheerlinck T. Custom-made triflanged acetabular components in the treatment of major acetabular defects. Short-term results and clinical experience. Acta Orthop Belg. 2017;83(3):341-50.

42.   Gladnick BP, Fehring KA, Odum SM, Christie MJ, Deboer DK, Fehring TK. Midterm Survivorship After Revision Total Hip Arthroplasty With a Custom Triflange Acetabular Component. The Journal of Arthroplasty. 2018;33(2):500-4.

Part II - Tool development and analysis

For the second and main thesis objective, we developed a semi-automatic 3D-CT assessment tool to analyze the positioning of CTACs. Patients were included and analyzed. This scientific paper is the main end-product of this master thesis (TM30004). Additional modeling methods can be found in the Appendix H Part II – Matlab script.

Accuracy of Positioning Custom Triflange Acetabular Components in THA Revision and Tumor Resection Surgery – A 3D-CT Assessment Study

Abstract

Introduction In recent years, there has been an increasing interest in custom triflange acetabular components (CTAC) for revision and oncological surgery. The aim of this study was to evaluate the surgical accuracy of positioning CTACs in patients receiving either total hip arthroplasty (THA) revision or tumor resection surgery, using a novel 3D analyzing technique.

Method This retrospective cohort study included 35 patients (27 tumor and 8 THA revision cases), between February 2017 and March 2021. All patients received a CTAC. The planned and achieved implant position were assessed by means of a developed semi-automatic 3D-CT assessment method. The primary outcomes were the cup angles described as inclination, anteversion and cup rotation, and the translation of center of rotation (COR), pubic flange, ischial flange and ilium flange in three planes.

Results The mean deviation, between planned and achieved, in inclination was 0.5° (SD: 3.9°), in anteversion 1.2° (SD: 6.1°) and in cup rotation 0.6° (SD: 3.2°). The mean deviation in COR in the sagittal plane was -0.8 mm (SD: 3.2), in the coronal plane -0.4 mm (SD: 6.3) and in the axial plane 0,6 mm (SD: 6,1). Translation of the ischial flange showed the largest aberration (median absolute value: 7.0 mm), followed by the pubic flange (6.4 mm) and the ilium flange (5.3 mm).

Discussion A semi-automatic method to analyze the 3D position of CTAC was presented in this study. The results show good agreement between the planned and achieved implant position in patients receiving THA revision or tumor resection surgery. 89% of the components in this study were accurately positioned according to our criteria.

Keywords Bone defects, custom-made implants, pelvic discontinuity, revision total hip arthroplasty, tumor, reconstruction, acetabular

1. Introduction

The surgical management of large pelvic bone defects remains technically challenging (1, 2). Surgical repair of periacetabular bone defects related with THA revision are dependent on bone stock of the acetabular dome, medial wall, anterior and posterior pelvic column and pelvic ring continuity. Small defects can successfully be reconstructed by bone impaction grafting with or without mesh reconstruction, by off-the-shelf reinforcement rings, by triflange acetabular cages or by a combination of the mentioned options. Larger constructs or major hip altering procedures are needed, if there is gross bone loss, discontinuity of the pelvic ring or tumor resection (3). These techniques often are insufficient or suboptimal in patients who had multiple total hip arthroplasty (THA) revision procedures or who need large tumor resections.

The greatest challenges in THA revision surgery are the classified Paprosky types IIIA and IIIB, which are defined as the most severe acetabular defects characterized by destruction of supporting structures (4, 5), see Appendix C – Definitions, for the Paprosky definition. Besides Paprosky type III defects, pelvic tumors are challenging to reconstruct due to the complexity of the anatomy and the large anatomical structures that often must completely be removed and rebuild. These reconstructions are classified by the zone of pelvic resection (Enneking type I, II, III, IV) (6), see Appendix C – Definitions, for Enneking definition. Although several studies have reported encouraging results, the optimal surgical technique for Paprosky type III defects and pelvic tumor resection reconstruction has not been established (1, 7, 8). Previously proposed reconstructive procedures for THA revision surgery include jumbo acetabular cups, oblong acetabular cups, titanium

pedestal cups and antiprotrusio cages. (7-14). For pelvic tumor resection, reconstructive procedures include the use of the LUMiC, saddle prosthesis and custom made pelvic implants.

In recent years, there has been an increasing interest in custom made pelvic implants for revision and oncologic surgery, Figure 1. This technology has evolved substantially during the past decade and provides an advanced approach to tumor resection or revision surgery (15). Using pre-operative planning software, the surgeon has the possibility to determine the exact component positioning, the component shape, location and length of the screws (15). Additionally, the current 3D additive manufacturing techniques give the ability to intraoperatively check the bone and implant positioning with an additional similar sterile printed model. Furthermore, computer-assisted intraoperative navigation and patient specific instruments (PSI) are available tools used to enhance implant positioning. As a result, custom made acetabular components have been proposed as a solution to treat patients with severe acetabular defects and patients receiving large tumor resections.

During surgery, the pre-operative planning is of great importance, as the custom made implant apts one exact position. It is necessary to assess the exact executed position of the post-operative implant, in order to determine the exactness of the surgical placement. Throughout this paper, the term 'Surgical accuracy' will refer to the exactness

of the surgical placement of a custom triflange acetabular component (CTAC) compared to the pre-operative planning.

The orientation of an acetabular implant can be described by its anteversion and inclination. Lewinnek et al. (1978) proposed a 'safe zone' of cup inclination of 40° ± 10° and anteversion of 15° ± 10° (16). Murray et al. (1993) defined three different methods for the measurement of acetabular orientation; operative, radiographic and anatomical (17). The different methods of measurement depend on its application and cause minor measurement differences. A more extensive description of the different measurement methods can be found in Appendix C - Definitions. Inapt inclination and anteversion is associated with an increased chance of implant dislocation and greater susceptibility to wear due to improper loads (18, 19). Therefore, correct cup placement is essential.

Several researches reported on the surgical accuracy of positioning printed pelvic implants. However, most writers focused on the accuracy of 2D images rather than 3D images. Studies reporting the accuracy of the 3D position of the implant were limited by small cohorts and focused solitary on THA revision surgery. Previous research comparing the pre-operative planning position with the post-operative position of a 3D printed pelvic implant proposed several methods for the calculation of the position (20-23), see Appendix D – Methods for position calculation for details. All

Figure 1. OSSIS custom triflange acetabular component (CTAC). a) 3D print of pelvic bone. b) OSSIS custom made acetabular implant. c) Pre-operative planning of CTAC including screw positioning.
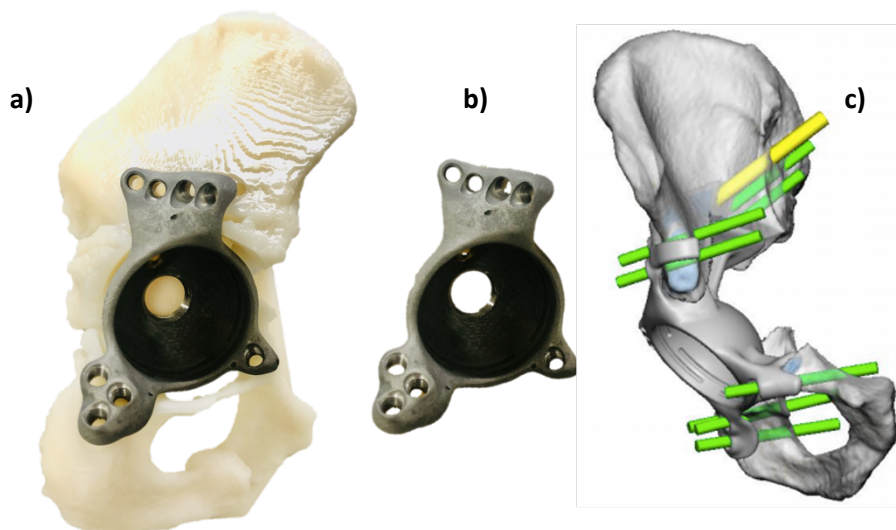
of these studies investigated the deviation of the inclination and anteversion. As component rotation in tri-flanged components affects the position of screw holes and consequently may affect implant fixation, additional measurements on cup rotation and flange translation could be of added value. However, rotation of the cup and translation of the center of rotation (COR) was studied occasionally and no research was found on the translation of the implant flanges.

To our knowledge, no cohort data is available on 3D pelvic implant positioning in tumor reconstructions and only sparsely on THA revision surgery with limited cohorts. The aim of this study was to evaluate the surgical accuracy of positioning CTAC, in six degrees of freedom, in patients receiving THA revision or tumor resection surgery. A novel semi-automatic 3D-CT assessment technique was developed for analysis. Second, a surgical accuracy comparison was performed on the use of intraoperative navigation, the surface size of the implant, and between tumor and THA revision indications.

2. Method

A multi-center retrospective cohort study of patients with massive acetabular bone defects was conducted. All patients underwent THA revision surgery or tumor reconstructions with a CTAC (OSSIS Limited, Christchurch, New Zealand) in Australia. Primary outcomes measures were the planned versus achieved inclination and anteversion, their difference in rotation, and the translation of the center of rotation (COR), Pubic Flange, Ischial Flange, and the Ilium Flange in millimeters. Secondary outcomes include the surgical accuracy of use of navigation during surgery, the surface size of the implant, and between tumor or THA revision indications. Ethical approval was obtained from the participating institutions ethics committees and patients were anonymized throughout the study.

2.1 Patients
Inclusion criteria for selecting the subjects were patients, regardless of age, who received a OSSIS CTAC between February 2017 and March 2021, underwent surgery at one of the three hospitals that participate in the study (Sydney, Perth, or Brisbane), and had an available pre- and post-operative pelvic (PET)-CT. Exclusion criteria were unavailable post-operative (PET)-CTs, no acetabular component in the implant design, and patients who did not give informed consent for participating in the study. Indications for the use of CTACs were massive acetabular bone defects due to acetabular aseptic loosening (AL), implant failure, periprosthetic joint infection, osteolysis, multiple dislocations, or tumor.

2.2 Implants
All patients received a pre-operative CT scan of the pelvis. Based on the acquired CT scan, a 3D computer-aided model of the pelvis was generated by a semi-automatic bone segmentation algorithm (Mimics, Materialize, Leuven, Belgium). A proposal

Figure 2. *Schematic representation of the development of a custom made acetabular implant*

| Pre-operative CT scan | Pre-operative 3D models | Planning 3D models | Printed Implant ready for surgery |
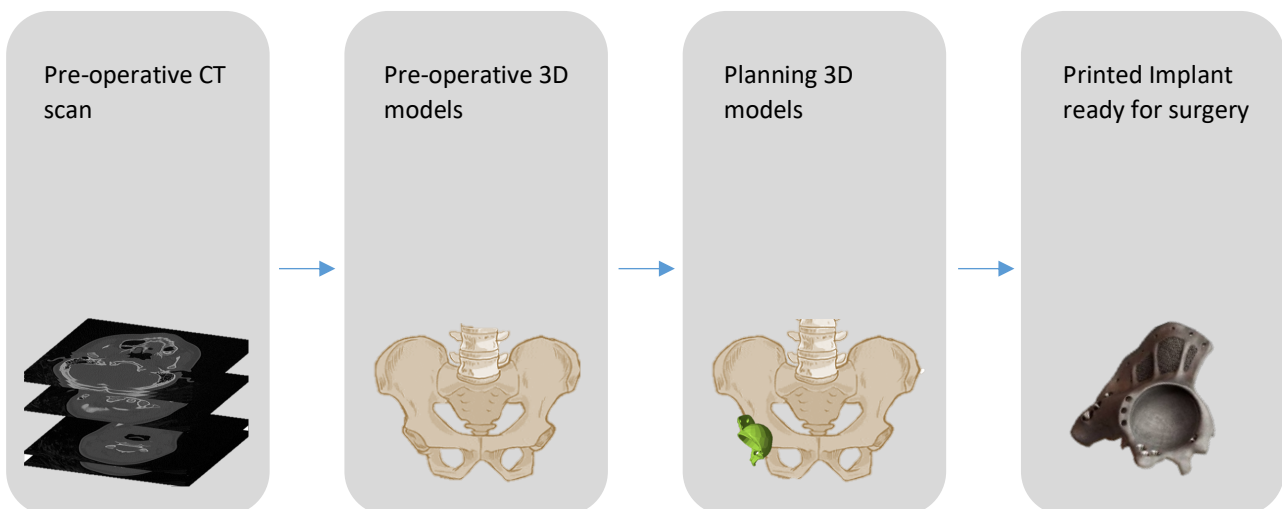
for a CTAC was presented by the implant manufacturer. The final design was determined with specific input from the surgeon where the quality of the remaining acetabular bone, the positioning of the optimal inclination (INCL), anteversion (AV), center of rotation (COR), surgical approach and placement of the screws, was respected. The implant was subsequently printed in 3D with titanium. The process of developing a CTAC is schematically represented in Figure 2. Although each implant design differ, the traditional triflange implant typically consist of one pubic flange, one ischial flange, and one larger iliac flange.

2.3 Operative Procedure

Surgery was performed under general anesthesia, with regional or spinal techniques where possible, and prophylactic intravenous antibiotics per protocol. For oncologic resections, the majority of the procedures were completed in a single-stage via supine position modified iliofemoral approach, where possible, with an anterior superior iliac spine osteotomy with abductor release. Pelvic osteotomy sites were determined using patient specific cutting guides, a trial implant was used to finalize resection and precise implant positioning, and navigation was used in some cases.

For THA revision cases, a modified anterolateral or direct anterior approach (abductor sparing) was used. Any residual hardware from prior surgeries (acetabular cup, screws, plates and/or meshes or other components) were removed when necessary according to the pre-operative planning, and the remaining pelvic bone was refashioned with reamers or rongeurs to provide a viable stable surface to accommodate the CTAC. The implant with its specific matching contours, and features such as flanges and hooks, was positioned according to predetermined bony landmarks, with the aid of sterile 3d printed bone models.

In most cases, a non-locking screw was initially placed to achieve stability and implant compression against the bone, followed by multiple fixed angle locking screws. Locking guides were used to achieve pre-determined screw trajectories. For resections involving the peri-acetabular region (P2), the hip joint was reconstructed with a cemented femoral stem or a proximal femoral replacement (Exeter or Global Modular Replacement System, Stryker, Mahwah, New Jersey, United States). On the acetabular side, a semi- constrained polyethylene Snap-Fit cup (Bioimpianti, Milan, Italy) or Tripolar component (Corin) was cemented into the 3DPI acetabular dome, using antibiotic loaded (gentamycin) polymethylmethacrylate (PMMA) cement.

Closure was achieved through reattachment of the anterior superior iliac spine osteotomy using large fragment screws, absorbable suture to inguinal ligament, abdominal wall and gluteal fascia, with wounds closed over suction drains. Post-operatively all patients were admitted to the intensive care unit (ICU). They received six weeks thromboprophylaxis (low molecular weight heparin) and antibiotics (intravenous vancomycin and cefepime followed by oral cephalexin). Patients remained on bed rest until muscle control was regained. Rehabilitation followed under physiotherapist supervision and guidance.

2.4 Postoperative Analysis

To determine the accuracy of the positioning of CTACs, 3D computer-aided models of the pelvis and implant were generated from the pre-operative and post-operative (PET)-CT. After aligning the models, the position of the achieved implant was compared to the planned position. A more detailed description of the analysis methods is provided in the next paragraphs (2.5 to 2.12).

Traditionally, the orientation of an acetabular implant may be described by its anteversion and inclination. However, as component rotation in triflanged components affects the position of screw holes and subsequently may affect implant fixation, implant positioning was described in six degrees of freedom in this study: inclination (°), anteversion (°), cup rotation (°), and translation in three planes (mm). Translation of the implant was described for COR, pubic flange, ischial flange and the ilium flange. We developed an automatic analysis algorithm (MATLAB R2019b, Mathworks) based on anatomic and implant landmark selection. A schematic overview of the analysis method can be found in Figure 3 . The developed

Figure 3. *Schematic representation of the 3D-CT analysis method*
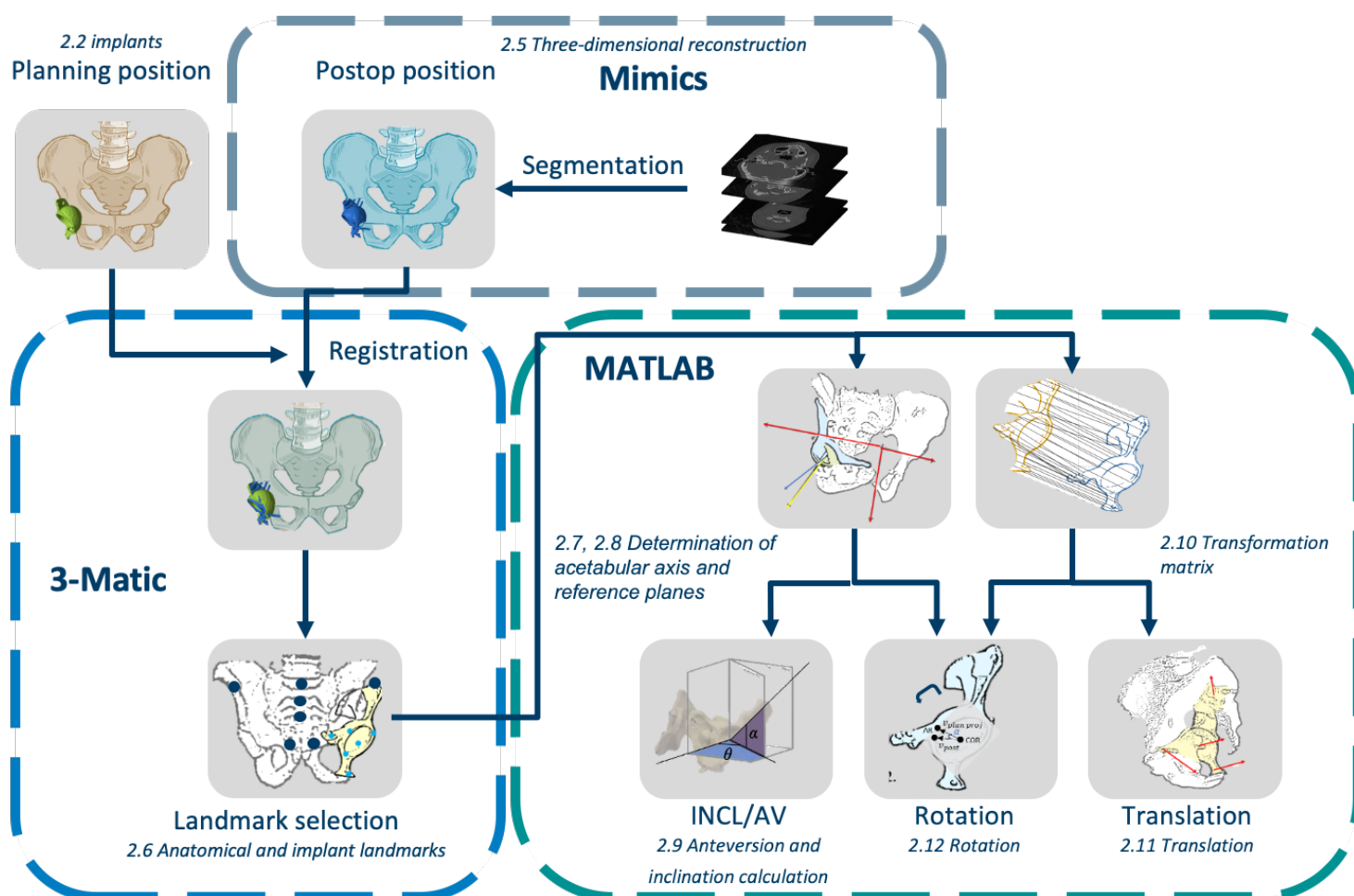
semi-automatic script of the analysis can be found in Appendix H – Matlab script.

2.5 Three-dimensional reconstruction

The 3D models of the pelvis and the implant were extracted from the pre-operative and postoperative Digital Imaging and Communications in Medicine (DICOM) data, preferably CT-data. 3D models were extracted using an image thresholding technique (Mimics, Materialize, Leuven, Belgium). This technique classifies pixels that meet a given grayscale criteria to regard as belonging to the target, while other pixels are relegated to the background (24). Subsequently, the targeted pixels were converted into 3D surface (STL) models. Once the 3D models were extracted, the planned pelvic model was aligned towards the post-operative pelvic model. Aligning of the pelvic 3D models was achieved using a iterative closest point (ICP) algorithm (3-Matic, Materialize, Leuven, Belgium). The registration performed was based on surface registration, focused on sacrum alignment. Sacrum alignment was chosen as the sacral region is connected to the lumbar spine, and is therefore not translocated during surgery. Second, a copy of the planned implant was created and aligned towards the post-operative implant for the comparison of two identical 3D implant models. After aligning the 3D models, each model was exported as Binary Standard Triangle Language (STL) file. See Appendix G – Protocol for pre-processing, for a detailed description.

Figure 4. *Anatomical and implant landmark selection. ASIS = anterior superior iliac spine; PT = pubic tubercle; SC = sacral crest; COR = center of rotation*
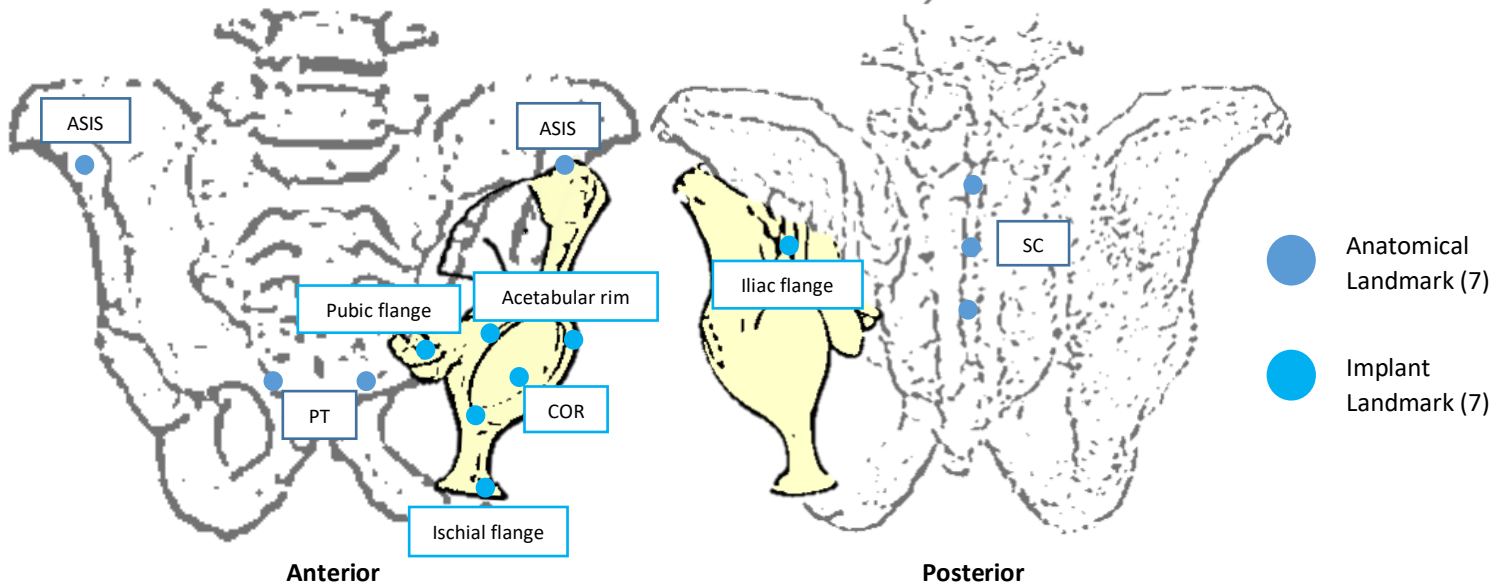
2.6 Anatomical and implant landmarks

Subsequently, anatomical landmarks on the planned pelvis and implant were chosen to acquire five anatomical reference planes (3-Matic, Materialize, Leuven, Belgium). Several methods are currently described in literature for the determination of anatomical pelvic planes (25). The anatomical pelvic planes in this study were determined by adapting the anatomical landmark selection procedure used by Wang et al. (2017) (26).

Three equally placed landmarks on the acetabular implant rim were marked, used to obtain the acetabular planes. Further, bilateral anterior superior iliac spine (ASIS) landmarks, and bilateral pubic tubercle (PT) landmarks were chosen to determine the coronal plane. Three landmarks of the sacral crest (SC) were labeled, used to acquire the sagittal planes. Three central landmarks near the screw holes were chosen on the triflange edges, respectively; pubic flange, ischial flange, and ilium flange, Figure 4. In case a flange was not present at the implant design, the corresponding implant landmark was not selected. Last, the center of rotation of the acetabular cup of the implant was selected. As the implant acetabular cups were hemispheres, the center of rotation (COR) was based on the middle point of an

acetabular sphere. The acetabular hemisphere was fitted based on 4 points selected on the surface of the acetabular cup. The anatomical landmarks were manually labelled. In case a part of an important pelvic bone was missing in the 3D model due to large bone resections or targeted CT acquisition, the contralateral side was mirrored to reconstruct the missing anatomy. Coordinates of each anatomical landmark (x,y,z) were exported for automatic calculation of the inclination, anteversion, cup rotation and translation of the implant.

2.7 Determination of the acetabular axis

The implant landmarks of the acetabular rim are located on a plane, called the acetabular plane. The acetabular plane can be defined as the normal vector of the acetabular plane. This normal vector was calculated and named as the acetabular axis, Figure 5. The acetabular axis was calculated using the coordinates of the three acetabular rim landmarks. From these coordinates, two vectors where calculated. Vector $\overrightarrow{AB}$ connecting acetabular rim landmark 1 with acetabular rim landmark 2. Vector $\overrightarrow{AC}$ represent an arrow connecting acetabular rim landmark 1 with acetabular rim landmark 3, Equation 1. The normal vector of the acetabular plane was calculated using

the cross product of the two vectors in three-dimensional space, Equation 2.

$$AB = ab_1\hat{\imath} + ab_2\hat{\jmath} + ab_3\hat{k}$$
$$AC = ac_1\hat{\imath} + ac_2\hat{\jmath} + ac_3\hat{k}$$

Eq. 1

$$n = AB \, X \, AC$$
$$= \begin{vmatrix} \hat{\imath} & \hat{\jmath} & \hat{k} \\ ab_1 & ab_2 & ab_3 \\ ac_1 & ac_2 & ac_3 \end{vmatrix}$$

Eq. 2

Equation 1 and 2. *Describing the mathematical calculation of a normal vector.* **Eq. 1** *Mathematical representation of the linearly independent vectors $\overrightarrow{AB}$ and $\overrightarrow{AC}$.* **Eq. 2** *Mathematical representation of the cross product of $\overrightarrow{AB}$ and $\overrightarrow{AC}$ resulting in a vector perpendicular to both vectors, thus normal to the plane. The formula is written as a 3x3 determinant.*

2.8 Determination of reference axes

As the use of the anterior pelvic plane (APP) is recommended for the assessment of acetabular cup orientation by the International Society of Biomechanics (25), the coronal plane in this study was described as the APP. When a patient is placed in supine position during imaging, the difference between the APP and the coronal plane is represented as the pelvic tilt (27). However, when calculating the position of the implant of the same person, the pelvic tilt is similar and can therefore be neglected in this analysis. Consequently, the determination of the APP was based on the conceptual framework by Wang et al. (2017) (26). The APP is defined as the tangential plane of the pelvis determined by four pelvic landmarks; two bilateral ASIS, and two bilateral PT. The three of these anatomical landmarks where mathematically converted into a normal vector of the APP plane and was named as the frontal axis, Figure 5 and Equation 1 and 2. The sagittal plane was defined by the midline of the bilateral ASIS and the three SC landmarks. Mathematical conversion of these midline and two SC landmarks resulted in a normal vector of the sagittal plane and was named as the transverse axis, Figure 5 and Equation 1 and 2.

Once the frontal and transverse axis were known, the normal vector of the transverse plane was calculated. As the transverse plane was perpendicular to the APP and sagittal plane; mathematically, the cross product of the frontal and transverse axis resulted in a normal vector of the transverse plane, Equation 3. This normal vector was named as the longitudinal axis, Figure 5.

Figure 5. *Frontal, transverse and longitudinal axis (red), planned acetabular axis (yellow) and post-operative acetabular axis (blue)*
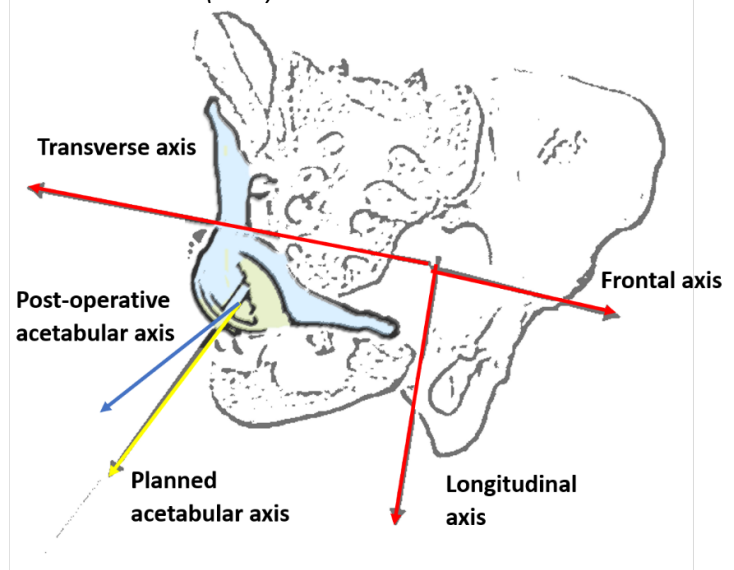
$$n_{Trans} = \overrightarrow{n_{APP}} \, X \, \overrightarrow{n_{Sag}}$$
$$= \begin{vmatrix} \hat{\imath} & \hat{\jmath} & \hat{k} \\ n_{APP_1} & n_{APP_2} & n_{APP_3} \\ n_{Sag_1} & n_{Sag_2} & n_{Sag_3} \end{vmatrix}$$

Eq. 3

Equation 3. *Mathematical representation of the cross product $\overrightarrow{n_{APP}}$ and $\overrightarrow{n_{Sag}}$ resulting in a vector perpendicular to both normal vectors, thus the normal vector of the transverse plane. The formula is written as a 3x3 determinant.*

2.9 Anteversion and inclination calculation

To measure the anteversion (AV) and inclination (INC), the radiographic definition described by Murray et al. (1993) was chosen (17). Prior to analyzing the angles, the acetabular axis was projected onto the APP, Equation 4. Thereafter, the radiographic anteversion (RA) was calculated

as the angle between the acetabular axis and the acetabular axis projected on the coronal plane, Equation 5. Radiographic inclination (RI) is described as the angle between the longitudinal axis of the patient and the acetabular axis projected on the coronal plane, Equation 5. Thus, $\vec{n}$ represent the acetabular axis projected on the APP. $\vec{m}$ represent the acetabular axis or the longitudinal axis, conditional to calculating the anteversion or inclination.

$$Proj_{A axis \, on \, APP} = \frac{\overrightarrow{n_{APP}} X (\overrightarrow{n_{APP}} X \overrightarrow{n_p})}{|\overrightarrow{n_{APP}}|^2} \qquad Eq. \, 4$$

Equation 4. *Mathematical representation of the projection of the acetabular axis onto the APP. $\overrightarrow{n_{APP}}$ represent the APP and $\overrightarrow{n_p}$ represent either the planned acetabular plane or the post-operative acetabular plane.*

$$\alpha = \cos^{-1} \frac{\vec{n} \vec{m}}{|\vec{n}||\vec{m}|} \qquad Eq. \, 5$$

Equation 5. *Mathematical representation of the angle calculation. The angle is calculated in degrees between vector $\vec{n}$ and $\vec{m}$.*

2.10 Transformation matrix

To determine the discrepancy in millimeters between the postoperative and the planned position of the implant, a second analyzing method was developed, figure 3. A point cloud was created from both the planned as the post-operative implant STL files. The point cloud was generated by the conversion of the surfaces meshes of a STL file into a point cloud.

Once the point clouds of the planned and the achieved implant were extracted, a landmark transform method to determine the rotation and translation of the implant was applied to the data. This landmark transform is a type of transformation whose rule is based on multiplication of a vector by a matrix. The 4 by 4 transformation matrix uses homogeneous coordinates, which allow to distinguish between points and vectors. This matrix can be used to directly transform an object from one point in a coordinate system to another along one or more of the three axes. The matrix consist of sub-transformations such as translations, rotations and/or scaling.

The transformation method in this study is based on point correspondence and uses the singular value decomposition of a matrix derived from the point clouds as previously reported by Soderkvist el al. (1993) and Challis et al. (1995) (28) (29). Accordingly, an optimal alignment was achieved between the planned and post-operative point cloud whereas the sum of the squared error was zero. The squared error in this study was zero because the two created point clouds were identical. The method is visualized in Figure 6.

2.11 Translation

Once the transformation matrix was established, any given point on the 3D model of the planning implant could be transformed towards the postoperative location using Equation 6. Thus, the previously chosen implant landmarks; COR, pubic flange, ischial flange, and ilium flange on the planning, were transformed towards the post-operative position. Following the transformation of these points, the discrepancy between the planning and the post-operative position of the four points were calculated, described in millimeters (mm), Equation 7 and Figure 7. In case

Figure 7. *Translation direction vector for the COR, Pubic flange, Ischial flange and Iliac flange.*
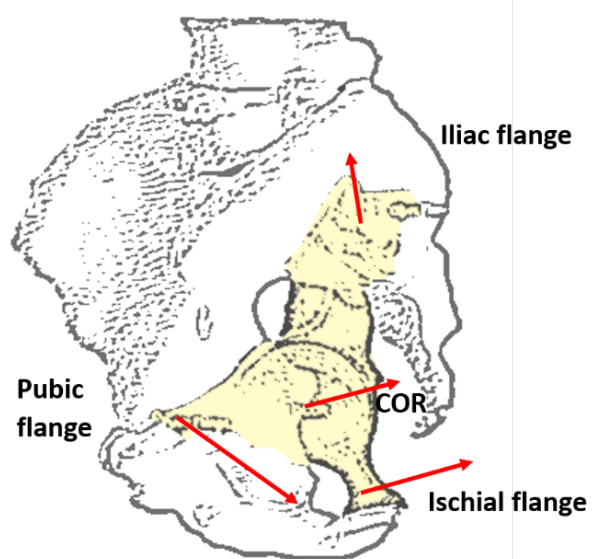
Figure 6. *Representation of point cloud transformation based on Singular Value*

$$Error = Rplan_i + t - post_i$$
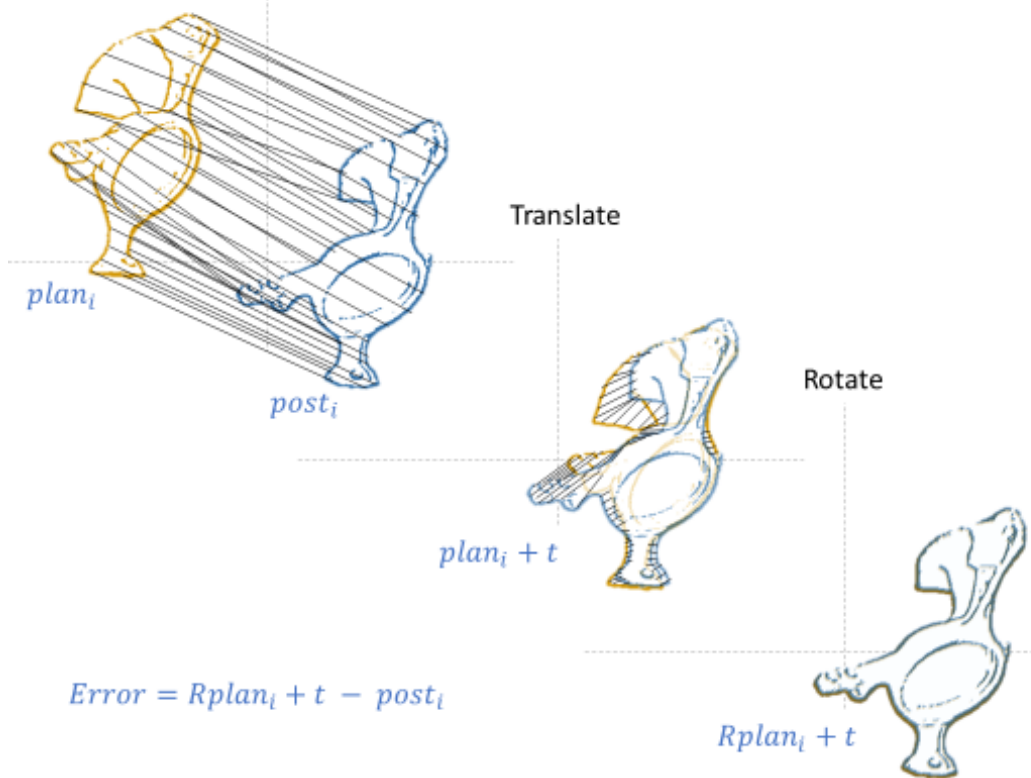
a flange did not exist on the implant, the missing flange was not included in the analysis.

$$\begin{bmatrix} x' \\ y' \\ z' \\ 1 \end{bmatrix} = \begin{bmatrix} r_{11} & r_{12} & r_{13} & p \\ r_{21} & r_{22} & r_{23} & q \\ r_{31} & r_{32} & r_{33} & r \\ 0 & 0 & 0 & 1 \end{bmatrix} * \begin{bmatrix} x \\ y \\ z \\ 1 \end{bmatrix} \qquad \text{Eq. 6}$$

Equation 6. *Mathematical representation of the transformation of a point (x,y,z) towards another point (x',y',z') in a three-dimensional space. This matrix represents rotations followed by a translation. r_{11} to r_{33} represent the rotation matrix, and p, q, r form a translation vector.*

$$\begin{bmatrix} x' \\ y' \\ z' \\ 1 \end{bmatrix} - \begin{bmatrix} x \\ y \\ z \\ 1 \end{bmatrix} = \begin{bmatrix} x' - x \\ y' - y \\ z' - z \\ 1 - 1 \end{bmatrix} \qquad \text{Eq. 7}$$

Equation 7. *Subtraction of two points with coordinates (x,y,z) and transformed coordinates (x',y',z').*

In an effort to determine the possible influence of implant migration on the results, as the time between surgery and follow-up surgery was variable. The relationship between the COR translation in mm and the time in days between surgery and follow-up imaging was plotted in a graph.

2.12 Rotation

In order to identify the rotation angle of the acetabular cup, a method was introduced based on the angle displacement between a planned and achieved vector. First, a vector was created between the planned COR and one acetabular rim landmark. In addition, a second vector was created between the achieved COR and the same acetabular rim landmark at the post-operative position, Figure 8a. The second step in this process was to project the created planned vector on to the post-operative acetabular plane, Figure 8a and Equation 8. The angle of rotation was represented as the angle between the two vectors, Figure 8b The angle was calculated by Equation 5. Thus, $\vec{n}$ represent the planned vector projected on the post-operative acetabular plane. $\vec{m}$ represent the

Figure 8. *Measurement of the angle cup rotation. a) Vector between COR and the acetabular rim landmark, for both the planned as for the achieved position. b) Planned vector projected on the post-operative acetabular plane, from which the angle rotation is calculated in degrees (α).*

Planned implant   Postop implant

Postop implant
with projected
planned vector
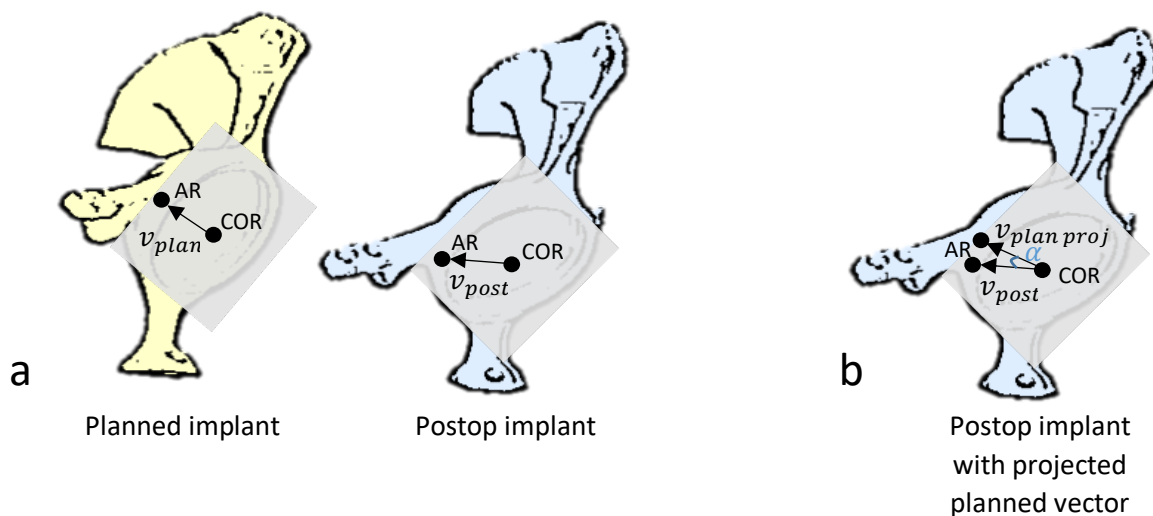
post-operative vector on the post-operative acetabular plane.

$$Proj_{planned\ vector} = \frac{\overrightarrow{n_{post}}X\left(\overrightarrow{n_{post}}X\overrightarrow{v_{plan}}\right)}{\left|\overrightarrow{n_{post}}\right|^2} \qquad \text{Eq. 8}$$

Equation 8. *Mathematical representation of the projection of the planned vector onto the post-operative acetabular plane. $\overrightarrow{n_{post}}$ represent the post-operative acetabular plane and $\overrightarrow{v_{plan}}$ represent the planned vector between the COR and the point on the acetabular rim.*

2.13 Statistical methods

Data management and statistical analysis were performed using SPSS (Statistics 25, IBM). Descriptive statistics were used to present quantitative data. Continuous variables were reported as mean, mean absolute value (MA, described as the absolute values of the mean) and standard deviation (SD) in case of normally distributed data, and as median absolute value and percentiles in case of not normally distributed data. Categorical variables were expressed as the number of cases or percentage. Components were labelled as adequately positioned when the achieved CTAC is within 10 degrees from the planned orientation (20, 21). The comparison between the planned position and the achieved position was performed using the paired t-test. Secondary outcomes were calculated using a non-parametric Mann-Whitney U test. 95% confidence intervals (CI) were extracted using the paired t-test and the one-sample t-test. Significance levels were set at a p-value of < 0.05.

3. Results

During the inclusion period, 103 patients (104 implants) received a CTAC, of which 34 patients (35 implants) met the inclusion criteria. A total of 69 patients were excluded: 62 due to unavailability of the post-operative (PET)-CTs, 3 due to a missing acetabular component in the CTAC design, 3 due to not giving informed consent and 1 patient was excluded due to the limited quality of the post-operative imaging. These included patients underwent acetabular THA revision or tumor resection surgery with a custom-made acetabular implant (OSSIS Limited, Christchurch, New Zealand), between February 2017 and March 2021,

at several hospitals in Australia (Sydney, Brisbane and Perth). The average age at the time of surgery was 49 years (range 16-78). 21 (60%) males and 14 (40%) females were included in the study. 27 patients received surgery due to tumor indication and 8 patients were included due to THA revision surgery. 2 of the revised patients were classified as Paprosky type IIIA and 6 as Paprosky type IIIB, with 3 of 8 patients encountering pelvic discontinuity. Tumor patients were classified by the zone of resection (Enneking Type I, II, III, IV). 5 cases had incomplete patient data. Individual patient and cohort characteristics are reported in Tables 1 and 2

Table 1. Individual patient Characteristics

Case	Age	Gender	Primary diagnosis	If THA revision; Paprosky classification, pelvic discontinuity	If Tumor; Enneking resection Type	Side	Surgical Approach	Device	Navigation
1	57	Male	Tumor	NA	type II	Left	iliofemoral	Hemipelvis	No
2	58	Male	Tumor	NA	type I-II	Left	iliofemoral	Hemipelvis	No
3	34	Male	Tumor	NA	type I-II	Right	iliofemoral	Hemipelvis	No
4	41	Female	Tumor	NA	type II	Right	iliofemoral	Hemipelvis	No
5	16	Female	Tumor	NA	type I-II	Right	iliofemoral	Hemipelvis	No
6	22	Female	THA Revision	3B, No	NA	Right	Anterolateral	AceOs Plus	No
7	71	Male	Tumor	NA	type II - III	Left	iliofemoral	Hemipelvis	No
8	78	Male	THA Revision	3A, No	NA	Left	Anterolateral	AceOs Plus	No
9	44	Male	Tumor	NA	type I-II -III	Right	iliofemoral	Hemipelvis	No
10	65	Male	Tumor	NA	type II	Right	iliofemoral	Hemipelvis	No
11	51	Male	Tumor	NA	type II	Right	iliofemoral	Hemipelvis	No
12	68	Female	Tumor	NA	type II	Left	iliofemoral	Hemipelvis	No
13	70	Male	Tumor	NA	type II	Right	iliofemoral	Hemipelvis	No
14	39	Male	Tumor	NA	type II	Right	iliofemoral	Hemipelvis	No
15	29	Male	Tumor	NA	type II- III	Left	iliofemoral	Hemipelvis	No
16	43	Female	Tumor	NA	type II	Left	iliofemoral	Hemipelvis	No
17	31	Female	Tumor	NA	type I-II	Left	iliofemoral	Hemipelvis	No
18	66	Female	THA Revision	3B, Yes	NA	Left	posterior	AceOs	No
19	63	Male	Tumor	NA	type II- III	Right	iliofemoral	Hemipelvis	Yes
20	69	Female	Tumor	NA	type II- III	Left	iliofemoral	Hemipelvis	Yes
21	33	Male	Tumor	NA	type II	Right	anterolateral	Hemipelvis	Yes
22	56	Female	THA Revision	3B, No	NA	Left	Posterior	AceOs	Yes
23	49	Female	Tumor	NA	type II- III	Left	iliofemoral	Hemipelvis	Yes
24	57	Male	THA Revision	3A, No	NA	Left	posterior	AceOs Plus	Yes
25	71	Female	THA Revision	3B, Yes	NA	Left	posterior	AceOs Plus	Yes
26	73	Female	THA Revision	3B, No	NA	Right	posterior	AceOs	No
27	*	Male	Tumor	NA	type I-II	Right	iliofemoral	*	Yes
28	21	Male	Tumor	NA	type I-II	Left	iliofemoral	Hemipelvis	Yes
29	69	Male	Tumor	NA	type I-II -III	Left	iliofemoral	Hemipelvis	Yes
30	*	Female	Tumor	NA	type I-II	Right	iliofemoral	*	Yes
31	18	Male	Tumor	NA	type I-II	Right	iliofemoral	Hemipelvis	Yes
32	22	Male	Tumor	NA	type I-II	Left	iliofemoral	Hemipelvis	Yes
33	*	Male	Tumor	NA	type I-II	Right	Posterolateral Extended	*	No
34	*	Male	Tumor	NA	type II -III	Left	Anterolateral	*	No
35	*	Female	THA Revision	3B, Yes	NA	Right	Posterior	*	No

NA = not applicable

* = unknown

Table 2. Summary of patient characteristics

		Mean	Range
Age [years]		49	16 to 78
		N	Percentage
Gender	Male	21	60%
	Female	14	40%
Anatomical Position	Right	17	49%
	Left	18	51%
Device type	Hemipelvis	23	66%
	AceOS	3	9%
	AceOS plus	4	11%
	unkown	5	14%
Indication	Tumor	27	77%
	Revision	8	23%
If THA revision, Paproksy classification	3A	2 of 8	25%
	3B	6 of 8	75%
Pelvic discontinuity	Yes	3 of 8	38%
	No	5 of 8	62%
If tumor, Enneking classification	type I-II	10 of 27	37%
	type II	9 of 27	33%
	type II - III	6 of 27	22%
	type I-II -III	2 of 27	8%
Navigation	Yes	13	37%
	No	22	63%

3.1 Individual outcomes

The planned and achieved inclination and anteversion for each case is presented in Table 3. In addition, the individual difference between the planned and achieved inclination, anteversion and rotation was described in the same table. Using a 10° benchmark for defining correct positioning, 34 (97%) components were positioned within 10° of the planned inclination. Another 33 (94%) components were positioned within 10° of the planned anteversion. 33 (94%) components were not rotated by more than 10° compared to the planning. In total, 31 (89%) components were positioned within 10° from the planned inclination, anteversion and rotation. From this data, we can see that one case (case 18) was malpositioned from the planned anteversion and rotation, respectively; -12.2° and 10.7°. Closer inspection of

the individual translation table in Appendix E – Individual translation data, revealed differences between patient cases. In contrast to case 18, case 2 showed a larger translation of the COR (9.8 mm) without any large rotations. Case 5 showed a larger anteversion (29,6°) and translation (COR translation vector 44,1 mm) than planned. The visualization of the planned and achieved implant position of case 18, case 2 and case 5 can be seen in Figure 9.

Table 3. Individual inclination (INCL), anteversion (AV) and cup rotation

	INCL (°)			AV (°)			Rotation (°)
Case	Planned	Postop	Δ°	Planned	Postop	Δ°	Δ°
1	40,8	42,8	2,0	25,4	24,1	-1,3	1,0
2	45,9	46,5	0,6	25,9	23,1	-2,8	1,9
3	42,2	37,9	-4,3	18,6	23,1	4,6	-0,2
4	45,3	43,7	-1,6	34,2	32,4	-1,8	0,1
5	49,4	53,3	3,9	4,2	33,8	29,6	1,4
6	38,3	36,4	-1,9	21,6	19,9	-1,8	2,2
7	48,4	50,1	1,7	17,9	18,0	0,0	0,6
8	39,2	34,5	-4,8	23,9	27,4	3,5	10,5
9	43,0	39,7	-3,4	17,5	13,0	-4,5	-1,1
10	38,1	42,4	4,3	17,6	22,1	4,5	2,2
11	36,7	37,4	0,8	15,1	14,9	-0,2	0,4
12	43,5	43,7	0,2	23,6	23,6	0,0	1,8
13	41,5	40,0	-1,5	18,4	24,9	6,5	0,1
14	41,8	38,7	-3,1	16,4	18,4	1,9	4,2
15	41,3	39,4	-2,0	13,4	13,2	-0,2	2,0
16	40,1	48,8	8,7	16,6	20,3	3,6	-0,9
17	41,5	42,4	0,9	19,0	26,0	7,1	1,3
18	47,6	56,1	8,5	23,2	11,0	-12,2	10,7
19	40,8	38,2	-2,6	22,1	24,9	2,8	0,1
20	44,5	43,3	-1,2	23,3	21,4	-1,9	-0,2
21	40,1	39,9	-0,2	24,4	25,2	0,8	-0,1
22	47,9	46,0	-1,8	32,6	35,5	2,9	-4,7
23	39,1	36,2	-2,8	24,3	28,6	4,3	-1,5
24	40,0	44,9	4,8	21,6	23,3	1,7	-1,3
25	40,8	38,9	-1,9	16,9	14,9	-2,0	1,5
26	27,6	41,8	14,2	16,3	11,7	-4,6	-2,5
27	44,5	44,7	0,2	11,7	11,8	0,1	-0,5
28	46,7	47,8	1,2	16,8	14,7	-2,1	-1,6
29	35,2	36,2	1,0	13,6	16,5	2,9	1,4
30	44,8	45,2	0,4	22,1	23,5	1,4	-0,8
31	43,3	43,4	0,1	22,7	24,7	2,1	-1,7
32	49,6	45,9	-3,6	12,9	11,8	-1,1	-2,5
33	45,4	44,6	-0,9	27,7	30,7	3,1	1,9
34	36,5	37,9	1,4	15,3	13,8	-1,5	-6,1
35	38,6	40,0	1,3	9,8	6,2	-3,7	0,9

Universiteit Leiden TUDelft Delft University of Technology Erasmus ERASMUS UNIVERSITEIT ROTTERDAM

Figure 9. *Visualization of implant placement for case 18, case 2, and case 5. Yellow = planned, blue = achieved*

Case 18   Case 2   Case 5
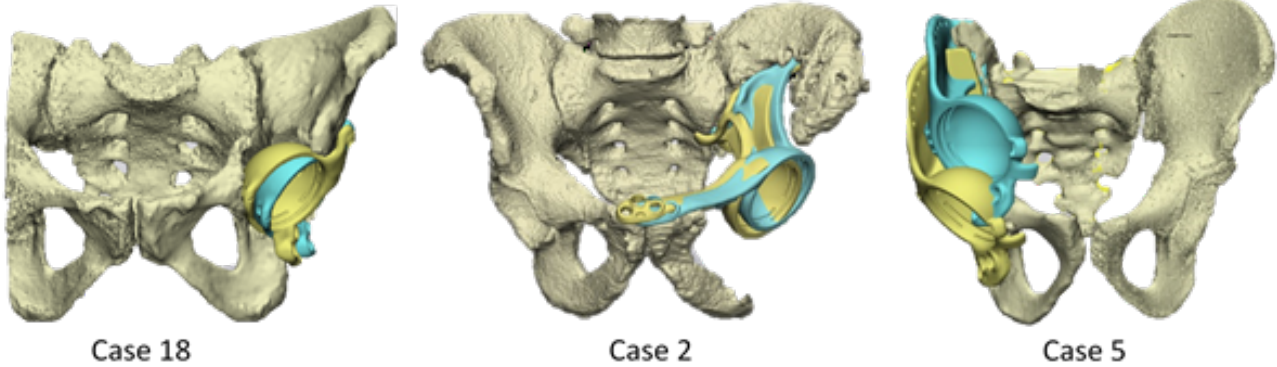
Primary outcomes

As shown in Table 4 and Table 5, the mean difference, between planned and achieved, was not significant. The mean inclination was 0.5° (Mean absolute (MA): 2.7°; standard deviation (SD): 3.9°, 95% confidence interval (CI): -0.8°, 1.9°). Whereas the planned anteversion showed a mean difference of 1.2° (MA: 3.6°; SD: 6.1°, 95% CI: -0.9°, 3.3°). The mean deviation of cup rotation from planned was 0.6° (MA: 2.1°; SD: 3.2°, 95% CI: -0.5°, 1.7°). The mean translation between the planned and achieved COR was -0.8 mm (MA: 2.4; SD: 3.2, 95% CI: -1.9, 0.4) in the sagittal plane, -0.4 mm (MA: 3.8; SD: 6.3, 95% CI: -2.6, 1.8) in the coronal plane and 0.6mm (MA: 2.8; SD: 6.1, 95% CI: -1.6, 2.7) in the axial plane. Figure 10 represents the planned and achieved position of case 4, which was described as an accurate placement and similar to the average. Figure 11 shows the average translation direction vectors of the COR, pubic flange, ischial flange and iliac flange.

Figure 10. *Visualization of implant placement for case 4. Yellow = planned, blue = achieved*
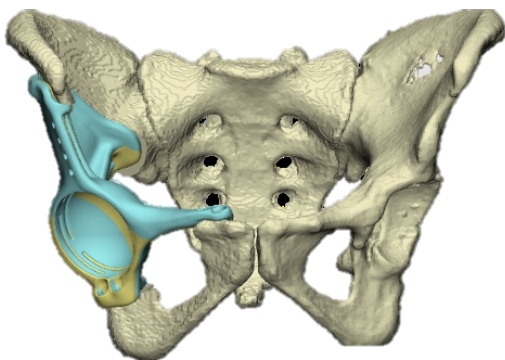
Table 4. Summary of primary outcomes

		Mean	Mean of ABS*	SD Mean
INCL	Plan (°)	42,0	-	4,4
	Post (°)	42,5	-	4,9
	Δ (°)	0,5	2,7	3,9
AV	Plan (°)	19,6	-	6,0
	Post (°)	20,8	-	7,0
	Δ (°)	1,2	3,6	6,1
Δ Rotation (°)		0,6	2,1	3,2
Δ COR	Sa [mm]	-0,8	2,4	3,2
	Co [mm]	-0,4	3,8	6,3
	Ax [mm]	0,6	2,8	6,1
Δ COR Vector		-	5,9	7,2
Δ Pubic Flange	Sa [mm]	-0,1	3,4	4,8
	Co [mm]	-0,6	3,1	5,7
	Ax [mm]	0,8	3,1	7,4
Δ Pubic Flange Vector		-	6,4	8,4
Δ Ischial Flange	Sa [mm]	-1,1	2,5	3,1
	Co [mm]	-1,1	4,8	8,6
	Ax [mm]	0,7	3,2	6,0
Δ Ischial Flange Vector		-	7,0	8,7
Δ Ilium Flange	Sa [mm]	-1,3	2,6	3,2
	Co [mm]	0,2	2,3	3,1
	Ax [mm]	-0,3	3,0	3,9
Δ Ilium Flange Vector		-	5,3	3,0

Δ : difference; Plan : planned; Post : postoperative; INCL : inclination, AV : anteversion; COR : centre of rotation; Sa : Sagittal; Co : Coronal; Ax : Axial; Mean of ABS : mean of absolute values

Legend

Rotation:	Frontal +, Dorsal -
Sagittal:	Medial +, Lateral -
Coronal:	Dorsal +, Frontal -
Axial:	Cranial +, Caudal -

Figure 11. *Visualization of the average translation direction vectors for the COR, public flange, ischial flange and ilium flange. Each red vector represent an average translation vector and it's direction. All vectors are 10 times magnified.*
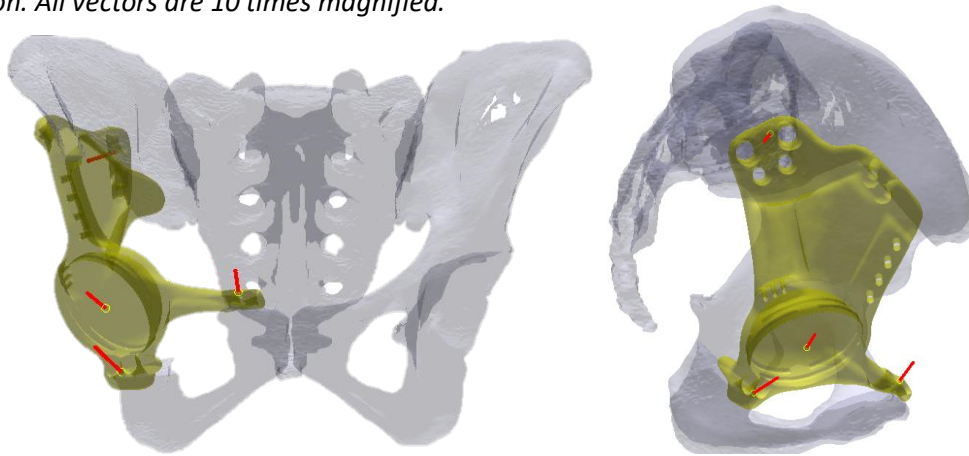
As component rotation in tri-flanged components affects the position of screw holes and consequently may affect implant fixation, the mean translation per flange is described in Table 4. Translation of the ischial flange showed the largest deviation (MA 7.0 mm), followed by the pubic flange (MA 6.4 mm) and the ilium flange (MA 5.3 mm). Individual translation vectors were presented in Appendix I – Individual accuracy data.

In an effort to determine the influence of implant migration on the results, the relationship between the COR translation and the time between surgery and follow-up imaging was visualized, see Appendix F – migration graph. No relationship was seen between longer follow-up imaging duration and larger COR deviations.

3.3 Secondary outcomes

This study showed no significant influence on the use of navigation or the size of the implant, median respectively; navigation (yes vs no): 1,2° vs 2,0° (inclination), 2,0° vs 3,3° (anteversion), 1,4° vs 1,6° (rotation) and 3,3 mm vs 4,6 mm (COR vector); implant size (small vs large): 1,9° vs 1,4° (inclination), 3,0° vs 2,1° (anteversion), 1,5° vs 1,3° (rotation) and 3,9 mm vs 4,3 mm (COR vector). The accuracy of positioning between tumor indications and revision indications showed a significant difference in favor of tumor indications; (tumor vs THA revision) 1.5° vs 3.4° (inclination), 2.1° vs 3.2° (anteversion), 1.3° vs 2.4° (rotation) and 4.0 mm vs 4.6 mm (COR vector). The sub-group statistics are shown in Table 6.

Table 5. Primary outcomes

		N	Mean	Std. Deviation	Std. Error Mean	95% CI		p-value*
						Lower	Upper	
Planning vs Post-operative	Δ Inclination (°)	35	0,5	3,9	0,7	-0,8	1,9	0,43
	Δ Anteversion (°)	35	1,2	6,2	1,0	-0,9	3,3	0,26
	Δ Rotation (°)	35	0,6	3,2	0,5	-0,5	1,7	0,19
	Δ COR sagittal [mm]	35	-0,8	3,3	0,6	-1,9	0,4	0,16
	Δ COR coronal [mm]	35	-0,4	6,4	1,1	-2,6	1,8	0,70
	Δ COR axial [mm]	35	0,6	6,2	1,0	-1,6	2,7	0,60

* Paired t-test

Table 6. Secondary outcomes

			N	Median of ABS*	Percentiles 25th	Percentiles 75th	p-value**
Navigation vs Non-Navigation	Δ Inclination (°)	Yes	13	1,2	0,4	2,6	0,34
		No	22	2,0	1,3	4,3	
	Δ Anteversion (°)	Yes	13	2,0	1,4	2,8	0,15
		No	22	3,3	1,5	4,6	
	Δ Rotation (°)	Yes	13	1,4	0,5	1,6	0,12
		No	22	1,6	0,9	2,2	
	Δ COR vector [mm]	Yes	13	3,3	2,0	6,1	0,13
		No	22	4,6	2,8	8,3	
Small vs Large implant*	Δ Inclination (°)	Small	18	1,9	1,3	4,8	0,12
		Large	17	1,4	0,8	2,6	
	Δ Anteversion (°)	Small	18	3,0	1,8	4,3	0,26
		Large	17	2,1	1,3	2,9	
	Δ Rotation (°)	Small	18	1,5	0,9	2,5	0,54
		Large	17	1,3	0,6	1,9	
	Δ COR vector [mm]	Small	18	3,9	2,4	6,1	0,44
		Large	17	4,3	3,0	6,9	
Tumor vs Revision	Δ Inclination (°)	Tumor	27	1,5	0,9	3,0	0,02
		THA Revision	8	3,4	1,9	6,7	
	Δ Anteversion (°)	Tumor	27	2,1	1,2	4,0	0,22
		THA Revision	8	3,2	1,9	4,2	
	Δ Rotation (°)	Tumor	27	1,3	0,5	1,9	0,02
		THA Revision	8	2,4	1.4	7,6	
	Δ COR vector [mm]	Tumor	27	4,0	2,6	6,8	0,99
		THA Revision	8	4,6	2,5	6,0	

* Median of ABS = median of absolute values

** Mann-Whitney U test

*** Groups based on surface size. Cut-off point was set at the median surface size

4. Discussion

This study was designed to determine the accuracy of placing CTACs in patients undergoing THA revision or pelvic tumor reconstruction surgery. Overall, the observed planned and achieved implant positions were in good agreement for inclination, anteversion, rotation and COR translation, where the measured mean difference was respectively; 0.5° (SD: 3,9°), 1.2° (SD: 6,2°), 0.6° (SD: 3,2°), and 5,9 mm for COR translation (SD: 7,2 mm). With a 10° offset set as benchmark for malposition, 34 (97%) of the components were positioned within 10° of the planned inclination, 33 (94%) were positioned within 10° of the planned anteversion and 33 (94%) components were not rotated by more than 10°. In total, 31 (89%) components were positioned within 10° from the planned inclination, anteversion and rotation. Focusing on the translation of the implant, the ischial flange showed the largest translation, followed by the pubic flange and the ilium flange.

Secondary outcomes reported higher deviations in cup angles and translation for non-navigation cases. However this was not significant, possibly due to the limited cohort size. Notwithstanding the relative limited sample, the findings suggest that implant positioning in THA revision cases was less accurate in comparison to the tumor resection cases. Furthermore, implant size had limited effect on the deviations in cup angle and translation of the implant.

The results of this study were in line with those of previous studies. Zampelis et al. (2021) reported an accurate placement of inclination, anteversion, rotation and the COR; respectively 3,6° (inclination), -2,8° (anteversion), -1,2° (rotation)

and a COR median translation of -0,5 mm, -0,6mm and 1,1 mm in three different planes (23). Whereas, Baauw et al. (2015) reported a median inclination difference of 2° and an anteversion difference of 5° (20). Previous studies reporting the accuracy of the positioning of CTACs using 3D analysis techniques are sparse and all focused on THA revision surgery.

To the best of our knowledge, this is the largest study in which 3D data that was acquired for the pre-operative planning of a CTAC has been compared with CT data on the post-operative position. Assessment of the 3D position of CTACs was achieved by developing a semi-automatic analysis method. Therefore, this method is almost insensitive to incorrect anatomical landmark positioning and measurement errors.

The findings may be limited by a few analysis uncertainties. Metal artefacts in (PET)-CT acquisition and implant adaptative manufacturing errors may influence the precision of the obtained pre-operative or post-operative DICOM, and may have caused segmentation errors. Another source of uncertainty was the variability in post-operative imaging follow-up time. Besides the measured surgeon's placement accuracy, the possible migration of the implant could have influenced the outcomes. No relationship was found between longer follow-up imaging duration and larger deviations, suggesting that the factor migration did not play a major role. No migration analysis was performed. Another possible limitation of this study is that no reversed engineering of the implant was executed.

Furthermore, as the patient's anatomy and DICOM data differed in asperity, manual segmentation and registration of the STL models may have resulted in random measurement errors. Although, these errors are expected to have a limited impact on the results, an inter- and intra-observer reliability study would be needed to analyze the accuracy of this semi-automatic measurement technique.

Manual anatomical landmark selection could have affected the individual inclination and anteversion. However, this did not influence our study outcomes, as this study uses one landmark reference plane for both the planned and achieved implant position. Last, although this is the largest cohort to study 3D positioning of a CTAC, the cohort size is limited.

Traditionally, the orientation of an acetabular implant can be described by its anteversion and inclination. However, as component rotation in tri-flanged components affects the position of screw holes, it consequently may affect implant fixation. Therefore, implant positioning was described in six degrees of freedom in this study; inclination, anteversion, component rotation, and COR/flange translation in 3 planes. The relevance of small degrees of component rotation and flange translation displacement is yet undetermined. Although, the relevance most likely depends on individual component design and patient anatomy, measurements in six degrees of freedom should be considered in future CTAC studies.

The patient's records were consulted in case of mispositioning of the implant. For case 18, it stated that more bone loss was found during surgery than observed on the pre-operative CT, from which the implant was designed. Second, navigation was unexpectedly unavailable during the surgery of case 18, interrupting the surgeon's normal. Patient's surgery records of cases 2 and 5 were not available.

In this study, the largest flange displacement was found for the ischial and pubic flange. A possible explanation for this is that the pubic and ischial bone may experience extra movement compared to the iliac bone, due to greater mobility of the pubic symphysis relative to the sacroiliac joint. As a result, displacement of the ischial and pubic bone might occur during surgery, rather than inaccurate implant positioning. Further research should be undertaken to investigate pelvic bone displacement during pelvic resections where the pelvic ring is interrupted. Another possible explanation is that it is caused by the narrow visibility during surgery. The ischial flange is usually the most difficult flange to adequately position due

Universiteit Leiden

TUDelft Delft University of Technology

Erasmus
ERASMUS UNIVERSITEIT ROTTERDAM

to the deep position and large enclosing soft tissue component.

Larger accuracy deviations were found for THA revision patients compared to the tumor resection group. This result may partly be explained by the decreased image quality due to metal artefacts in the pre-operative CT image of the revised implant. Difficulties that arise following the pre-operative planning, and press fitting of the custom component, occur when intra-operative acetabular defects differ from those seen on the pre-operative imaging. In addition, limited bone quality due to previous THA and revisions may complicate the surgery. Whereas, during tumor resection, wide surgical margins and intact bone may facilitate the procedure of implant positioning.

The indication for receiving a custom-made acetabular component were major acetabular defects or large tumor resections. The studied cohort was defined as high complexity cases (Paprosky types 3A/B). Therefore, the results in this study may be compared with other implant studies due to the use of the Paproksy classification. However, the Paproksy classification of types 3A and 3B does not differentiate between these major defects, where off-the-shelf implant techniques are insufficient, and minor 3A and 3B defects where off-the-shelf implants are sufficient. We have to debate whether the Paprosky classification is sufficient for staging these major defects.

This research assessed, in six degrees of freedom, the accuracy of the planned versus achieved implant placement in THA revision and tumor reconstruction surgery. Malposition of the implant compared to the planned position does not imply the patient will experience a poor clinical outcome. A natural progression of this work is to analyze the clinical outcomes belonging to the CTAC (mal)position. The association between the (mal)position of an implant, implant migration patterns and the long-term follow-up and survival of an implant, is a valuable area for future research.

5. Conclusion

To our knowledge, this is the largest 3D positioning study assessing CTACs. A semi-automatic method to analyze the accuracy of positioning CTACs in THA revision and tumor patients was presented in this study. The achieved implant position showed good agreement to the pre-operative planned position. 89% of the components in this study were accurately positioned according to our criteria.

References

1.   De Martino I, Strigelli V, Cacciola G, Gu A, Bostrom MP, Sculco PK. Survivorship and Clinical Outcomes of Custom Triflange Acetabular Components in Revision Total Hip Arthroplasty: A Systematic Review. The Journal of Arthroplasty. 2019;34(10):2511-8.
2.   Di Laura A, Henckel J, Wescott R, Hothi H, Hart AJ. The effect of metal artefact on the design of custom 3D printed acetabular implants. 3D Printing in Medicine. 2020;6(1).
3.   Issack PS, Nousiainen M, Beksac B, Helfet DL, Sculco TP, Buly RL. Acetabular component revision in total hip arthroplasty. Part II: management of major bone loss and pelvic discontinuity. Am J Orthop (Belle Mead NJ). 2009;38(11):550-6.
4.   Telleria JJM, Gee AO. Classifications In Brief: Paprosky Classification of Acetabular Bone Loss. Clinical Orthopaedics and Related Research®. 2013;471(11):3725-30.
5.   Paprosky WG, Perona PG, Lawrence JM. Acetabular defect classification and surgical reconstruction in revision arthroplasty. The Journal of Arthroplasty. 1994;9(1):33-44.
6.   Enneking WF, Spanier SS, Goodman MA. A system for the surgical staging of musculoskeletal sarcoma. Clin Orthop Relat Res. 1980(153):106-20.
7.   Barlow BT, Oi KK, Lee YY, Carli AV, Choi DS, Bostrom MP. Outcomes of Custom Flange Acetabular Components in Revision Total Hip Arthroplasty and Predictors of Failure. J Arthroplasty. 2016;31(5):1057-64.

8.	Wilson RJ, Freeman TH, Jr., Halpern JL, Schwartz HS, Holt GE. Surgical Outcomes After Limb-Sparing Resection and Reconstruction for Pelvic Sarcoma: A Systematic Review. JBJS Reviews. 2018;6(4).

9.	Woo S-H, Sung M-J, Park K-S, Yoon T-R. Three-dimensional-printing Technology in Hip and Pelvic Surgery: Current Landscape. Hip & Pelvis. 2020;32(1):1.

10.	Abolghasemian M, Tangsataporn S, Sternheim A, Backstein D, Safir O, Gross AE. Combined trabecular metal acetabular shell and augment for acetabular revision with substantial bone loss: a mid-term review. Bone Joint J. 2013;95-b(2):166-72.

11.	Banerjee S, Issa K, Kapadia BH, Pivec R, Khanuja HS, Mont MA. Systematic review on outcomes of acetabular revisions with highly-porous metals. Int Orthop. 2014;38(4):689-702.

12.	Beckmann NA, Weiss S, Klotz MC, Gondan M, Jaeger S, Bitsch RG. Loosening after acetabular revision: comparison of trabecular metal and reinforcement rings. A systematic review. J Arthroplasty. 2014;29(1):229-35.

13.	Sculco PK, Ledford CK, Hanssen AD, Abdel MP, Lewallen DG. The Evolution of the Cup-Cage Technique for Major Acetabular Defects: Full and Half Cup-Cage Reconstruction. J Bone Joint Surg Am. 2017;99(13):1104-10.

14.	Berry DJ. Antiprotrusio cages for acetabular revision. Clin Orthop Relat Res. 2004(420):106-12.

15.	Berasi CC, Berend KR, Adams JB, Ruh EL, Lombardi AV. Are Custom Triflange Acetabular Components Effective for Reconstruction of Catastrophic Bone Loss? Clinical Orthopaedics and Related Research®. 2015;473(2):528-35.

16.	Lewinnek GE, Lewis JL, Tarr R, Compere CL, Zimmerman JR. Dislocations after total hip-replacement arthroplasties. J Bone Joint Surg Am. 1978;60(2):217-20.

17.	Murray D. The definition and measurement of acetabular orientation. The Journal of Bone and Joint Surgery British volume. 1993;75-B(2):228-32.

18.	Grant AD, Sala DA, Schwarzkopf R. Femoro-acetabular impingement: the diagnosis—a review. Journal of Children's Orthopaedics. 2012;6(1):1-12.

19.	Higa M, Tanino H, Abo M, Kakunai S, Banks SA. Effect of acetabular component anteversion on dislocation mechanisms in total hip arthroplasty. J Biomech. 2011;44(9):1810-3.

20.	Baauw M, van Hellemondt GG, van Hooff ML, Spruit M. The accuracy of positioning of a custom-made implant within a large acetabular defect at revision arthroplasty of the hip. Bone Joint J. 2015;97-b(6):780-5.

21.	Weber M, Witzmann L, Wieding J, Grifka J, Renkawitz T, Craiovan B. Customized implants for acetabular Paprosky III defects may be positioned with high accuracy in revision hip arthroplasty. International Orthopaedics. 2019;43(10):2235-43.

22.	Durand-Hill M, Henckel J, Di Laura A, Hart AJ. Can custom 3D printed implants successfully reconstruct massive acetabular defects? A 3D-CT assessment. Journal of Orthopaedic Research. 2020.

23.	Zampelis V, Flivik G. Custom-made 3D-printed cup-cage implants for complex acetabular revisions: evaluation of pre-planned versus achieved positioning and 1-year migration data in 10 patients. Acta Orthopaedica. 2021;92(1):23-8.

24.	Zhang J, Yan CH, Chui CK, Ong SH. Fast segmentation of bone in CT images using 3D adaptive thresholding. Computers in Biology and Medicine. 2010;40(2):231-6.

25.	Wu G, Siegler S, Allard P, Kirtley C, Leardini A, Rosenbaum D, et al. ISB recommendation on definitions of joint coordinate system of various joints for the reporting of human joint motion—part I: ankle, hip, and spine. Journal of Biomechanics. 2002;35(4):543-8.

26.	Wang RY, Xu WH, Kong XC, Yang L, Yang SH. Measurement of acetabular inclination and anteversion via CT generated 3D pelvic model. BMC Musculoskeletal Disorders. 2017;18(1).

27.	Babisch JW, Layher F, Amiot L-P. The Rationale for Tilt-Adjusted Acetabular Cup Navigation. JBJS. 2008;90(2).

28.	Challis JH. A procedure for determining rigid body transformation parameters. Journal of Biomechanics. 1995;28(6):733-7.

29.	Söderkvist I, Wedin PA. Determining the movements of the skeleton using well-configured markers. J Biomech. 1993;26(12):1473-7.

Acknowledgements

I would like to express my sincere appreciation to the supervisors for their support and efforts throughout this project. Demien, thank you for your endless enthusiasm, critical clinical perception and for suggesting and organizing this project. I enjoyed learning from you and I appreciated my clinical days in the hospital together. I look forward to continuing working together on the article and hopefully soon drink a beer on a terrace to celebrate the acceptance for publication. Bart, I want to thank you for your passion and infinite ideas, your technical knowledge throughout this project, and for always being available for questions without seeing each other in real life for more than a year. You taught me to ask for help in time and set boundaries during my project. Prof Nelissen, thank you for your excitement and interest in this project. I'm very happy that I had to opportunity to be part of the department for a long period.

Furthermore, I want to thank Sascha for his hard work and patience throughout the project. You got a lot of extra work when we came to the conclusion that it was not possible for me to go to Sydney and get the patient data myself. Without you, it was not possible to run this project. Thank you Bethany and Natalie for the dedication, good ideas, and fast communication. Without you both, we were not able to include so many patients in the study.

At last, I would like to thank my friends and family for their ongoing support throughout this period.

Appendices

Detailed search strategy Pubmed;

1. ("Arthroplasty, Replacement, Hip"[Mesh] OR "Hip Prosthesis Implantation"[tw] OR "Hip Prosthesis Implantations"[tw] OR "Hip Replacement Arthroplasty"[tw] OR "Hip Replacement Arthroplasties"[tw] OR "Hip Arthroplasty"[tw] OR "Hip Arthroplasties"[tw] OR "Hip Prosthesis"[Mesh] OR "Hip Prosthesis"[tw] OR "Hip Prostheses"[tw] OR "hip surgery"[tw] OR "Hip/surgery"[mesh] OR "Total Hip"[tw] OR "Total Hip Replacements"[tw] OR "Total Hip Replacement"[tw] OR "THA"[tw] OR "THR"[tw] OR (("Arthroplasty"[Mesh] OR "Prosthesis"[tw] OR "Prostheses"[tw] OR "Replacement"[tw] OR "reconstruction"[tw] OR reconstruct*[tw] OR "triflange"[tw] OR triflang*[tw]) AND ("Hip"[tw] OR "Hips"[tw]))) AND ("revision"[tw] OR revisi*[tw] OR reviz*[tw] OR "Reoperation"[Mesh] OR "Reoperation"[tw] OR "Reoperation"[tw] OR Reoperat*[tw] OR "Re-operation"[tw] OR Re-operat*[tw] OR "Prosthesis Failure"[mesh] OR "Arthroplasty, Replacement, Hip/adverse effects"[Mesh] OR "Hip Prosthesis/adverse effects"[Mesh] OR "failure"[tw] OR failure*[tw] OR "failed"[tw] OR "AAOS "[tw] OR "acetabular defect"[tw] OR "acetabular defects"[tw] OR "acetabular deficiency"[tw] OR "acetabular deficiencies"[tw] OR "acetabulum defect"[tw] OR "acetabulum defects"[tw] OR "acetabulum deficiency"[tw] OR "acetabulum deficiencies"[tw] OR "Paprosky"[tw] OR Paprosky*[tw] OR "Bone Defects"[tw] OR "bone defect"[tw] OR "pelvic defect"[tw] OR "pelvic defects"[tw] OR "pelvis defect"[tw] OR "pelvis defects"[tw] OR "bone loss"[tw] OR "Osteolysis"[mesh] OR "Osteolysis"[tw])

2. ("custom"[tw] OR "custom-made"[tw] OR "custommade"[tw] OR custom-mad*[tw] OR custommad*[tw] OR "customized"[tw] OR "customised"[tw] OR "custom design"[tw] OR custom design*[tw] OR "customization"[tw] OR "customisation"[tw] OR "custom triflange"[tw] OR "personalized"[tw] OR "personalised"[tw] OR "patient specific"[tw] OR patientspecif*[tw] OR "Precision Medicine"[Mesh] OR "ossis"[tw] OR "implant cast"[tiab] OR "implantcast"[tiab] OR "materialise"[tiab])

3. ("Acetabulum"[Mesh] OR "Acetabulum"[tw] OR acetabul*[tw] OR "acetabular"[tw] OR acetabular*[tw] OR "acetabular component"[tw] OR "acetabular components"[tw]))

OR

1. ("Arthroplasty, Replacement, Hip"[mesh] OR "Hip Prosthesis Implantation"[tw] OR "Hip Prosthesis Implantations"[tw] OR "Hip Replacement Arthroplasty"[tw] OR "Hip Replacement Arthroplasties"[tw] OR "Hip Arthroplasty"[tw] OR "Hip Arthroplasties"[tw] OR "Hip Prosthesis"[mesh] OR "Hip Prosthesis"[tw] OR "Hip Prostheses"[tw] OR "Total Hip"[tw] OR "Total Hip Replacements"[tw] OR "Total Hip Replacement"[tw] OR "THA"[tw] OR "THR"[tw] OR (("Arthroplasty"[mesh] OR "Prosthesis"[tw] OR "Prostheses"[tw] OR "Replacement"[tw] OR "reconstruction"[tw] OR reconstruct*[tw] OR "triflange"[tw] OR triflang*[tw]) AND ("Hip"[tw] OR "Hips"[tw]))) AND ("revision"[tw] OR revisi*[tw] OR reviz*[tw] OR "Reoperation"[mesh] OR "Reoperation"[tw] OR "Reoperation"[tw] OR Reoperat*[tw] OR "Re-operation"[tw] OR Re-operat*[tw] OR "Prosthesis Failure"[mesh] OR "Arthroplasty, Replacement, Hip/adverse effects"[mesh] OR "Hip Prosthesis/adverse effects"[mesh] OR "failure"[tw] OR failure*[tw] OR "failed"[tw] OR "AAOS "[tw] OR "acetabular defect"[tw] OR "acetabular defects"[tw] OR "acetabular deficiency"[tw] OR "acetabular deficiencies"[tw] OR "acetabulum defect"[tw] OR "acetabulum defects"[tw] OR "acetabulum deficiency"[tw] OR "acetabulum deficiencies"[tw] OR "Paprosky"[tw] OR Paprosky*[tw] OR "Bone Defects"[tw] OR "bone defect"[tw] OR "pelvic defect"[tw] OR "pelvic defects"[tw] OR "pelvis defect"[tw] OR "pelvis defects"[tw] OR "bone loss"[tw] OR "Osteolysis"[mesh] OR "Osteolysis"[tw])

2. ("custom"[ti] OR "custom-made"[ti] OR "custommade"[ti] OR custom-mad*[ti] OR custommad*[ti] OR "customized"[ti] OR "customised"[ti] OR "custom design"[ti] OR custom design*[ti] OR "customization"[ti] OR "customisation"[ti] OR "custom triflange"[ti] OR "personalized"[ti] OR "personalised"[ti] OR "patient specific"[ti] OR patientspecif*[ti] OR "Precision Medicine"[majr] OR "ossis"[tw] OR "implant cast"[ti] OR "implantcast"[ti] OR "materialise"[ti])

Template 12-2017 protocol (medisch) wetenschappelijk onderzoek met bestaande (patiënten)gegevens (niet-WMO) in het LUMC

---

1.   **Informatie over onderzoeker en opdrachtgever**

1.1 **Titel onderzoek**	**Accuracy of positioning of custom 3D titanium printed pelvic implants in large pelvic bone defect reconstruction.**
1.2 **Onderzoeker(s)**	Willemijne Meurs, Master student Technical Medicine, Technical University Delft, Tel: +31616431825 Email: willemijnemeurs@hotmail.com Demien Broekhuis, MSc, MD, Dept. Orthopaedics, Leiden University Medical Center, Postzone J11-R, Kamer J-11-72, PO Box 9600, 2300 RC Leiden, The Netherlands Tel: +31 71 5263606 Email: d.broekhuis@lumc.nl Rob G.H.H Nelissen, Prof, PhD, MD, Head of Department, Dept. Orthopaedics, Leiden University Medical Center, Postzone J11-R, Room J-11-72, PO Box 9600, 2300 RC Leiden, The Netherlands Tel: +31 71 52 63606 / 63613 Email: R.G.H.H.Nelissen@lumc.nl Bart L. Kaptein, PhD, Ir, Dept. Orthopaedics, Leiden University Medical Center, Postzone J11-R, Room J-11-73, PO Box 9600, 2300 RC Leiden, The Netherlands Tel: +31715264542 Email: B.L.Kaptein@lumc.nl Lennard A. Koster, MSc, Dept. Orthopaedics, Leiden University Medical Center, Postzone J11-R, Room J-11-73, PO Box 9600, 2300 RC Leiden, The Netherlands Tel: +31 71 5264542 Email: l.a.koster@lumc.nl Richard Boyle, MD, Dept. Orthopaedics, Chris O'Brien Lifehouse Clinic B, Level 2 119-143, Camperdown, Australia Tel: +61 2 8064 0310 Email: info@boyleorthopaedics.com Sascha Karunaratne, MSc, Research Officer, Dept. Orthopaedics, Royal Prince Alfred Hospital, Level 9, Building 89, PO Box M157, Camperdown, Australia

	Tel: +61 2 9515 3210 Email: sascha.karunaratne@health.nsw.gov.au
1.3 **Opdrachtgever(s)/sponsor(en)**	Department of Orthopaedics, LUMC
1.4 **Protocoldatum**	17-06-2020

2. Doel van het onderzoek

2.1 **Onderzoeksvraag/doelstelling(en)** **van het onderzoek**	**Main study parameters:** The aim of this study is to evaluate the surgical positioning of patient specific/custom 3D titanium printed pelvic implants (3DPI) in patients with large pelvic defects. **Objective 1,** Acquiring the post-operative position of the implant (expressed as the Tx, Ty, Tz (translation) and Rx, Ry, Rz (rotation) coordinates of the implant center of gravity point), relative to the pre-operative position plan. (These Tx, Ty, Tz /Rx, Ry, Rz coordinates and found alterations in positioning can be rewritten to i.e. the anatomical planes; sagittal / coronal / transversal) **Objective 2,** localizing the post-operative position of specified implant contact areas (i.e. tree points in tri-flage designs, or an average point in every cluster of screws) relative to the the pelvic bone, compared to these points in the pre-operative plan. This can provide additional insight into potential repetitive/generalized implant placement errors, allowing for future improvements. **Objective 3** (possible): Evaluating the possible association between acquired implant positioning accuracy and clinical factors such as gender, age, BMI, previous interventions, pre-op radiotherapy. pelvic location and positioning accuracy correlating to functional outcomes and complications. Measurement time of functional outcomes are short pre-operative and post-operative after one year. The complications are measured at the time of the file investigation, so this will differ for each patient. **Objective 4** (possible): internal validation of the implant position measurement technique used in this study, by means of calculating the intra-observer variability between measurements based on identical and/or subsequent (PET)-CT scans and identifying margins of error.

3. Onderzoeksopzet

3.1 a. Algemene beschrijving van de onderzoeksopzet (design)	The surgical management of large pelvic bone defects is technically challenging. Due to the high load of mechanical forces acting on this bone, the complex anatomy and deep-seated location with nearby critical neurovascular and visceral structures (1,2). In patients with massive pelvic defects (i.e. after tumor resection or failed total hip arthroplasty) patient specific implants can be very helpful in the management of large bone defects. Large bone defects cannot be easily bridged by the standard implants (1). Therefore, Patient Specific Implants (3DPI) are increasingly used (3). To our knowledge, to date no cohort data is available on 3DPI implant positioning in tumour reconstructions and only sparsely in hip revision surgery (4,5). The aim of this study is to evaluate the acquired post-operative 3DPI position compared to the pre-operative plan in a retrospective cohort of patients in which the 3DPIs are implanted in a standard surgical manner (i.e. no intra-operative navigation tools). To evaluate the surgical placement of 3DPI, radiological data from patients who received a 3DPI between 2013 and 2020 in hospitals in Sydney, Australia are assessed. Preoperative planning stereolithography (STL) files and imaging data will be compared with the postoperative imaging data (PET-CT/conventional CT). In Mimics Research 21.0 (Materialise NV, Leuven, Belgium), the postoperative bone and 3DPI will be segmented to create 3D bone and implant models. After segmentation, the postoperative models are aligned with the preoperative planning models. With these models, calculations can be made to examine the implant position and attachment to the pelvic bone. This visualizes the rotation and translation differences between the planned and achieved models. With that, alignment calculations and a ratio of implant insertion discrepancy between the pre-operative implant planning and the achieved postoperative implant insertion will be calculated. The results obtained from this study will describe the surgical position evaluation of inserted 3DPIs in the pelvic after tumor resection surgery. These results could be of great importance for future 3DPI placement strategies. This is a retrospective cohort study based on the surgical placement of 3D titanium printed custom pelvic implant (3DPI). All necessary anonymized STL files and pre-/postoperative imaging data will be transferred or taken back to the LUMC. Patient data will be identified with a study specific identification code, and in no circumstances patient details will be available to any member of the research team other than the one who collected the data in hospitals in Sydney. All used data collected from surgical procedures are performed in the recent years. Therefore, no patient registration is performed and no clinical data is gathered.

3.2 **a. Wanneer wordt het onderzoek uitgevoerd?**	The study starts at the beginning of September 2020
b. Wat is de beoogde einddatum van het onderzoek?	The study ends at May 2021
3.3 **Gaat het om onderzoek met uitsluitend bestaande (patiënt)gegevens (retrospectief) en niet met nog te genereren gegevens (prospectief)?**	yes
3.4 **Met welk *type* gegevens wordt onderzoek gedaan?**	The 3D model datasets (STL files of implants and pelvic bone) and retrospective imaging datasets (post-operative PET-CT/conventional CT and pre-operative CT scans) used for this study are derived from previous pelvic reconstruction cases, designed by OSSIS Limited (New Zealand, origin of 3D models) and acquired in the Chris O'Brien Hospital or other local radiology locations, Australia (not LUMC) between 2013 and 2020. All patients have signed a consent allowing for their anonymized data to be used for scientific research. All data used in this study is subject to written patient consent. Datasets were acquired specifically for the reconstructive cases. All pre-operative patient information from the 3D model datasets are removed by OSSIS Limited and a unique identification number is added which for the researchers is not retractable to the patient. All post-operative imaging datasets are collected by one of the researchers at the hospitals in Sydney. This data is stored on one laptop and securely send to the LUMC. An external storage is used for back-up of the data. This is in collaboration with orthopedic surgeons in the Chris O'Brien Lifehouse hospital in Sydney, Australia. The data is anonymized before taking it to the LUMC. All digital 3D model files are transferred to the researchers via a secured fileshare platform (https://www.sharefile.com/) and stored on the LUMC internal server only accessible after system login with personal login details which are only available to members of the research team. The key-file will be kept by one of the original surgical / rehab team members, which is not available for the researchers.
3.5	Gender

Indien er informatie uit patiëntendossiers wordt gebruikt: beschrijf om *welke* informatie het gaat.	Age
	BMI
	Indication for 3DPI
	Date of surgery
	Location of pelvic reconstruction/resection (according to Enneking classification P1-4)
	Number of previous surgical interventions to site
	Pre-operative radiotherapy
	Implant specific complications (according to the Henderson tumour implant complication classification)
	Functional hip scores pre and post-operatively when available (see OSSIS consent form, looks like they have gathered these)
	Date of (PET) CT scans
3.6 **Op welke periode hebben de gegevens betrekking?**	2013-2020

4. Databeheer en privacy

4.1 **a. Wordt in het kader van *dit* onderzoek aan patiënten/betrokkenen toestemming gevraagd voor het gebruik van hun (medische) gegevens?** **b. Indien geen toestemming wordt gevraagd: licht toe waarom geen toestemming wordt gevraagd.**	Yes All data used in this study is subject to this written patient consent. A written consent is obtained per patient for the use of the post-operative data. If no consent is obtained, the patient will not be included in the study.
4.2 **Is er in het verleden aan patiënten/betrokkenen toestemming gevraagd voor het gebruik van (medische) gegevens voor wetenschappelijk onderzoek?**	Yes This is done by the 3D printed implant manufacturer (OSSIS). Written consent was given pre-operatively by the patients consenting to the use of the data for research, at the time of indication for a 3D printed implant.
4.3 **a. Is er sprake (geweest) van een behandelrelatie tussen de**	No, all patients subjected to this study are treated in hospitals in Sydney, Australia.

onderzoeker(s) of de afdeling van de onderzoeker(s) en de patiënten van wie de status wordt ingezien? (zie ook hierna onder 4.8)	
b. Is de behandelrelatie nog actueel of is deze inmiddels beëindigd?	Not applicable
4.4 **Is het waarschijnlijk dat patiënten uit de onderzoekspopulatie inmiddels zijn overleden?**	No
4.5 **Van hoeveel patiënten worden gegevens gebruikt?**	Around approximately 50 patients
4.6 **Hebben patiënten de (algemene) mogelijkheid gehad bezwaar te maken tegen het (gecodeerd/geanonimiseerd) gebruik van hun (medische) gegevens?**	Yes
4.7 **Wordt er van het gebruik van (medische)gegevens voor wetenschappelijke doeleinden aantekening gemaakt in de status van de desbetreffende patiënt(en)?**	No
4.8 **a. Door wie worden de benodigde gegevens uit de patiëntendossiers gehaald?**	Willemijne or a research officer in Sydney Chris O'Brien Lifehouse
4.9 **Worden er tot de persoon herleidbare gegevens ter beschikking gesteld aan de onderzoeker(s)?**	No, all information will be anonymized and coded using a unique identification number.
4.10 **Indien codering plaatsvindt: wanneer vindt codering plaats, door wie en op welke wijze?**	The identification number is added by one of the original surgical / rehab team members in the hospital at time of data extraction and anonymization.
4.11	Yes

Is er een melding gedaan van de voorgenomen gegevens verwerking via: https://www.albinusnet.nl/weten-en-regelen/onderzoek/integriteit-en-privacy/meldenverzamelenonderzoeksdata	
4.12 **Indien van toepassing: waar worden de gecodeerde gegevens bewaard en wie hebben er toegang tot de gecodeerde gegevens?** **Indien van toepassing: waar worden de ongecodeerde gegevens bewaard en wie hebben er toegang tot de ongecodeerde gegevens?**	All 3D model data (OSSIS Limited) will be handled confidentially. The data will be treated anonymously and all patient data will received an unique identification number. The data collected in the hospitals in Sydney is anonymously secured at a laptop with login codes only accessible to members of the research team. All digital 3D model files are transferred to the LUMC via a secured fileshare platform (https://www.sharefile.com/) and stored on the LUMC internal server only accessible after system login with personal login details which are only available to members of the research team.
4.13 **Welke technische en organisatorische maatregelen zijn er getroffen ter voorkoming van verlies, diefstal of ongeautoriseerd gebruik van de onderzoeksdata? Wordt er bijvoorbeeld gebruik gemaakt van een datasafe?**	See above (4.12)
4.14 **Door wie wordt de sleutel van de code beheerd?**	OSSIS and Chris O'Brien Lifehouse hospital Sydney The key-file will be kept by one of the original surgical / rehab team members, which is not available for the researchers.
4.15 **Vindt er uitwisseling van (onderzoeks)gegevens plaats met (een) andere instelling(en) binnen Nederland en/of de EU?**	No
4.16 **a. Vindt er uitwisseling van de (onderzoeks)gegevens plaats met een andere instelling/instantie buiten de EU?** **b. Wordt aan de desbetreffende patiënten toestemming gevraagd voor het uitwisselen van persoonsgegevens met een land buiten de EU?**	Yes outside of EU, the data is transferred from Australia/New Zealand to the Netherlands: • OSSIS Limited New Zealand (origin of 3D model data) • Chris O'Brien Lifehouse, Sydney (origin of imaging data) Yes, all pre-operative data used in this study is subject to a written patient consent. A written consent is obtained per patient for the use of the post-operative data. If no consent is obtained, the patient will not be included in the study.

	OSSIS Limited will provide all the digital STL files of the implants, the resected bone models, locking head screws and STL files of the screw trajectories. The digital files are sent to the researchers via a secured fileshare platform (https://www.hightail.com/) and stored on the LUMC internal server only accessible to members of the research team.
	All patient information from the imaging datasets, pre/post-operative (PET-)CT scans, are personally collected by one of the researches at the hospitals in Sydney. This is in collaboration with orthopedic surgeons in the Chris O'Brien Lifehouse hospital in Sydney, Australia. The data is anonymized before taking them to the LUMC. The key-file will be kept by one of the original surgical / rehab team members, which is not available for the researchers.
4.17 **Hoe lang worden de (onderzoeks)gegevens bewaard? Indien de gegevens langer of korter dan de standaardtermijn van 15 jaar worden bewaard graag toelichten waarom.**	15 years

5. Onderzoekspopulatie

5.1 **Inclusie-/selectiecriteria**	Patients are eligible for inclusion if 1) they received a 3DPI, ranging from only (partial) P2 resection to a larger P1-2-3 resection reconstruction (all OSSIS custom 3D pelvic implant models) 2) when they have signed the written patient consent.
5.2 **Exclusiecriteria**	Patients are excluded if; 1) no post-operative PET-CT or CT is available; 2) post-op (PET) CT is of insufficient quality to perform analysis.

6. Statistische analyse

6.1 **a. Primaire uitkomstmaat** **b. Indien van toepassing: secundaire uitkomstmaat**	**Objective 1,** Acquiring the post-operative position of the implant (expressed as the Tx, Ty, Tz (translation) and Rx, Ry, Rz (rotation) coordinates of the implant center of gravity point), relative to the pre-operative position plan. (These Tx, Ty, Tz /Rx, Ry, Rz coordinates and found alterations in positioning can be rewritten to i.e. the anatomical planes; sagittal / coronal / transversal)

Universiteit Leiden

TUDelft Delft University of Technology

ERASMUS UNIVERSITEIT ROTTERDAM

	Objective 2, localizing the post-operative position of specified implant contact areas (i.e. tree points in tri-flage designs, or an average point in every cluster of screws) relative to the the pelvic bone, compared to these points in the pre-operative plan. This can provide additional insight into potential repetitive/generalized implant placement errors, allowing for future improvements.
	Objective 3 (possible): Evaluating the possible correlation between acquired implant positioning accuracy and clinical factors such as gender, age, BMI, previous interventions, pre-op radiotherapy. pelvic location and positioning accuracy correlating to functional outcomes and complications. Measurement time of functional outcomes are short pre-operative and post-operative after one year. The complications are measured at the time of the file investigation, so this will differ for each patient.
	Objective 4 (possible): internal validation of the implant position measurement technique used in this study, by means of calculating the intra-observer variability between measurements based on identical and/or subsequent (PET)-CT scans and identifying margins of error.
6.2 **a. Statistische analyse primaire uitkomstmaat** -	Descriptive statistics on misalignments of the 3DPI between the pre-operative implant planning and the achieved post-operative implant position.

7. Bijlagen en literatuurverwijzingen

7.2 **Literatuurverwijzingen**	(1)G. Chen, A. Muheremu, L. Yang, et al. Three-dimensional printed implant for reconstruction of pelvic bone after removal of giant chondrosarcoma: a case report. *J Int Med Res*. 2020;48(4) (2) K. C. Wong, S. M. Kumta, N. V. Geel & J. Demol et al. One-step reconstruction with a 3D-printed, biomechanically evaluated custom implant after complex pelvic tumor resection, Computer Aided Surgery, 2015. 20:1, 14-23 (3) C. Fang, H. Cai, E. Kuong et al. Surgical applications of three-dimensional printing in the pelvis and acetabulum: from models and tools to implants. Unfallchirurg 122. 2019, 278-285 (4) M. Baauw, G.G. van Hellemondt, M. L. Van Hooff et al. The accuracy of positioning of a custom-made implant within a large acetabular defect at revision arthroplasty of the hip. Soc. Of Bone & Joint Surgery. 2015, 780(5) (5) M. Weber, L. Witzmann, J. Wieding et al. Customized implants for acetabular Paprosky III defects may be positioned with high accuracy in revision hip arthroplasty. International Orthopaedics. 2018; 43(10): 2235-2243

Paprosky classification

The paprosky classification is a common used classification system for acetabular bone loss in THA revision. The classification is anatomical orientated and assesses specific bone structures for deficit, rather than staging based on volumetric bone loss. It is focused on "the presence or absence of an intact acetabular rim and its ability to provide rigid support for an implanted acetabular component" (3). The classification is divided into three types, for each consecutive the severity of bone loss increases. Type 2 and 3 defects are further divided into subgroups. Type 3 defects, described in this study," have extensive global erosion of the acetabulum with attenuation or destruction of all supporting structures and greater than 2cm of hip center migration" (1). Some of these defects include pelvic discontinuity. A type 3A defect is described as moderate-to-severe destruction of the acetabular walls and posterior column. The acetabular rim is deficient from 10 o'clock to 2 o'clock and 30% to 60% of the supporting bone structures are destructed. A type 3B defect, is defined as the most severe acetabular defects characterized by destruction of supporting structures including both the wall and columns. The acetabular rim is deficient from 9 o'clock to 5 o' clock and more than 60% of the supporting bone is destructed (1). See Figure 1.
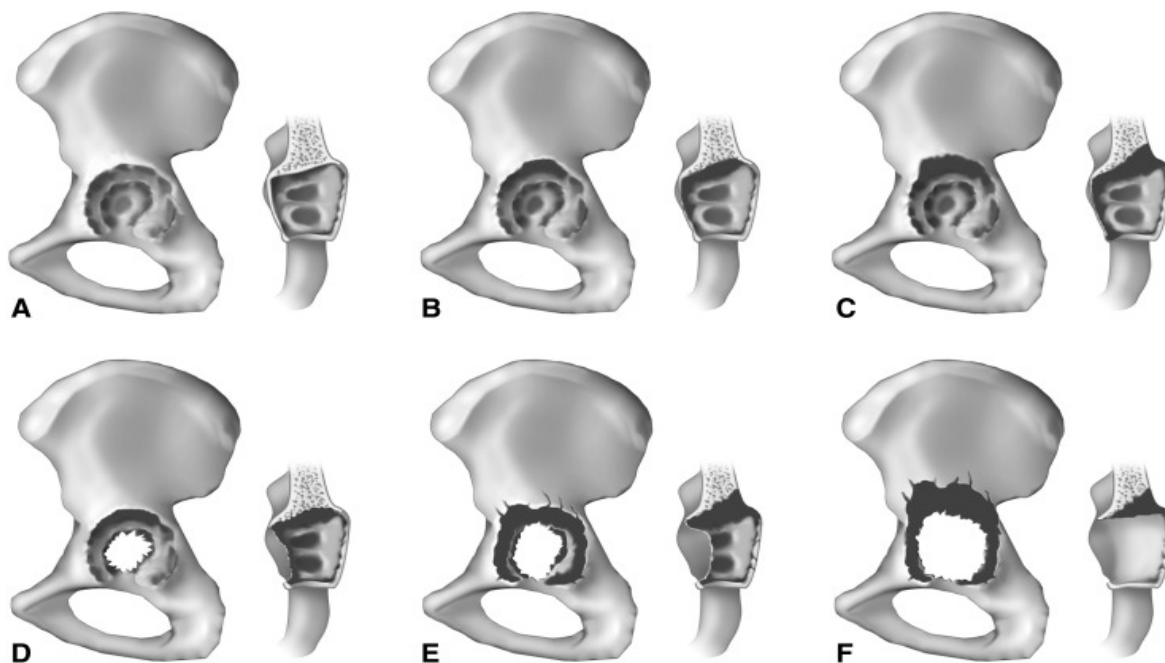
Figure 1. Paprosky classification. A) Type 1. B) Type 2A. C) Type 2B. D) Type 2C. E) Type 3A. F)

Figure 2. Classification of pelvic resections according to Enneking (4).

Enneking classification

The location of pelvic tumors and the requirement for en bloc resections can be described into three types. Type I includes resection of the ilium bone. Type II resections involve the acetabulum and type III resections involve the ischium and pubic rami. As tumor resections can be large, a combination of types is possible (5). See Figure 2 (4).
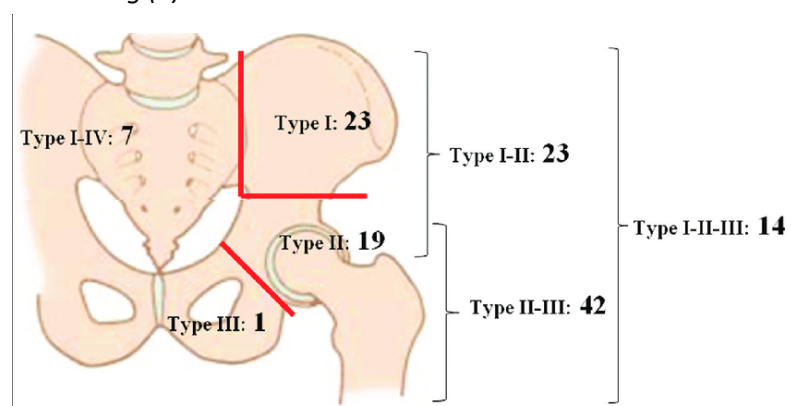
Inclination and Anteversion measurement methods by Murray et al. (1993)

Murray et al. (1993) defined three different methods for the measurement of acetabular orientation; operative, radiographic and anatomical (6). The operative anteversion (OA) is described as the angle between the longitudinal axis of the patient and the acetabular axis as projected on the sagittal plane. The operative inclination (OI) is therefore the angle between the acetabular axis and the sagittal plane. The orientation of the acetabulum can be determined postoperatively on antero-posterior (AP) radiographs and 3D images using the radiographic definition. Radiographic anteversion (RA) is known as the angle between the acetabular axis and the acetabular axis projected on the coronal plane.

Radiographic inclination (RI) is described as the angle between the longitudinal axis of the patient and the acetabular axis projected on the coronal plane. Anatomical anteversion (AA) is defined as the angle between the transverse axis and the acetabular axis projected on the transverse plane. Anatomical inclination (AI) is represented as the angle between the acetabular axis and the longitudinal axis (6). See Figure 3 (2).

Figure 3. Operative, radiographic and anatomical reference systems for the calculation of the inclination and anteversion (2).
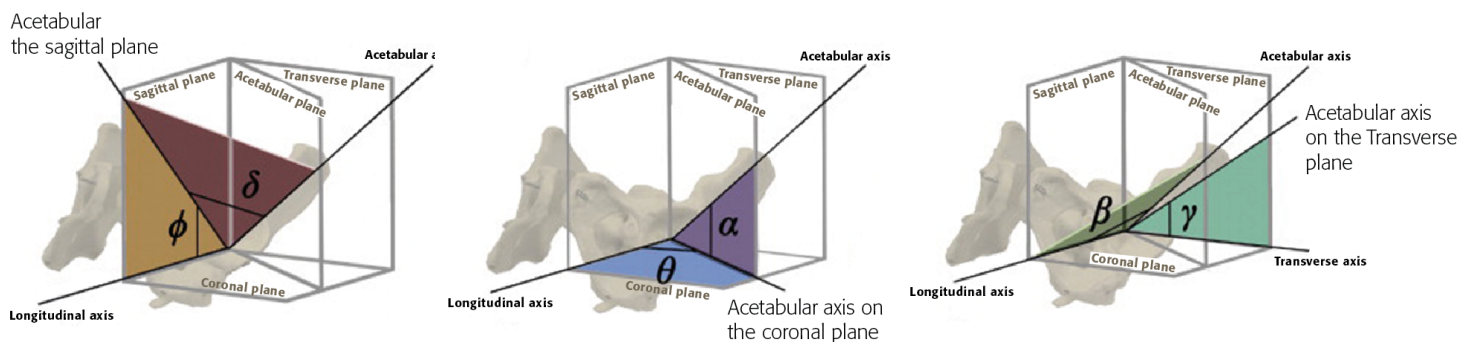
References

1.   Telleria JJM, Gee AO. Classifications In Brief: Paprosky Classification of Acetabular Bone Loss. Clinical Orthopaedics and Related Research®. 2013;471(11):3725-30.
2.   Harrison CL, Thomson AI, Cutts S, Rowe PJ, Riches PE. Research Synthesis of Recommended Acetabular Cup Orientations for Total Hip Arthroplasty. The Journal of Arthroplasty. 2014;29(2):377-82.
3.   Paprosky WG, Perona PG, Lawrence JM. Acetabular defect classification and surgical reconstruction in revision arthroplasty. The Journal of Arthroplasty. 1994;9(1):33-44.
4.   Angelini A, Calabrò T, Pala E, Trovarelli G, Maraldi M, Ruggieri P. Resection and reconstruction of pelvic bone tumors. Orthopedics. 2015;38(2):87-93.
5.   Enneking WF, Spanier SS, Goodman MA. A system for the surgical staging of musculoskeletal sarcoma. Clin Orthop Relat Res. 1980(153):106-20.
6.   Murray D. The definition and measurement of acetabular orientation. The Journal of Bone and Joint Surgery British volume. 1993;75-B(2):228-32.

D. Supplementary material Part II – Methods for position calculation

Table 7; Published studies on the accuracy of the positioning CTACs (37, 38, 42, 43, 45, 55, 57).

Author	Year	(Pre/Post) Assessment	Imaging	Outcome measures	Registration type	Software	Coordinate system
				Position assessment methods			
Friedrich et al	2014	Post	X-ray	Vertical, horizontal distance (mm)	-	-	-
				Alpha COR (mm)			
Baauw et al.	2015	3D-CT pre-post	CT	Alpha INCL, AV, rotation (degrees)	N/A	N/A	ISB
Li et al.	2016	Post	X-ray	Vertical, horizontal distance (mm)	-	-	-
				Alpha COR (mm)		Mimics,	
Weber et al.	2018	3D-CT pre-post	CT	Alpha INCL, AV (degrees)	N/A	SolidWorks	N/A
				COR (mm)			
Walter et al.	2020	Pre-post	X-ray	Vertical, horizontal, alpha, COR distance (mm)	-	-	-
				Vertical, horizontal distance, leg length discrepancy (mm)			
Burastero et a	2020	Post	X-ray	INCL (degrees)	-	-	-
				Alpha COR (mm)	Landmark	ScanIP,	Local coordinate
Durand-Hill et	2020	3D-CT pre-post	CT	Alpha INCL, AV, rotation (degrees)	registration	Meshlab	system
				Alpha COR (mm)			Orthogonal
Zampelis et al	2020	3D-CT pre-post	CT	Alpha INCL, AV, rotation (degrees)	N/A	Mimics	coordinate system

* N/A: information not available

E. Supplementary material Part II – Individual Translation data

Individual Translation data of COR, Pubic flange, Ischial flange and ilium flange

Table 8. Individual translation of COR, Pubic Flange, Ischial Flange, Ilium Flange

Case	COR Sagittal [mm]	Coronal [mm]	Axial [mm]	Δ Vector	Pubic Flange Sagittal [mm]	Coronal [mm]	Axial [mm]	Δ Vector	Ischial Flange Sagittal [mm]	Coronal [mm]	Axial [mm]	Δ Vector	Ilium Flange Sagittal [mm]	Coronal [mm]	Axial [mm]	Δ Vector
1	-1,9	2,0	0,6	2,8	-2,5	1,7	-1,9	3,6	-3,4	2,8	0,5	4,4	1,7	0,2	1,3	2,1
2	-8,5	2,2	4,5	9,8	-10,4	1,3	-1,1	10,5	-	-	-	-	-5,5	-2,4	6,7	9,0
3	-0,1	-1,7	0,8	1,9	2,9	-1,3	3,3	4,6	1,3	-3,1	0,3	3,4	-7,5	-0,9	-3,3	8,3
4	0,5	-0,5	0,1	0,7	0,0	-1,1	-0,4	1,2	1,1	0,0	0,9	1,5	-0,2	-3,6	0,6	3,6
5	8,3	-28,0	33,1	44,1	14,0	-26,8	39,8	49,9	0,4	-38,4	27,1	47,0	-6,3	-0,4	4,3	7,6
6	1,1	3,2	-2,9	4,5	-	-	-	-	1,2	5,0	-2,0	5,5	-0,6	-1,1	-1,2	1,7
7	-3,1	-2,2	-5,3	6,6	-3,5	-2,6	-8,4	9,5	-	-	-	-	-0,5	-1,8	-5,7	6,0
8	-1,2	2,2	-0,5	2,5	4,8	5,3	-2,5	7,6	-4,6	8,1	1,0	9,4	-3,0	-4,7	-0,2	5,6
9	-0,4	6,8	-3,1	7,5	-3,3	1,2	-0,6	3,6	-	-	-	-	-3,8	0,2	-0,2	3,8
10	-2,9	-4,2	0,6	5,1	-1,3	-3,8	1,0	4,1	-6,2	-5,2	-0,2	8,1	-0,1	0,0	-2,8	2,8
11	-0,7	-0,4	0,8	1,2	-0,9	-0,4	0,3	1,0	-1,0	-0,3	0,8	1,3	0,5	-0,7	0,9	1,3
12	0,9	0,1	2,3	2,4	1,9	1,3	0,6	2,4	0,0	0,7	2,7	2,8	1,4	-1,7	2,9	3,6
13	0,3	-8,1	-4,6	9,4	3,8	-3,6	0,3	5,3	-1,2	-9,4	-6,5	11,5	-4,5	-3,9	-7,1	9,3
14	-1,7	-3,6	0,8	4,1	1,0	-1,4	0,6	1,8	-4,4	-2,1	2,0	5,2	-7,0	-5,5	1,9	9,2
15	-1,0	-1,4	-3,3	3,7	1,1	2,5	-3,0	4,0	-0,7	0,9	-2,0	2,3	-4,3	-3,7	-1,3	5,9
16	-3,6	1,0	-0,3	3,8	-4,2	0,6	0,2	4,2	-	-	-	-	4,8	7,2	-4,1	9,6
17	-0,4	-8,0	-2,0	8,3	1,9	-6,7	-0,2	7,0	-3,0	-9,3	-4,1	10,6	-4,1	1,8	-6,9	8,3
18	-6,0	10,1	2,0	11,9	-9,3	12,4	-5,2	16,3	-8,7	14,6	11,2	20,4	2,0	2,6	7,8	8,5
19	6,4	-2,4	-0,7	6,9	9,0	1,0	4,4	10,1	-	-	-	-	-0,7	0,2	-1,8	1,9
20	-0,2	-0,6	-1,8	1,9	-1,1	-2,1	-1,5	2,8	1,0	0,2	-1,2	1,6	-1,0	-2,3	-1,3	2,8
21	-0,5	-3,4	1,6	3,8	-0,2	-3,4	2,1	4,0	-0,7	-3,6	1,4	4,0	-0,8	-3,0	1,5	3,4
22	-1,3	5,4	-2,6	6,2	0,4	3,0	1,2	3,2	0,8	2,7	-5,3	6,0	-3,3	8,3	-6,4	11,0
23	-1,8	-0,1	-0,2	1,8	1,2	2,7	7,7	8,2	-1,6	-1,8	-1,8	3,0	-3,1	0,6	-1,6	3,6
24	0,8	0,9	0,0	1,1	-0,6	-0,1	0,0	0,6	-1,1	-0,7	-1,2	1,7	4,4	3,6	0,5	5,7
25	1,2	2,0	-0,8	2,4	1,5	2,5	-1,5	3,3	1,7	3,6	1,0	4,1	-0,2	-1,5	0,6	1,6
26	-4,1	3,4	1,9	5,7	-9,1	0,4	-3,4	9,8	-3,3	3,7	2,4	5,5	4,5	6,7	8,4	11,7
27	1,0	1,7	0,2	2,0	0,8	1,4	0,3	1,6	1,1	1,4	0,0	1,8	1,5	2,2	-0,3	2,7
28	-2,8	3,3	0,2	4,3	-5,7	-1,1	-1,1	5,9	-1,9	3,0	0,2	3,5	1,4	2,6	0,0	3,0
29	0,8	-3,1	0,6	3,3	3,0	1,4	-0,4	3,4	-	-	-	-	-0,1	-0,2	-1,1	1,1
30	2,2	-0,6	-1,9	3,0	2,5	-0,8	-0,8	2,7	2,1	-1,4	-2,7	3,7	1,6	2,3	-2,9	4,0
31	-2,6	-3,6	-4,4	6,2	-2,1	-3,9	-0,8	4,5	-2,3	-4,7	-5,6	7,6	-4,4	0,6	-6,2	7,6
32	5,4	-0,5	-2,8	6,1	5,2	-1,1	-1,8	5,6	8,1	-1,0	-2,2	8,4	0,3	-0,4	-2,6	2,7
33	-1,8	-1,8	3,1	4,0	0,1	-1,1	3,4	3,6	-3,3	-1,2	3,0	4,7	-5,4	0,1	3,1	6,2
34	-6,2	12,0	5,3	14,5	-	-	-	-	-	-	-	-	-1,1	2,8	6,5	7,2
35	-3,0	3,3	-1,8	4,7	-4,2	3,6	-3,3	6,5	-2,8	5,8	0,5	6,5	-0,6	1,5	0,2	1,6

F. Supplementary material Part II – Migation graph

Migration graph. Translation of the COR versus time to follow-up imaging.

COR displacement vs Time till post-operative imaging
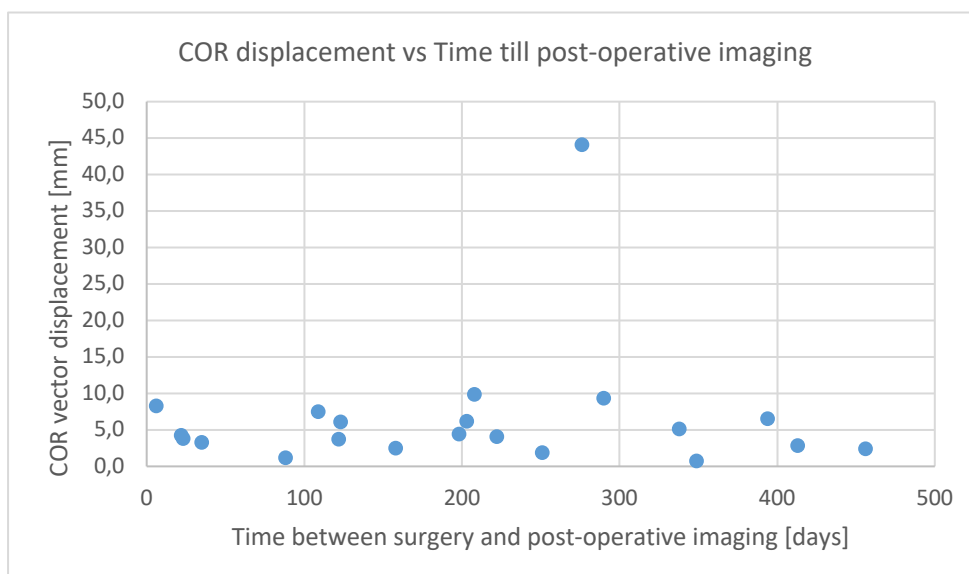
G. Supplementary material Part II – Protocol for pre-processing

Protocol Mimics/3-Matic (19-01-2021)

Mimics

Planning:

- Open OSSIS mimics file
- (Re)create Parts with names; Planning Pelvis, Planning Component, Planning Screws,
  - Check if all anatomical landmarks are represented on Planning Pelvis.
    - If not; Create part Planning Removed bone (for anatomical landmarks if necessary)

Post-op: Import DICOM data

- Segment Pelvis, Implant
- Create Parts with names; Postop Pelvis, Postop Component

See Figure 1.

Save as STL Binary, Post-op STLs to Postop folder, Planning STLs to Planning Folder

Figure 1. Mimics segmentation
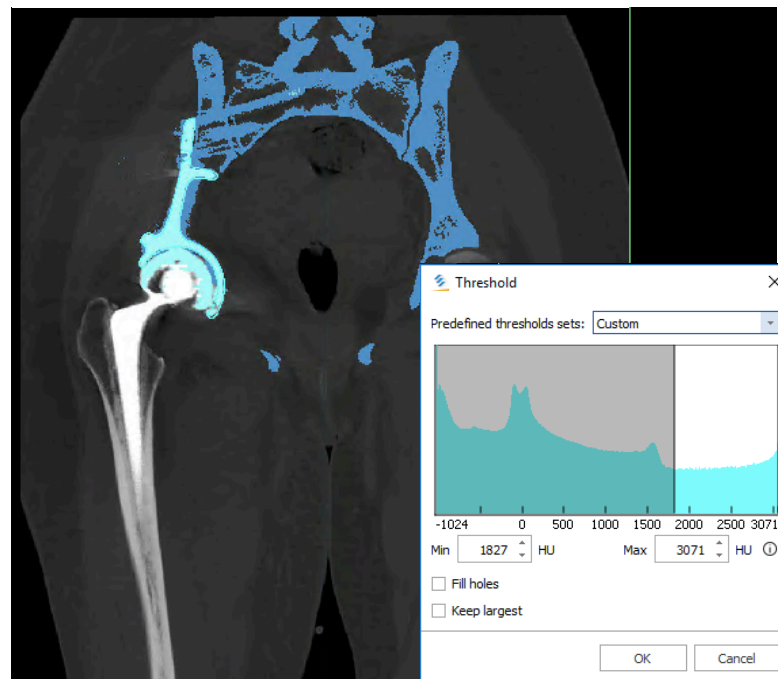
3-Matic

1. Import STL files; Planning Pelvis, Component and Screws, Postop Pelvis and Component.
2. Translate/Rotate function; Move towards Postop Pelvis.
   a. Main entity; Planning Pelvis,
   b. Moving along entities; Planning Component and Screws. (Removed bone)
3. Global registration; (repeat until perfect)
   a. Fixed entity; Postop Pelvic,
   b. Moving entity; Planning Pelvis,
   c. Moving along entities; planning Component and Screws. (Removed bone)

See Figure 2.

Figure 2. 3-Matic Registration

Now you can see the difference between the implant position of the planning and the post-operative situation.

4. Hide everything except for the Planning Component and Screws and Postop Component
5. Duplicate Planning Component and Screws; Rename: Postop Component_OSSIS, Postop Screws_OSSIS

Now we will select the anatomical landmarks

1. Select 3 points on the acetabular rim on both the Planning Component and duplicate them. Rename; AR_1_Plan, AR_2_Plan, AR_3_Plan, AR_1_Post, AR_2_Post, AR_3_Post

2. Create 2 points on the left and right Anterior Superior Iliac Spine (ASIS) point on the Planning Pelvis. Rename; ASIS_l, ASIS_r
3. Create 2 points on the left and right pubic tubercles on the Planning Pelvis. Rename; PT_l, PT_r
4. Create 3 points on the sacral crests on the Planning Pelvis. Rename; SC_1, SC_2, SC_3.
5. Create a sphere in the Planning acetabular rim by selecting 3 points inside the hemisphere cup. Duplicate and Rename; COR_Plan, COR_Post
6. Select 3 points on the triflangle cup near the screw holes. 1. Pubis flangle, 2. Ischium flangle, 3. Ilium flange. In case one is missing, click an alternative point and write down. Duplicate and Rename; Screw1_Plan, Screw2_Plan, Screw3_Plan, Screw1_Post, Screw2_Post, Screw3_Post.

See Figure 3.

Figure 3. *3-Matic Landmark selection*

7. Global registration; (repeat until perfect)
    a. Fixed entity; Postop Component,
    b. Moving entity; Postop Component_OSSIS,
    c. Moving along entities; Postop Screws_OSSIS, AR_1_Post, AR_2_Post, AR_3_Post, COR_Post, Screw1_Post, Screw2_Post, Screw3_Post.
8. Hide Postop Component and Screws.
9. Create part comparison analysis; Entity; Postop Component_OSSIS, Target entity; Planning Component
10. Note maximum displacement in excel sheet
11. Copy all points with Ctr-C

Save STL models; Planning Component, Postop Component_OSIS, Planning Pelvis to main folder patient

Mimics

12. Open the corresponding images/models Mimics file
13. Paste all 13 points in the Mimics file and check if the points correspond on the Postop 3d Models
14. Export points; txt…; Analysis; (save in Main folder patient)
    a. Name AR_plan; AR_1_Plan, AR_2_Plan, AR_3_Plan,
    b. Name AR_post; AR_1_Post, AR_2_Post, AR_3_Post
    c. Name ASISPT; ASIS_l, ASIS_r, PT_l, PT_r
    d. Name SC; SC_1, SC_2, SC_3
    e. Name COR_Plan; COR_Planning
    f. Name COR_Post; COR_Postop
    g. Name Screw1_Plan, Screw2_Plan, Screw3_Plan; Screw_Plan
    h. Name Screw1_Post, Screw2_ Post, Screw3_ Post; Screw_ Post

See Figure 4.

Figure 4. *Mimics Check points*
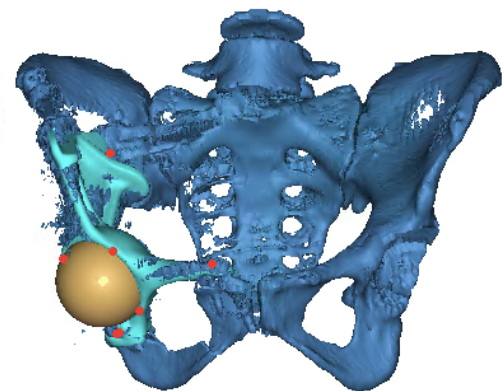
H. Supplementary material Part II – Matlab script

Matlab script developed for the 3D-CT analysis method

```matlab
% Accuracy of positioning of custom 3D titanium printed pelvic implants in large pelvic bone defect
reconstruction
% Willemijne Meurs
% 18-02-2021
% Short final version

% For this script you will need external scripts; stlread.m and soder.m

clc
clear all
close all

%% read txt and STL files  (anatomical landmarks and STL models)
% ---- FILL IN! -----

Side = 1; % Right implant = 1, Left implant = -1 (Important for axial plane)
ID = '3Dpi_Id4'; % Patientnumber in file path

% Standard: debug = 0
% In case Transformation matrix is incorrect, fill in debug = 1,
debug = 0;

%%
% Import STLs and anatomical landmarks (same method for all txt files)
PP = 'R:\Research\2020_Australia\Patient data\Sydney\';
AR_plan = '\AR_plan.txt'; % Find file name
AR_plan = readmatrix(strcat(PP,ID,AR_plan)); % Read txt file
AR_plan = AR_plan(:,2:4); % Remove NaN data
AR_post = '\AR_post.txt';
AR_post = readmatrix(strcat(PP,ID,AR_post));
AR_post = AR_post(:,2:4);
SC = '\SC.txt';
SC = readmatrix(strcat(PP,ID,SC));
SC = SC(:,2:4);
ASIS_PT = '\ASISPT.txt';
ASIS_PT = readmatrix(strcat(PP,ID,ASIS_PT));
ASIS_PT = ASIS_PT(:,2:4);
Screw_plan = '\Screw_Plan.txt';
Screw_plan = readmatrix(strcat(PP,ID,Screw_plan));
Screw_plan = Screw_plan(:,2:4);
Screw_post = '\Screw_Post.txt';
Screw_post = readmatrix(strcat(PP,ID,Screw_post));
Screw_post = Screw_post(:,2:4);
COR_Plan = '\COR_Planning.txt';
COR_Plan = readmatrix(strcat(PP,ID,COR_Plan));
COR_Post = '\COR_Postop.txt';
COR_Post = readmatrix(strcat(PP,ID,COR_Post));
COR = [COR_Plan ; COR_Post ; (COR_Post - COR_Plan)];
COR = COR(:,2:4);

% read STL files (Planning Pelvis, Planning Component, Postop Component)
postop_implant = '\Postop Component_OSSIS.stl';
postop_implant = stlread(strcat(PP,ID,postop_implant));
plan_implant = '\Planning Component.stl';
plan_implant = stlread(strcat(PP,ID,plan_implant));
pelvis = '\Planning Pelvis.stl';
pelvis = stlread(strcat(PP,ID,pelvis));

% Screw; 1. pubis, 2. ischium, 3. ilium

%% Calculate Acetabular axis Planning and Postop
% Calculate Planning Acetabular axis
AB = AR_plan(2,:) - AR_plan(1,:); % Vector AB
AC = AR_plan(3,:) - AR_plan(1,:); % Vector AC
n_plan = cross(AB,AC); % Normal vector of Planning acetabular plane Crossproduct AB x AC

% automatically correct vector direction
```

```matlab
if n_plan(3) < 0 %Caudal direction (correct)
    n_plan = n_plan;
elseif n_plan(3) > 0 % Cranial direction (incorrect, change direction)
    n_plan = -n_plan;
end


fprintf('Check if answers are 90 ')
acosd(dot(AB,n_plan)/(norm(AB)*norm(n_plan))) % Check if normal vs coordinate vector is 90 degrees

% Create Planning Acetabular plane (a*x+b*y+c*z+d)=0
d_plan = -AR_plan(1,:)*n_plan'; % dot product
[X_plan,Y_plan] = meshgrid(AR_plan(:,1),AR_plan(:,2)); % create grid for plane
z_plan = (-n_plan(1)*X_plan - n_plan(2)*Y_plan - d_plan)/n_plan(3); % calculate corresponding z


% Calculate Postop Acetabular axis
AB_post = AR_post(2,:) - AR_post(1,:); % Vector AB
AC = AR_post(3,:) - AR_post(1,:); % Vector AC
n_post = cross(AB_post,AC); % Normal vector of Postop acetabular plane Crossproduct AB x AC

% automatically correct vector direction
if n_post(3) < 0 %Caudal direction (correct)
    n_post = n_post;
elseif n_post(3) > 0 % Cranial direction (incorrect, change direction)
    n_post = -n_post;
end

acosd(dot(AB_post,n_post)/(norm(AB_post)*norm(n_post))) % Check if normal vs coordinate vector is 90
degrees

% Create Postop Acetabular plane (a*x+b*y+c*z+d)=0
d_post = -AR_post(1,:)*n_post'; % dot product
[X_post,Y_post] = meshgrid(AR_post(:,1),AR_post(:,2)); % make grid for plane
z_post = (-n_post(1)*X_post - n_post(2)*Y_post - d_post)/n_post(3); % calculate corresponding z


%% Calculate anatomical planes
% APP Plane
AB = ASIS_PT(4,:) - ASIS_PT(1,:); % Vector AB
CD = ASIS_PT(3,:) - ASIS_PT(2,:); % Vector CD
n_APP = cross(AB,CD); % Normal vector of APP Plane Crossproduct AB x CD
acosd(dot(AB,n_APP)/(norm(AB)*norm(n_APP))) % Check if normal vs coordinate vector is 90 degrees  #
cos(o)=(ac+bd)/(|(a b)|*|(cd)|)

% Create APP Plane
d = -ASIS_PT(1,:)*n_APP'; % dot product
[X_APP,Y_APP] = meshgrid(ASIS_PT(:,1),ASIS_PT(:,2)); % make grid for plane
z_APP = (-n_APP(1)*X_APP - n_APP(2)*Y_APP - d)/n_APP(3); % calculate corresponding z


% Sagittal Plane
mid_ASIS = [mean(ASIS_PT(1:2,1)) mean(ASIS_PT(1:2,2)) mean(ASIS_PT(1:2,3))]; % Midline ASIS
Sag = [SC; mid_ASIS]; %Combine SC with mid_ASIS for matrix with points
AB = Sag(1,:) - Sag(3,:); % Vector AB
CD = Sag(2,:) - Sag(4,:); % Vector CD
n_Sag = cross(AB,CD); % Normal vector of Sagittal plane; Crossproduct AB x CD
acosd(dot(AB,n_Sag)/(norm(AB)*norm(n_Sag))) % Check if normal vs coordinate vector is 90 degrees  #
cos(o)=(ac+bd)/(|(a c)|*|(bd)|)

% Create Sagittal Plane
d = -Sag(1,:)*n_Sag'; % dot product
[X_Sag,Y_Sag] = meshgrid(Sag(:,1),Sag(:,2)); % make grid for plane
z_Sag = (-n_Sag(1)*X_Sag - n_Sag(2)*Y_Sag - d)/n_Sag(3); % calculate corresponding z

% Create Transverse (Axial) Plane
n_Trans = cross(n_APP,n_Sag); % Normal vector of Transverse (axial) plane Cross product
acosd(dot(n_APP,n_Trans)/(norm(n_APP)*norm(n_Trans))) % Check if normal vs coordinate vector is 90
degrees  # cos(o)=(ac+bd)/(|(a b)|*|(cd)|)
d = -ASIS_PT(1,:)*n_Trans'; % dot product
[X_Trans,Y_Trans] = meshgrid(ASIS_PT(1:2,1),ASIS_PT(1:2,2)); % make grid for plane
z_Trans = (-n_Trans(1)*X_Trans - n_Trans(2)*Y_Trans - d)/n_Trans(3); % calculate corresponding z

% Summary
% n_plan = acetabular axis planning
% n_post = acetabular axis postop
% n_APP = Frontal axis (normal vector of APP (coronal) plane)
```

```matlab
% n_Sag = Transverse axis (normal vector of Sagittal plane)
% n_Trans = Longitudinal axis (normal vector of Transverse plane)


%% Inclination and Anteversion
% Projection of acetabular axis on APP (coronal) plane
%# To calculate the anteversion, we need to project the acetabular axis on the APP (coronal) plane.
Proj_AxetonCor_plan= (cross(n_APP,(cross(n_plan,n_APP))))/(norm(n_APP)^2); % Projection of Acetabular
Axis on Coronal (APP) plane
Proj_AxetonCor_post= (cross(n_APP,(cross(n_post,n_APP))))/(norm(n_APP)^2); % Projection of Acetabular
Axis on Coronal (APP) plane

% Radiological Anteversion calculation
%# Acetabular Axis // Acetabular axis projected on Coronal plane
AV_plan = acosd(dot(n_plan,Proj_AxetonCor_plan)/(norm(n_plan)*norm(Proj_AxetonCor_plan))); %
Radiological Anteversion Planning
AV_post = acosd(dot(n_post,Proj_AxetonCor_post)/(norm(n_post)*norm(Proj_AxetonCor_post))); %
Radiological Anteversion Postop
Delta_AV = (AV_post-AV_plan); % Difference Anterverion Planning vs Post

% Radiological Inclination calculation
%# Longitudinal axis (Transverse normal vector) // Acetabular axis projected on Coronal plane
INC_plan = acosd(dot(n_Trans,Proj_AxetonCor_plan)/(norm(n_Trans)*norm(Proj_AxetonCor_plan))); %
Radiological Inclination Planning
INC_post = acosd(dot(n_Trans,Proj_AxetonCor_post)/(norm(n_Trans)*norm(Proj_AxetonCor_post))); %
Radiological Inclination Postop
Delta_INC = (INC_post-INC_plan); % Difference Anterverion Planning vs Post

%% Transformation matrix - Use soder.m
% STL to point clouds
ptcloud_plan = pointCloud(plan_implant.vertices); % Create pointcloud of Planning Implant
cmatrix = ones(size(ptcloud_plan.Location)).*[1 1 0]; % Create YELLOW color for Planning point cloud
ptcloud_plan = pointCloud(plan_implant.vertices,'Color',cmatrix); % Pointcloud with yellow color
ptcloud_post = pointCloud(postop_implant.vertices); % Create pointcloud of Postop Implant
cmatrix = ones(size(ptcloud_post.Location)).*[0 0 1]; % Create BLUE color for Postop point cloud
ptcloud_post = pointCloud(postop_implant.vertices,'Color',cmatrix); % Pointcloud with blue color

% Vizualize merged point clouds
figure(1);
gridStep = 1;
PCmerge = pcmerge(ptcloud_plan,ptcloud_post,gridStep); %  Merge Planning and Postop point clouds
pcshow(PCmerge); %Vizualization of two pointclouds
xlabel('Axial(x) [mm]')
ylabel('Sagittal (y) [mm]')
zlabel('Coronal (z) [mm]')
title('PointCloud merge of Planning and Postoperative')
view(n_plan);


% From two 3D Point clouds to transformation matrix

% Create a SubSamp Dataset with only 5 points to speed up the process
SubSamp = randperm(ptcloud_plan.Count,5);
ptcloud_plan_5 = pointCloud(ptcloud_plan.Location(SubSamp,:));
ptcloud_post_5 = pointCloud(ptcloud_post.Location(SubSamp,:));

% [R,d,rms] = soder(x,y) -> y=R*x+d -> x = moving, y = fixed
%
% Note: Soder assumes points in rows of the x and y matrix
% (so an n x 3 matrix)
%
% For this reason, both the R and the d need to be transposed to provide
% a valid 4x4 transform matrix...
%
% Note that soder.m is a bit "old" code and may be optimized by removing
% the for loops...

[R,d,rms] = soder(ptcloud_plan_5.Location,ptcloud_post_5.Location); % use soder.m for creating
transformation matrix
TransFull = [R' [0 0 0]';[d', 1]];
tform = affine3d(TransFull); % Transformation matrix using soder.m

%% Check if correct Transformation matrix (Transformed points - Postoperative = 0)
ptCloudOut = pctransform(ptcloud_plan,tform); % Transformed Planning model with transformation
matrix. Result = Postop location
cmatrix = ones(size(ptCloudOut.Location)).*[1 1 1]; % Set color to White
ptCloudOut = pointCloud(ptCloudOut.Location,'Color',cmatrix);  % Add color to Transformed Point Cloud
```

```matlab
Checkpoints = ptcloud_post.Location-ptCloudOut.Location; % check if point cloud planning - point
cloud transformed planning  = 0

fprintf('Ans should only be < ...e-02. If not, previous transformation matrix is not correct. Affine
transformation matrix between Transformed Planning and Postoperative Implant')
max(Checkpoints)

% Debug!
% If Transformation matrix is not correct, check where the problem is in
% the image. debug = 1
if debug == 1
    linearIndexes = find(Checkpoints>abs(1e-03));  % Find elements with value more than e-03
    [rows, columns] = ind2sub(size(Checkpoints), linearIndexes);
    PCmerge2 = pcmerge(ptcloud_post,ptCloudOut,gridStep);
    pcshow(PCmerge2);
    title({'Merged postoperative implant with transformed implant', 'Color should be one color only
(light) to check if Transformation matrix is correct'})
    hold on

plot3(ptcloud_post.Location(rows(1),1),ptcloud_post.Location(rows(1),2),ptcloud_post.Location(rows(1)
,3),'o','Color','r')  % Find first mismatching point

plot3(ptcloud_post.Location(rows(ceil(end/2)),1),ptcloud_post.Location(rows(ceil(end/2)),2),ptcloud_p
ost.Location(rows(ceil(end/2)),3),'o','Color','r') % Find middle mismatching point

plot3(ptcloud_post.Location(rows(end),1),ptcloud_post.Location(rows(end),2),ptcloud_post.Location(row
s(end),3),'o','Color','r') % Find last mismatching point

elseif debug == 0
end

%% Translation of COR, Screw1, Screw2, Screw3 points
% (x)-plane = Sagittal plane
% (y)-plane = Coronal plane
% (z)-plane = Axial plane
% % Translation COR
TRCOR = transformPointsForward(tform,COR(1,:)); % TR*CORplan -> TR = Transformation matrix
TCOR = TRCOR - COR(1,:); % difference between transformed point (post) and Planning = Translation
DCOR = TCOR-COR(3,:); % Delta Transformed point and Postop point. Should be = 0 or very small
TCOR = [TCOR(1)*Side TCOR(2) TCOR(3)]; %Correct for right or left hip (For Sagittal Plane)

% Translation screw 1 - Pubis flangle [mm]
TRScrew1 = transformPointsForward(tform,Screw_plan(1,:)); % TR*Screw1plan -> TR = Transformation
matrix
TScrew1 =  TRScrew1(1,:) - Screw_plan(1,:); % difference between transformed point (post) and
Planning
DScrew1 = TRScrew1-Screw_post(1,:);  % Checkpoint if answer is correct, should be 0 since postop -
translated postop = 0
TScrew1 = [TScrew1(1)*Side TScrew1(2) TScrew1(3)]; %Correct for right or left hip

% Translation screw 2 - Ischium flangle [mm]
TRScrew2 = transformPointsForward(tform,Screw_plan(2,:)); % TR*Screw1plan -> TR = Transformation
matrix
TScrew2 =  TRScrew2(1,:) - Screw_plan(2,:); % difference between transformed point (post) and
Planning
DScrew2 = TRScrew2-Screw_post(2,:);  % Checkpoint if answer is correct, should be 0 since postop -
translated postop = 0
TScrew2 = [TScrew2(1)*Side TScrew2(2) TScrew2(3)];  %Correct for right or left hip

% Translation screw 3 - Ilium flangle [mm]
TRScrew3 = transformPointsForward(tform,Screw_plan(3,:)); % TR*Screw1plan -> TR = Transformation
matrix
TScrew3 =  TRScrew3(1,:) - Screw_plan(3,:); % difference between transformed point (post) and
Planning
DScrew3 = TRScrew3-Screw_post(3,:);  % Checkpoint if answer is correct, should be 0 since postop -
translated postop = 0
TScrew3 = [TScrew3(1)*Side TScrew3(2) TScrew3(3)];  %Correct for right or left hip

% Checkpoint. Answers should be < ...e-03
D = [DCOR;DScrew1;DScrew2;DScrew3]; % Matrix for checkpoint
rowNames = {'COR', 'Pubis Flangle','Ischium Flangle','Ilium Flangle'};
fprintf('Checkpoint! Answers should be < ...e-03 Otherwise Transformation matrix is not correct')
array2table(D,'RowNames',rowNames)

%% Rotation -> use projection.m function and SpinCalc.m function
% Axis-angle Rotations [x,y,z] in 3D [degrees]; From Transformation matrix to rotation around 3 axis
and angle
```

Universiteit Leiden

TUDelft Delft University of Technology

Erasmus ERASMUS UNIVERSITEIT ROTTERDAM

```matlab
% Use the SpinCalc.m function
Rmatrix = tform.T(1:3,1:3); % Get the rotation matrix from the translation matrix
Rangle = SpinCalc('DCMtoEV',Rmatrix,1,1); % Using the SpinCalc function to calculate the rotation
angle around the CT coordinate origin

% Transformation of AR_plan to AR_post using transformation matrix
TRAR = transformPointsForward(tform,AR_plan(1,:)); % Transformation of Acetabular rim point to postop
situation

% Projection of COR planning and post onto acetabular planes
[COR_proj_x COR_proj_y COR_proj_z] = projection(-n_plan(1),-n_plan(2),-
n_plan(3),d_plan,COR(1,1),COR(1,2),COR(1,3)); % Projection of COR onto acetabular plane planning
COR_proj = [COR_proj_x COR_proj_y COR_proj_z];
[TRCOR_proj_x TRCOR_proj_y TRCOR_proj_z] = projection(-n_post(1),-n_post(2),-
n_post(3),d_post,TRCOR(1,1),TRCOR(1,2),TRCOR(1,3)); % Projection of COR onto acetabular plane postop
TRCOR_proj = [TRCOR_proj_x TRCOR_proj_y TRCOR_proj_z];

% Create vectors from projected COR (on acetabular plane) to same point on
% acetabular rim (AR)
vAR_plan = AR_plan(1,:) - COR_proj; % Vector from projected COR planing to point
vAR_post = TRAR - TRCOR_proj; % Vector from projected COR postop to point

% Projection of Planning vector (vAR_plan) on postop acetabular plane
Proj_vARonAB= (cross(-n_post,(cross(vAR_plan,-n_post))))/(norm(-n_post)^2); % Projection of planning
vector on postop acetabular plane

% Rotation between two vectors on postop acetabular plane= Cup rotation
Rotation_Cup = acosd(dot(Proj_vARonAB,vAR_post)/(norm(Proj_vARonAB)*norm(vAR_post))); % Cup Rotation


%% Results
format bank % Two digids
% Radiological Anteversion and Inclination
Result = [AV_plan AV_post Delta_AV; INC_plan INC_post Delta_INC];
colNames = {'Planning [degrees]','Post-op [degrees]','Difference [degrees]'};
rowNames = {'Anteversion', 'Inclination'};
fprintf('+ answer = more anteversion/inclination than planned, - answer = less
anteversion/inclination')
AV_INC = array2table(Result,'VariableNames',colNames,'RowNames',rowNames)

% Translation COR, Screw1, Screw2 and Screw3
colNames = {'Sagittal(x) [mm]','Coronal (y) [mm]','Axial (z) [mm]'};
rowNames = {'COR', 'Pubis Flangle','Ischium Flangle','Ilium Flangle'};
Translation = [TCOR;TScrew1;TScrew2;TScrew3];
fprintf('Translation x,y,z [mm]; Sagittal: Medial +, Lateral -, Coronal: Dorsal +, Frontal -, Axial:
Cranial +,Caudal -')
Translation = array2table(Translation,'VariableNames',colNames,'RowNames',rowNames)

% Rotation of implant
colNames = {'[degrees]'};
rowNames = {'Implant Rotation','Rotation cup'};
fprintf('Rotation angle [degrees]')
Rotation = [Rangle(1,4);Rotation_Cup];
Rotation = array2table(Rotation,'VariableNames',colNames,'RowNames',rowNames) % Rotation angle
[degrees]

% Vector between rotation to vizualize direction
vDir = TRAR-(TRCOR_proj+Proj_vARonAB);


% Vizualization of Inclination/Anteversion planes (yellow = Planning acetabular axis, blue = Postop
acetabular axis, red = normal vectors coronal, sagittal, transverse)
figure(2);
quiver3(mean(AR_plan(:,1)),mean(AR_plan(:,2)),mean(AR_plan(:,3)),n_plan(1),n_plan(2),n_plan(3),0.2,'y
') % show scaled middlepoint normal vector
hold on
patch(plan_implant,'FaceColor',[0.8 0.8 1.0],'EdgeColor','y') % Show Pre-op implant
quiver3(mean(AR_post(:,1)),mean(AR_post(:,2)),mean(AR_post(:,3)),n_post(1),n_post(2),n_post(3),0.1,'b
') % if you want to change direction of normal vector
patch(postop_implant,'FaceColor',[0.8 0.8 1.0],'EdgeColor','b') % Show Pelvis
quiver3(mean(ASIS_PT(:,1)),mean(ASIS_PT(:,2)),mean(ASIS_PT(:,3)),n_APP(1),n_APP(2),n_APP(3),0.01,'r')
% show scaled middlepoint normal vector
quiver3(mean(Sag(:,1)),mean(Sag(:,2)),mean(Sag(:,3)),n_Sag(1),n_Sag(2),n_Sag(3),0.1,'r') % show
scaled middlepoint normal vector
quiver3(mean(ASIS_PT(1:2,1)),mean(ASIS_PT(:,2)),mean(ASIS_PT(:,3)),n_Trans(1),n_Trans(2),n_Trans(3),0
.000001,'r') % show scaled middlepoint normal vector
patch(pelvis,'FaceColor',[0.8 0.8 1.0],'EdgeColor','none') % Show Pelvis
```

Universiteit Leiden

TUDelft Delft University of Technology

Erasmus ERASMUS UNIVERSITEIT ROTTERDAM

```matlab
camlight('headlight');
material('dull');
title({'Normal vectors of anatomical planes and acetabular planes','Check if three normal vectors are
90degrees'})
axis equal
xlabel('x')
ylabel('y')
zlabel('z')

% Vizualization of the cup rotation direction
figure(3);
ax1= subplot(1,2,1);
quiver3(TRCOR_proj(1),TRCOR_proj(2),TRCOR_proj(3),Proj_vARonAB(1,1),Proj_vARonAB(1,2),Proj_vARonAB(1,
3),'r')
hold on
patch(postop_implant,'FaceColor',[0 0 1],'EdgeColor','none') % Show Post-op implant
title({'Vector rotation','angle between red and blue vector'})
patch(plan_implant,'FaceColor',[1 1 0],'EdgeColor','none') % Show Pre-op implant
plot3(TRCOR_proj(1,1),TRCOR_proj(1,2),TRCOR_proj(1,3),'o','Color','b') % Plot postop COR point
plot3(TRAR(1,1),TRAR(1,2),TRAR(1,3),'o','Color','b') % Postop point
quiver3(TRCOR_proj(1),TRCOR_proj(2),TRCOR_proj(3),vAR_post(1,1),vAR_post(1,2),vAR_post(1,3),'b')
quiver3(TRAR(1,1),TRAR(1,2),TRAR(1,3),vDir(1),vDir(2),vDir(3),10,'r')
camlight('headlight');
material('dull');
grid off
axis off
axis equal
ax2 = subplot(1,2,2);
plot3(TRCOR_proj(1,1),TRCOR_proj(1,2),TRCOR_proj(1,3),'o','Color','b') % Plot postop COR point
hold on
text(TRCOR_proj(1,1),TRCOR_proj(1,2),TRCOR_proj(1,3),'postop COR','Color','k')
plot3(TRAR(1,1),TRAR(1,2),TRAR(1,3),'o','Color','b') % Postop point
text(TRAR(1,1),TRAR(1,2),TRAR(1,3),'Acetabular Rim','Color','k')
quiver3(TRCOR_proj(1),TRCOR_proj(2),TRCOR_proj(3),vAR_post(1,1),vAR_post(1,2),vAR_post(1,3),'b')
quiver3(TRCOR_proj(1),TRCOR_proj(2),TRCOR_proj(3),Proj_vARonAB(1,1),Proj_vARonAB(1,2),Proj_vARonAB(1,
3),'r')
quiver3(TRAR(1,1),TRAR(1,2),TRAR(1,3),vDir(1),vDir(2),vDir(3),50,'r')
plot3((TRCOR_proj(1)+Proj_vARonAB(1,1)),(TRCOR_proj(2)+Proj_vARonAB(1,2)),(TRCOR_proj(3)+Proj_vARonAB
(1,3)),'o','Color','r')
title({'Rotation angle','Check direction of rotation; clockwise or anti-clockwise'})
axis equal
hlink = linkprop([ax1,ax2],{'CameraPosition','CameraUpVector'}); % link subplots for rotation
rotate3d on
grid off
axis off

% Plot to see Planning and Postop Translation.
figure(4);
patch(plan_implant,'FaceColor', [0 1 0],'EdgeColor','none','FaceAlpha',0.2);
view(n_APP);
xlabel('Sagittal (x) [mm]')
ylabel('Coronal (y) [mm]')
zlabel('Axial (z) [mm]')
title({'PointCloud of Postoperative Implant + COR, Pubis Flangle,Ischium Flangle,Ilium
Flangle','Yellow = Planning. Red = Postop','Red Vector indicates direction of translation'})
hold on
plot3(TRCOR(1,1),TRCOR(1,2),TRCOR(1,3),'o','Color','b','LineWidth',2) % Plot postop COR point
text(TRCOR(1,1),TRCOR(1,2),TRCOR(1,3),'COR','Color','k','LineWidth',2)
plot3(COR(1,1),COR(1,2),COR(1,3),'o','Color','y','LineWidth',2) % Plot planning COR point
plot3(Screw_plan(1,1),Screw_plan(1,2),Screw_plan(1,3),'o','Color','y','LineWidth',2) % Plot planning
Screw1 point
plot3(TRScrew1(1,1),TRScrew1(1,2),TRScrew1(1,3),'o','Color','b','LineWidth',2) % Plot Tansformed
Screw1 point
text(TRScrew1(1,1),TRScrew1(1,2),TRScrew1(1,3),'Pubic Flange','Color','k','LineWidth',2)
plot3(Screw_plan(2,1),Screw_plan(2,2),Screw_plan(2,3),'o','Color','y','LineWidth',2) % Plot planning
Screw1 point
plot3(TRScrew2(1,1),TRScrew2(1,2),TRScrew2(1,3),'o','Color','b','LineWidth',2); % Plot Tansformed
Screw2 pointplot3(Screw_plan(3,1),Screw_plan(3,2),Screw_plan(3,3),'o','Color','y') % Plot planning
Screw1 point
text(TRScrew2(1,1),TRScrew2(1,2),TRScrew2(1,3),'Ischium Flange','Color','k','LineWidth',2)
plot3(Screw_plan(3,1),Screw_plan(3,2),Screw_plan(3,3),'o','Color','y','LineWidth',2) % Plot planning
Screw1 point
plot3(TRScrew3(1,1),TRScrew3(1,2),TRScrew3(1,3),'o','Color','b','LineWidth',2) % Plot Tansformed
Screw3 point
text(TRScrew3(1,1),TRScrew3(1,2),TRScrew3(1,3),'Ilium Flange','Color','k','LineWidth',2)
patch(pelvis,'FaceColor', [0.8 0.8 1.0],'EdgeColor','none','FaceAlpha',0.4);
camlight('headlight');
```

```matlab
material('dull');
axis equal

% Translation
% Sagittal (X): Medial +, Lateral -
% Coronal (Y):  Dorsal +, Frontal -
% Axial (Z): Cranial +, Caudal -

% Vector indicating the direction of the translation (COR, Screw1, Screw2,
% Screw3)
vCOR = quiver3(COR(1,1),COR(1,2),COR(1,3),TCOR(1)*Side,TCOR(2),TCOR(3),30,'r','LineWidth',2);
vScrew1 =
quiver3(Screw_plan(1,1),Screw_plan(1,2),Screw_plan(1,3),TScrew1(1)*Side,TScrew1(2),TScrew1(3),30,'r',
'LineWidth',2);
vScrew2 =
quiver3(Screw_plan(2,1),Screw_plan(2,2),Screw_plan(2,3),TScrew2(1)*Side,TScrew2(2),TScrew2(3),30,'r',
'LineWidth',2);
vScrew3 =
quiver3(Screw_plan(3,1),Screw_plan(3,2),Screw_plan(3,3),TScrew3(1)*Side,TScrew3(2),TScrew3(3),30,'r',
'LineWidth',2);


% Save images automatically
f1 = '_merged';
f4 = '_vector';
jpeg = '.jpeg';
saveas(figure(1),fullfile([strcat(PP,ID)],[strcat(ID,f1,jpeg)]));
saveas(figure(4),fullfile([strcat(PP,ID)],[strcat(ID,f4,jpeg)]));

% Results to excel
if Side == 1
    Implant_Location = 'Right';
elseif Side == -1
    Implant_Location = 'Left';
end

xlsx = '.xlsx';
Analysis_results = 'Results';
cellID = {'Patient number';ID};
cellLoc = {'Implant Location';Implant_Location};
cell1 ={'Angle';'Anteversion'; 'Inclination'};
cell2 ={'Flange Position';'COR';'Pubis Flangle';'Ischium Flangle';'Ilium Flangle'};
cell3= {'Rotation';'Implant Rotation';'Acetabular Rim Rotation'};
writecell(cellID,fullfile([strcat(PP,ID)],[strcat(Analysis_results,xlsx)]),'Range','A1')
writecell(cellLoc,fullfile([strcat(PP,ID)],[strcat(Analysis_results,xlsx)]),'Range','B1')
writecell(cell1,fullfile([strcat(PP,ID)],[strcat(Analysis_results,xlsx)]),'Range','C1')
writetable(AV_INC,fullfile([strcat(PP,ID)],[strcat(Analysis_results,xlsx)]),'Range','D1');
writecell(cell2,fullfile([strcat(PP,ID)],[strcat(Analysis_results,xlsx)]),'Range','G1')
writetable(Translation,fullfile([strcat(PP,ID)],[strcat(Analysis_results,xlsx)]),'Range','H1');
writecell(cell3,fullfile([strcat(PP,ID)],[strcat(Analysis_results,xlsx)]),'Range','K1')
writetable(Rotation,fullfile([strcat(PP,ID)],[strcat(Analysis_results,xlsx)]),'Range','L1');


_____

%% Accuracy of positioning custom made acetabular implants
% Willemijne Meurs
% Vizualization of mean translation vectors
% 20-02-2021

COR1 = [-0.8 -0.4 0.6];
Pubis = [-0.1 -0.6 0.8];
Ischium = [-1.1 -1.1 0.7];
Ilium = [-1.3 0.2 -0.3];


figure;
xlabel('Sagittal(x) [mm]')
ylabel('Coronal (y) [mm]')
zlabel('Axial (z) [mm]')
title({'PointCloud of Postoperative Implant + COR, Pubis Flangle,Ischium Flangle,Ilium
Flangle','Yellow = Planning. Red = Postop','Red Vector indicates direction of translation'})
patch(plan_implant,'FaceColor', [1 1 0],'EdgeColor','none','FaceAlpha',0.4);
hold on
plot3(COR(1,1),COR(1,2),COR(1,3),'o','Color','y') % Plot planning COR point
plot3(Screw_plan(1,1),Screw_plan(1,2),Screw_plan(1,3),'o','Color','y') % Plot planning Screw1 point
plot3(Screw_plan(2,1),Screw_plan(2,2),Screw_plan(2,3),'o','Color','y') % Plot planning Screw1 point
```

```matlab
plot3(Screw_plan(3,1),Screw_plan(3,2),Screw_plan(3,3),'o','Color','y') % Plot planning Screw1 point
patch(pelvis,'FaceColor', [0.8 0.8 1.0],'EdgeColor','none','FaceAlpha',0.2);
camlight('headlight');
material('dull');
axis equal

% Vector indicating the direction of the translation (COR, Screw1, Screw2,
% Screw3) * Vector 10
vCOR = quiver3(COR(1,1),COR(1,2),COR(1,3),COR1(1)*Side,COR1(2),COR1(3),10,'r','LineWidth',3);
vScrew1 =
quiver3(Screw_plan(1,1),Screw_plan(1,2),Screw_plan(1,3),Pubis(1)*Side,Pubis(2),Pubis(3),10,'r','LineW
idth',3);
vScrew2 =
quiver3(Screw_plan(2,1),Screw_plan(2,2),Screw_plan(2,3),Ischium(1)*Side,Ischium(2),Ischium(3),10,'r',
'LineWidth',3);
vScrew3 =
quiver3(Screw_plan(3,1),Screw_plan(3,2),Screw_plan(3,3),Ilium(1)*Side,Ilium(2),Ilium(3),10,'r','LineW
idth',3);


_____


% Accuracy of positioning of custom 3D titanium printed pelvic implants in large pelvic bone defect
reconstruction
% Willemijne Meurs
% 16-03-2021
% Calculation Volume and area of each implant

% For this script you will need external scripts; stlVolume.m

clc
clear all
close all

patients_Sydney =
["3Dpi_Id1(A)","3Dpi_Id1(B)","3Dpi_Id2","3Dpi_Id4","3Dpi_Id8","3Dpi_Id11","3Dpi_Id12","3Dpi_Id13","3D
pi_Id17","3Dpi_Id20","3Dpi_Id21","3Dpi_Id22","3Dpi_Id26","3Dpi_Id29","3Dpi_Id36","3Dpi_Id80","LUMC_37
"];
patients_Perth =
["LUMC_22","LUMC_23","LUMC_24","LUMC_25","LUMC_26","LUMC_27","LUMC_28","LUMC_29","LUMC_30"];
patients_Brisbane =
["LUMC_31","LUMC_32","LUMC_33","LUMC_34","LUMC_35","LUMC_36","LUMC_38","LUMC_39","LUMC_40"];


PS = 'R:\Research\2020_Australia\Patient data\Sydney\';
PP = 'R:\Research\2020_Australia\Patient data\Perth\';
PB = 'R:\Research\2020_Australia\Patient data\Brisbane\';
path_implant = '\Planning Component.stl';
%%
Table = [];
a = 1;
for i = 1:length(patients_Sydney)
plan_implant(a) = stlread(strcat(PS,patients_Sydney(i),path_implant));
[volume,area] = stlVolume(plan_implant(i).vertices',plan_implant(i).faces');
Table(:,i)= [volume,area];
a = a +1;
end

Table = Table';

% Save to excel
xlsx = '.xlsx';
results = 'Sydney_patients';
PX = 'R:\Research\2020_Australia\Patient data\';
writematrix(Table,fullfile([strcat(PX)],[strcat(results,xlsx)]),'Range','B2')

%% Perth
Table = [];
a = 1;
for i = 1:length(patients_Perth)
plan_implant(a) = stlread(strcat(PP,patients_Perth(i),path_implant));
[volume,area] = stlVolume(plan_implant(i).vertices',plan_implant(i).faces');
Table(:,i)= [volume,area];
a = a +1;
end
```

```matlab
Table = Table';

% Save to excel
xlsx = '.xlsx';
results = 'Sydney_patients';
PX = 'R:\Research\2020_Australia\Patient data\';
writematrix(Table,fullfile([strcat(PX)],[strcat(results,xlsx)]),'Range','B19')

%% Brisbane
Table = [];
a = 1;
for i = 1:length(patients_Brisbane)
plan_implant(a) = stlread(strcat(PB,patients_Brisbane(i),path_implant));
[volume,area] = stlVolume(plan_implant(i).vertices',plan_implant(i).faces');
Table(:,i)= [volume,area];
a = a +1;
end

Table = Table';

% Save to excel
writematrix(Table,fullfile([strcat(PX)],[strcat(results,xlsx)]),'Range','B28')
```

I. Supplementary material Part II – Individual accuracy data

Individual accuracy data

Case 1

Angle	Planning	Postop	Δ (°)
AV	25,4	24,1	-1,3
INCL	40,8	42,8	2,0

	Rotation (°)	Direction
Acetabular Cup	1,0	Frontal

Flange position	Sagittal [mm]	Coronal [mm]	Axial [mm]
COR	-1,9	2,0	0,6
Pubis Flange	-2,5	1,7	-1,9
Ischial Flange	-3,4	2,8	0,5
Ilium Flange	1,7	0,2	1,3

Legend
Sagittal (x): Medial +, Lateral -
Coronal (y):   Dorsal +, Frontal -
Axial (z):   Cranial +, Caudal -

Legend
Vectors are factor 30 for visualisation of direction

■ Planning
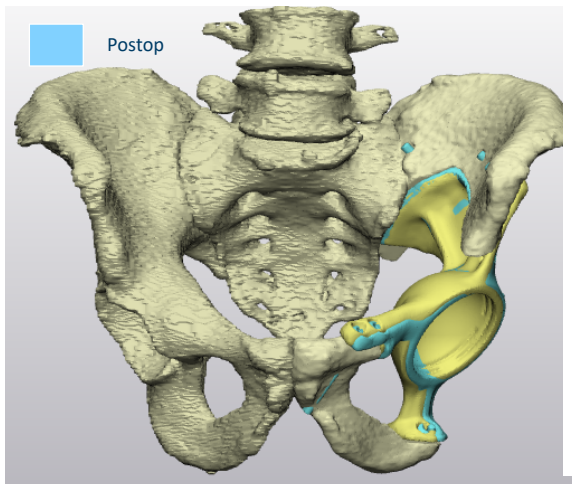
■ Postop

PointCloud of Postoperative Implant + COR, Pubis Flangle,Ischium Flangle,Ilium
Yellow = Planning. Red = Postop
Red Vector indicates direction of translation
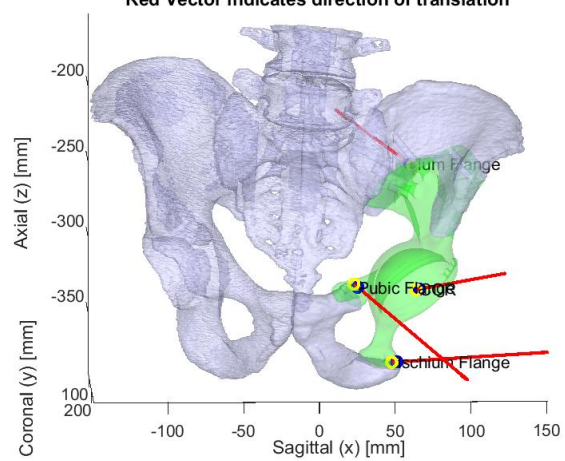
Case 2

Angle	Planning	Postop	Δ (°)
AV	25,9	23,1	-2,8
INCL	45,9	46,5	0,6

	Rotation (°)	Direction
Acetabular Cup	1,9	Frontal

Flange position	Sagittal [mm]	Coronal [mm]	Axial [mm]
COR	-8,5	2,2	4,5
Pubis Flange	-10,4	1,3	-1,1
Ischial Flange	-	-	-
Ilium Flange	-5,5	-2,4	6,7

Legend
Sagittal (x): Medial +, Lateral -
Coronal (y): Dorsal +, Frontal -
Axial (z): Cranial +, Caudal -

Legend
Vectors are factor 30 for visualisation of direction

Yellow — Planning
Postop
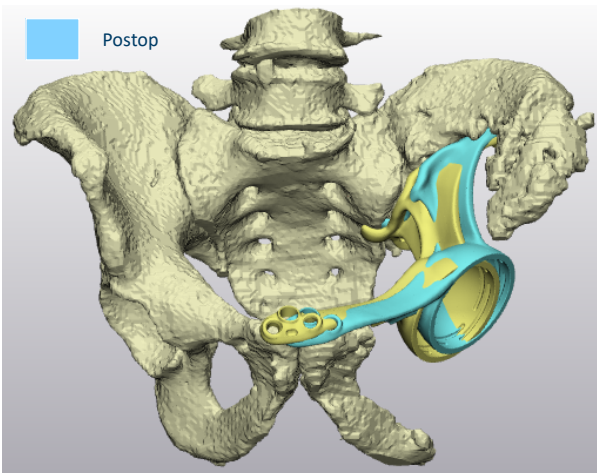
PointCloud of Postoperative Implant + COR, Pubis Flangle,Ischium Fl
Yellow = Planning. Red = Postop
Red Vector indicates direction of translation
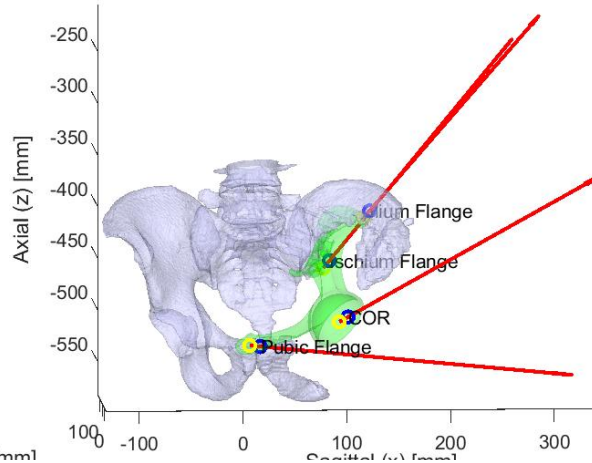
Case 3

Angle	Planning	Postop	Δ (°)
AV	18,6	23,1	4,6
INCL	42,2	37,9	-4,3

	Rotation (°)	Direction
Acetabular Cup	0,2	Dorsal

Flange position	Sagittal [mm]	Coronal [mm]	Axial [mm]
COR	-0,1	-1,7	0,8
Pubis Flange	2,9	-1,3	3,3
Ischial Flange	1,3	-3,1	0,3
Ilium Flange	-7,5	-0,9	-3,3

Legend
Sagittal (x): Medial +, Lateral -
Coronal (y): Dorsal +, Frontal -
Axial (z): Cranial +, Caudal -

Legend
Vectors are factor 30 for visualisation of direction
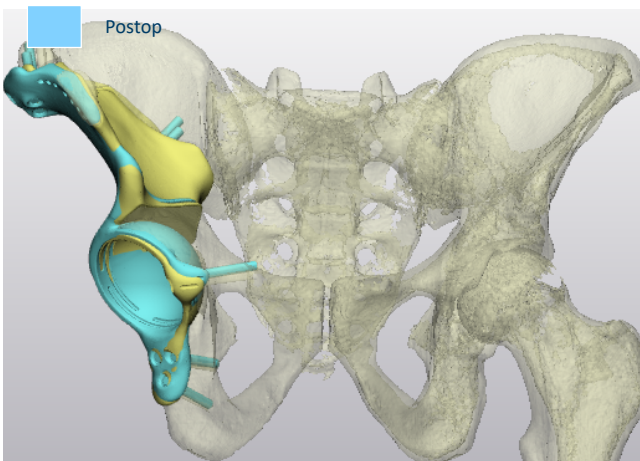
Planning
Postop

ntCloud of Postoperative Implant + COR, Pubis Flangle,Ischium Flangle,
Yellow = Planning. Red = Postop
Red Vector indicates direction of translation
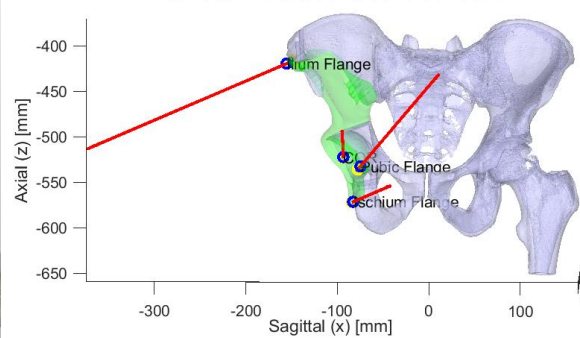
Case 4

Angle	Planning	Postop	Δ (°)
AV	34,2	32,4	-1,8
INCL	45,3	43,7	-1,6

	Rotation (°)	Direction
Acetabular Cup	0,1	Frontal

Flange position	Sagittal [mm]	Coronal [mm]	Axial [mm]
COR	0,5	-0,5	0,1
Pubis Flange	0,0	-1,1	-0,4
Ischial Flange	1,1	0,0	0,9
Ilium Flange	-0,2	-3,6	0,6

Legend
Sagittal (x): Medial +, Lateral -
Coronal (y): Dorsal +, Frontal -
Axial (z): Cranial +, Caudal -

Legend
Vectors are factor 30 for visualisation of direction
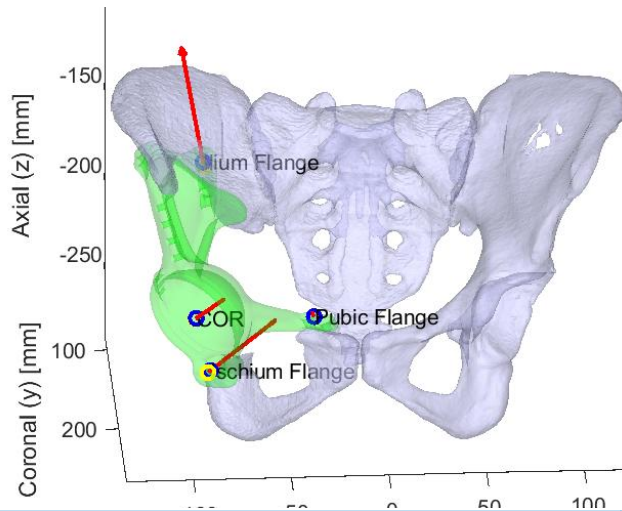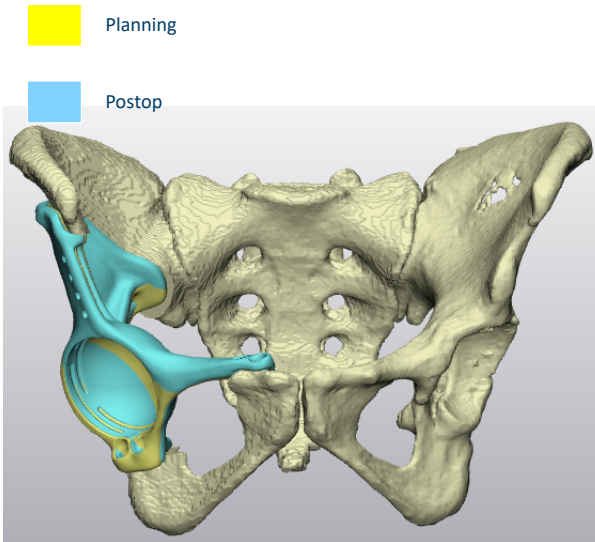
Planning

Postop

Case 5

Angle	Planning	Postop	Δ (°)
AV	4,2	33,8	29,6
INCL	49,4	53,3	3,9

	Rotation (°)	Direction
Acetabular Cup	1,4	Frontal

Flange position	Sagittal [mm]	Coronal [mm]	Axial [mm]
COR	8,3	-28,0	33,1
Pubis Flange	14,0	-26,8	39,8
Ischial Flange	0,4	-38,4	27,1
Ilium Flange	-6,3	-0,4	4,3

Legend
Sagittal (x): Medial +, Lateral -
Coronal (y): Dorsal +, Frontal -
Axial (z): Cranial +, Caudal -

Legend
Vectors are factor 30 for visualisation of direction

Planning

Postop

Universiteit Leiden

TUDelft Delft University of Technology

Erasmus
ERASMUS UNIVERSITEIT ROTTERDAM
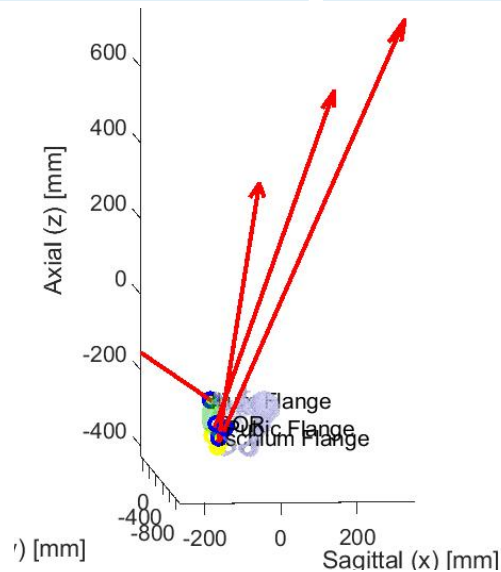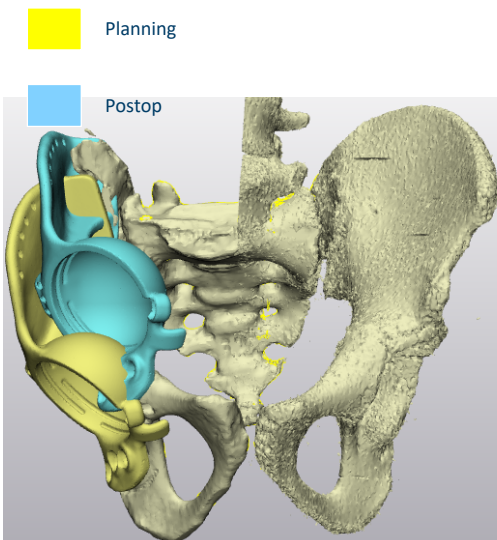
Case 6

Angle	Planning	Postop	Δ (°)
AV	21,6	19,9	-1,8
INCL	38,3	36,4	-1,9

	Rotation (°)	Direction
Acetabular Cup	2,2	Frontal

Flange position	Sagittal [mm]	Coronal [mm]	Axial [mm]
COR	1,1	3,2	-2,9
Pubis Flange	-	-	-
Ischial Flange	1,2	5,0	-2,0
Ilium Flange	-0,6	-1,1	-1,2

Legend
Sagittal (x): Medial +, Lateral -
Coronal (y): Dorsal +, Frontal -
Axial (z): Cranial +, Caudal -

Legend
Vectors are factor 30 for visualisation of direction
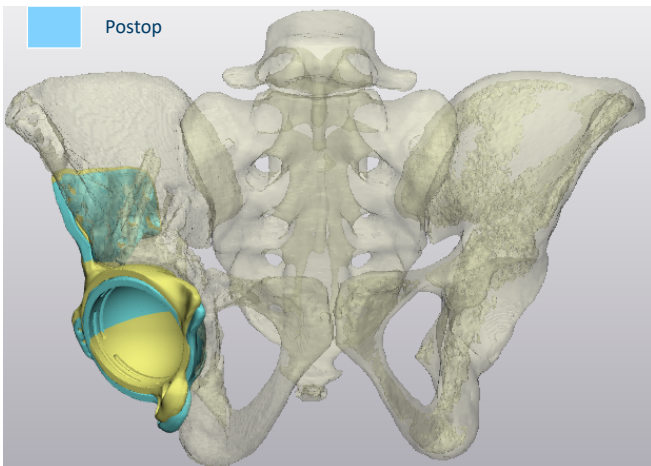
🟨 Planning
🟦 Postop

Cloud of Postoperative Implant + COR, Pubis Flangle, Ischium Fla
Yellow = Planning. Red = Postop
Red Vector indicates direction of translation
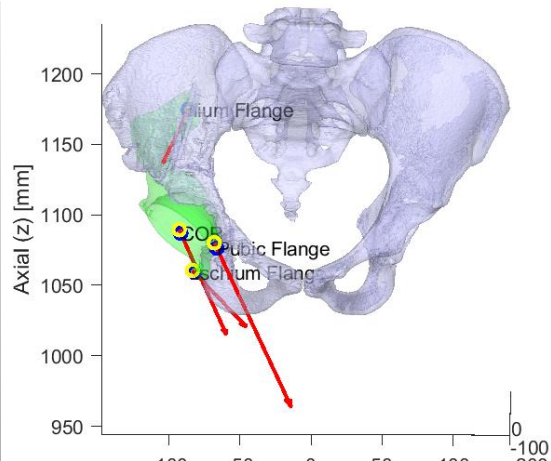
Case 7

Angle	Planning	Postop	Δ (°)
AV	17,9	18,0	0,0
INCL	48,4	50,1	1,7

	Rotation (°)	Direction
Acetabular Cup	0,6	Frontal

Flange position	Sagittal [mm]	Coronal [mm]	Axial [mm]
COR	-3,1	-2,2	-5,3
Pubis Flange	-3,5	-2,6	-8,4
Ischial Flange	-	-	-
Ilium Flange	-0,5	-1,8	-5,7

Legend
Sagittal (x): Medial +, Lateral -
Coronal (y): Dorsal +, Frontal -
Axial (z): Cranial +, Caudal -

Legend
Vectors are factor 30 for visualisation of direction

🟨 Planning
🟦 Postop

of Postoperative Implant + COR, Pubis Flangle, Ischium Flar
Yellow = Planning. Red = Postop
Red Vector indicates direction of translation

Universiteit Leiden

TUDelft Delft University of Technology

Erasmus ERASMUS UNIVERSITEIT ROTTERDAM
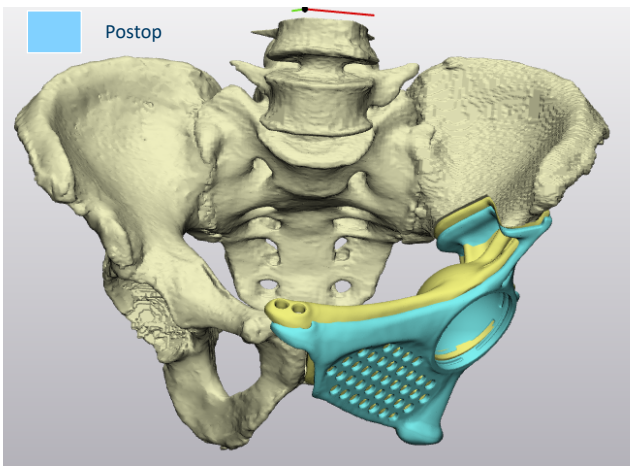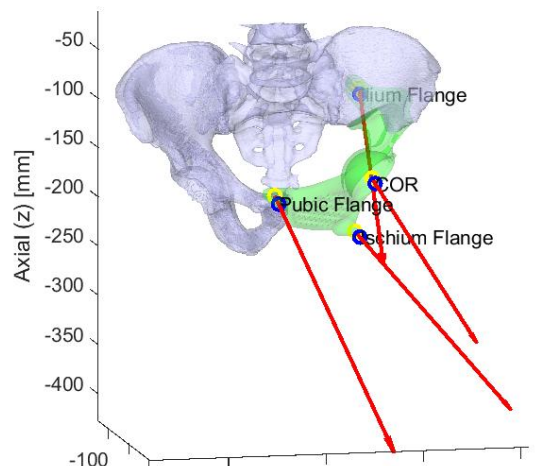
Case 8

Angle	Planning	Postop	Δ (°)
AV	23,9	27,4	3,5
INCL	39,2	34,5	-4,8

	Rotation (°)	Direction
Acetabular Cup	10,5	Frontal

Flange position	Sagittal [mm]	Coronal [mm]	Axial [mm]
COR	-1,2	2,2	-0,5
Pubis Flange	4,8	5,3	-2,5
Ischial Flange	-4,6	8,1	1,0
Ilium Flange	-3,0	-4,7	-0,2

Legend
Sagittal (x): Medial +, Lateral -
Coronal (y): Dorsal +, Frontal -
Axial (z): Cranial +, Caudal -

Legend
Vectors are factor 30 for visualisation of direction

Planning

Postop

PointCloud of Postoperative Implant + COR, Pubis Flangle,Ischium Flangle,Il
Yellow = Planning. Red = Postop
Red Vector indicates direction of translation
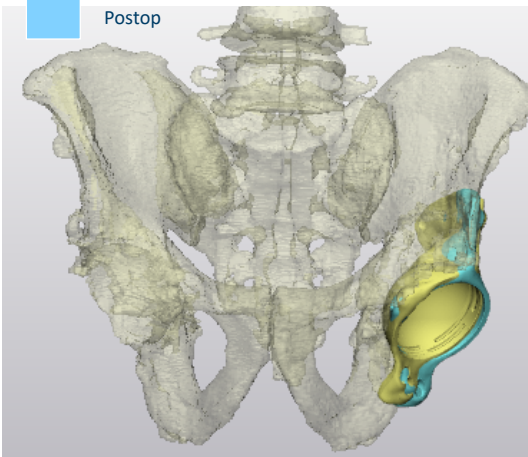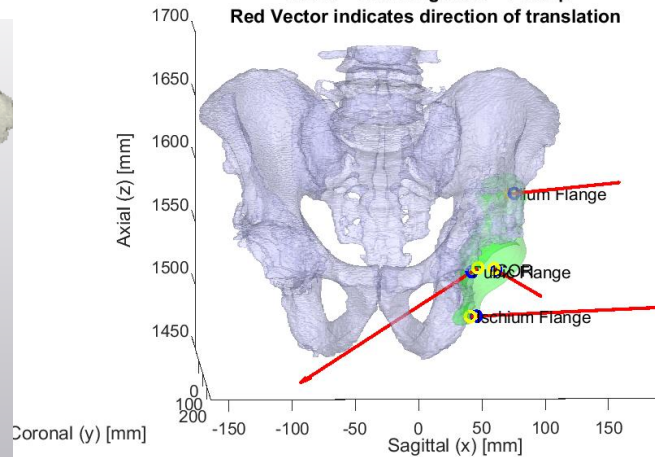
Case 9

Angle	Planning	Postop	Δ (°)
AV	17,5	13,0	-4,5
INCL	43,0	39,7	-3,4

	Rotation (°)	Direction
Acetabular Cup	1,1	Dorsal

Flange position	Sagittal [mm]	Coronal [mm]	Axial [mm]
COR	-0,4	6,8	-3,1
Pubis Flange	-3,3	1,2	-0,6
Ischial Flange	-	-	-
Ilium Flange	-3,8	0,2	-0,2

Legend
Sagittal (x): Medial +, Lateral -
Coronal (y): Dorsal +, Frontal -
Axial (z): Cranial +, Caudal -

Legend
Vectors are factor 30 for visualisation of direction

Planning

Postop

PointCloud of Postoperative Implant + COR, Pubis Flangle,Ischium Flangle,Il
Yellow = Planning. Red = Postop
Red Vector indicates direction of translation

Universiteit Leiden

TUDelft Delft University of Technology

Erasmus ERASMUS UNIVERSITEIT ROTTERDAM
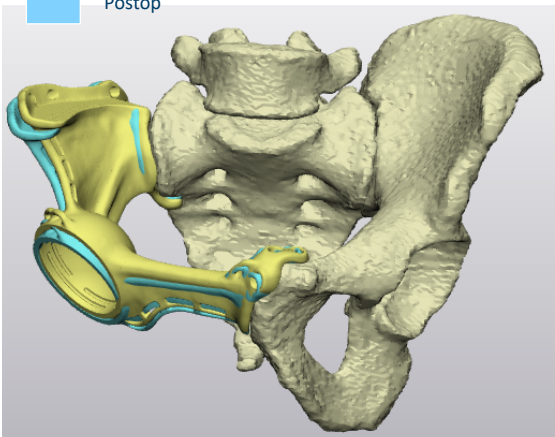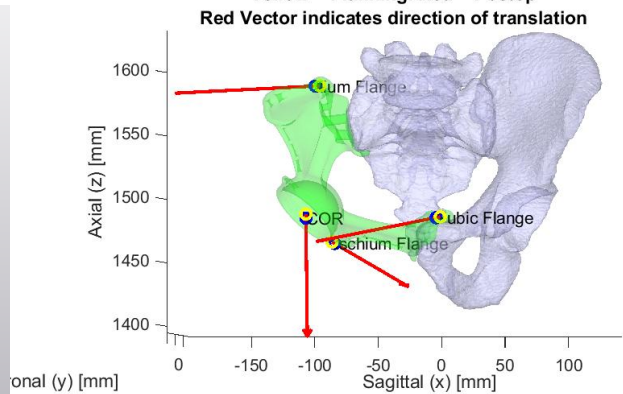
Case 10

Angle	Planning	Postop	Δ (°)
AV	17,6	22,1	4,5
INCL	38,1	42,4	4,3

	Rotation (°)	Direction
Acetabular Cup	2,2	Frontal

Flange position	Sagittal [mm]	Coronal [mm]	Axial [mm]
COR	-2,9	-4,2	0,6
Pubis Flange	-1,3	-3,8	1,0
Ischial Flange	-6,2	-5,2	-0,2
Ilium Flange	-0,1	0,0	-2,8

Legend
Sagittal (x):   Medial +, Lateral -
Coronal (y):   Dorsal +, Frontal -
Axial (z):   Cranial +, Caudal -

Legend
Vectors are factor 30 for visualisation of direction

Planning
Postop

PointCloud of Postoperative Implant + COR, Pubis Flangle,Ischium Flangle
Yellow = Planning. Red = Postop
Red Vector indicates direction of translation
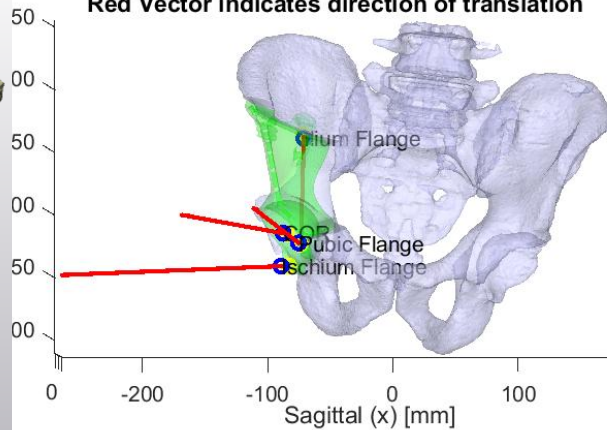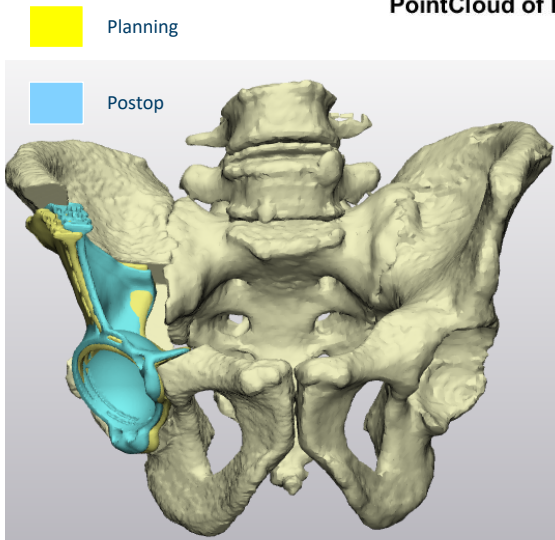
Case 11

Angle	Planning	Postop	Δ (°)
AV	15,1	14,9	-0,2
INCL	36,7	37,4	0,8

	Rotation (°)	Direction
Acetabular Cup	0,4	Frontal

Flange position	Sagittal [mm]	Coronal [mm]	Axial [mm]
COR	-0,7	-0,4	0,8
Pubis Flange	-0,9	-0,4	0,3
Ischial Flange	-1,0	-0,3	0,8
Ilium Flange	0,5	-0,7	0,9

Legend
Sagittal (x):   Medial +, Lateral -
Coronal (y):   Dorsal +, Frontal -
Axial (z):   Cranial +, Caudal -

Legend
Vectors are factor 30 for visualisation of direction

Planning
Postop

oud of Postoperative Implant + COR, Pubis Flangle,Ischium Flangle,Iliun
Yellow = Planning. Red = Postop
Red Vector indicates direction of translation

Universiteit Leiden

TUDelft Delft University of Technology

Erasmus ERASMUS UNIVERSITEIT ROTTERDAM
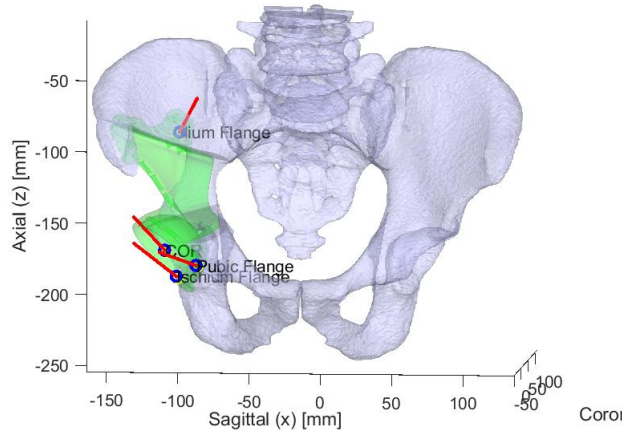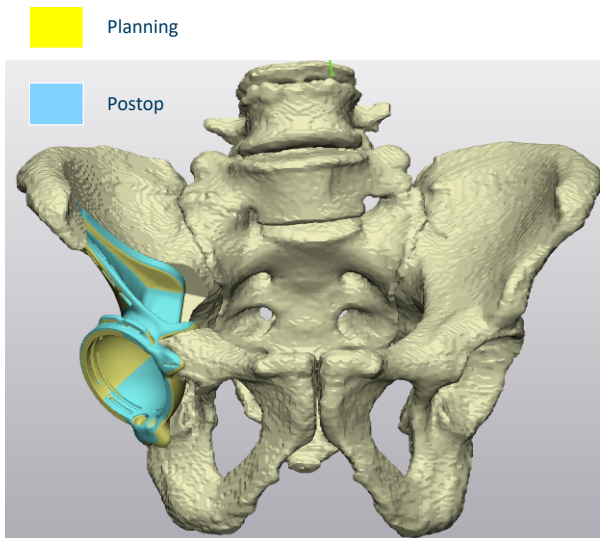
Case 12

Angle	Planning	Postop	Δ (°)
AV	23,6	23,6	0,0
INCL	43,5	43,7	0,2

	Rotation (°)	Direction
Acetabular Cup	1,8	Frontal

Flange position	Sagittal [mm]	Coronal [mm]	Axial [mm]
COR	0,9	0,1	2,3
Pubis Flange	1,9	1,3	0,6
Ischial Flange	0,0	0,7	2,7
Ilium Flange	1,4	-1,7	2,9

Legend
Sagittal (x): Medial +, Lateral -
Coronal (y): Dorsal +, Frontal -
Axial (z): Cranial +, Caudal -

Legend
Vectors are factor 30 for visualisation of direction

Planning

Postop

PointCloud of Postoperative Implant + COR, Pubis Flangle,Ischium Flangle,Iliu
Yellow = Planning. Red = Postop
Red Vector indicates direction of translation
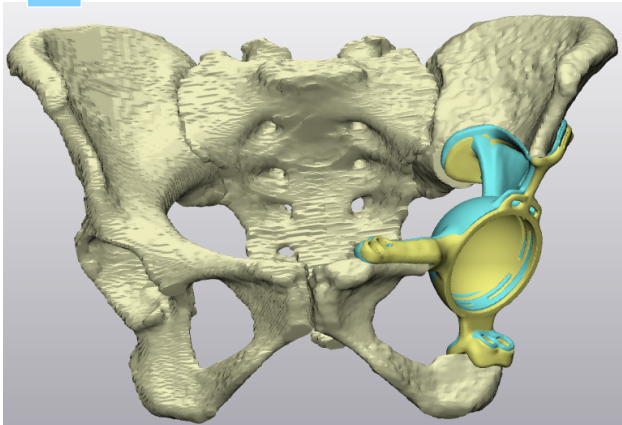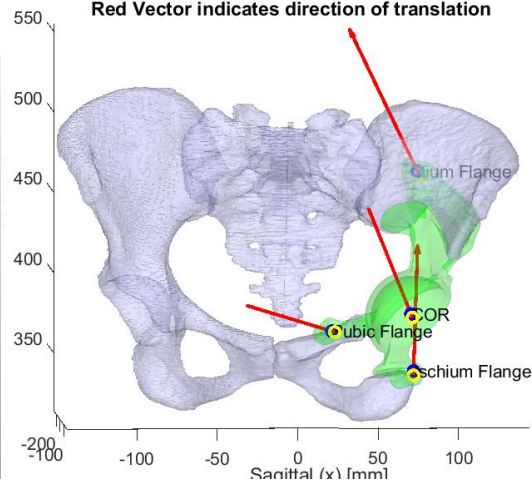
Case 13

Angle	Planning	Postop	Δ (°)
AV	18,4	24,9	6,5
INCL	41,5	40,0	-1,5

	Rotation (°)	Direction
Acetabular Cup	0,1	Frontal

Flange position	Sagittal [mm]	Coronal [mm]	Axial [mm]
COR	0,3	-8,1	-4,6
Pubis Flange	3,8	-3,6	0,3
Ischial Flange	-1,2	-9,4	-6,5
Ilium Flange	-4,5	-3,9	-7,1

Legend
Sagittal (x): Medial +, Lateral -
Coronal (y): Dorsal +, Frontal -
Axial (z): Cranial +, Caudal -

Legend
Vectors are factor 30 for visualisation of direction

Planning

Postop

PointCloud of Postoperative Implant + COR, Pubis Flangle,Ischium Flangle,Ilium
Yellow = Planning. Red = Postop
Red Vector indicates direction of translation

Universiteit Leiden

TU Delft Delft University of Technology

Erasmus UNIVERSITEIT ROTTERDAM

Case 14

Flange position	Sagittal [mm]	Coronal [mm]	Axial [mm]
COR	-1,7	-3,6	0,8
Pubis Flange	1,0	-1,4	0,6
Ischial Flange	-4,4	-2,1	2,0
Ilium Flange	-7,0	-5,5	1,9
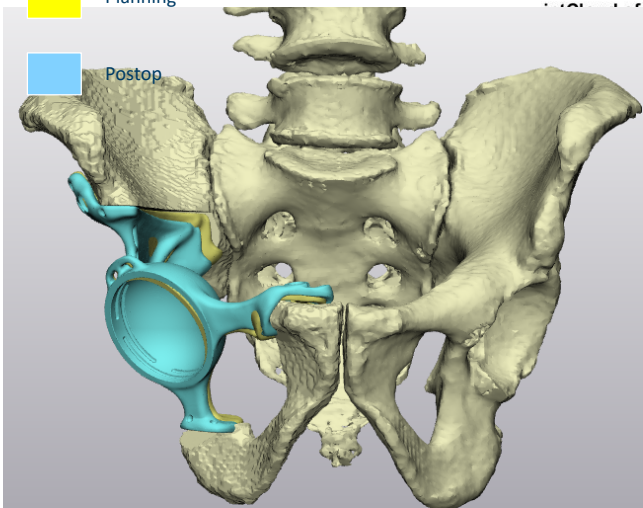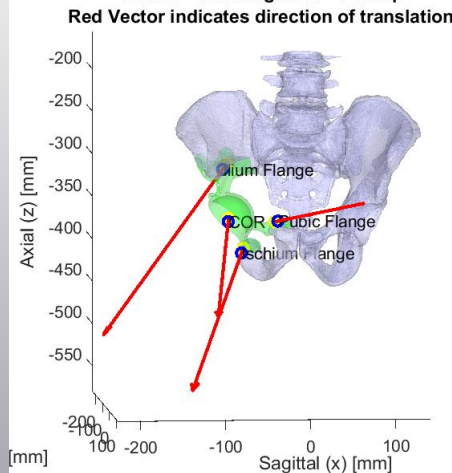
Angle	Planning	Postop	Δ (°)
AV	16,4	18,4	1,9
INCL	41,8	38,7	-3,1

	Rotation (°)	Direction
Acetabular Cup	4,2	Frontal

Legend
Sagittal (x): Medial +, Lateral -
Coronal (y): Dorsal +, Frontal -
Axial (z): Cranial +, Caudal -

Legend
Vectors are factor 30 for visualisation of direction

Planning

Postop

f Postoperative Implant + COR, Pubis Flangle,Ischium Flangle,Iliu
Yellow = Planning. Red = Postop
Red Vector indicates direction of translation

Case 15

Flange position	Sagittal [mm]	Coronal [mm]	Axial [mm]
COR	-1,0	-1,4	-3,3
Pubis Flange	1,1	2,5	-3,0
Ischial Flange	-0,7	0,9	-2,0
Ilium Flange	-4,3	-3,7	-1,3
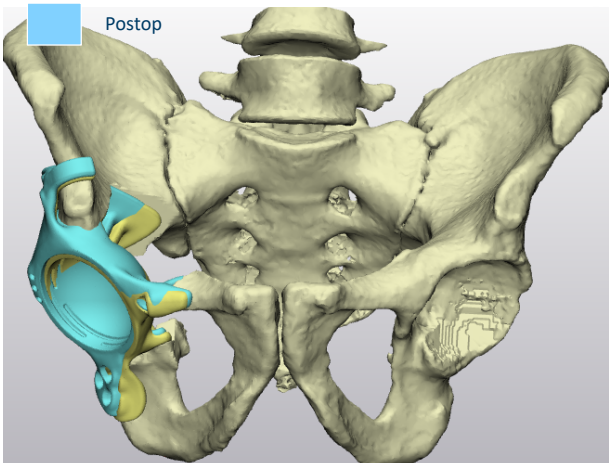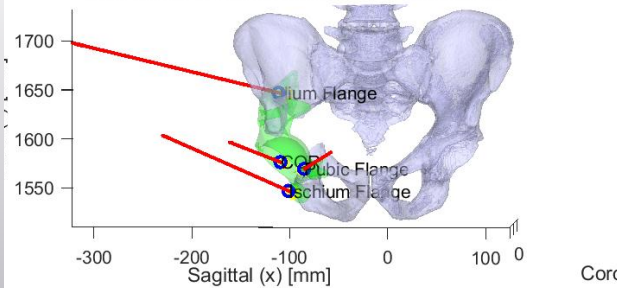
Angle	Planning	Postop	Δ (°)
AV	13,4	13,2	-0,2
INCL	41,3	39,4	-2,0

	Rotation (°)	Direction
Acetabular Cup	2,0	Frontal

Legend
Sagittal (x): Medial +, Lateral -
Coronal (y): Dorsal +, Frontal -
Axial (z): Cranial +, Caudal -

Legend
Vectors are factor 30 for visualisation of direction

Planning

Postop

ntCloud of Postoperative Implant + COR, Pubis Flangle,Ischium Flangle,Iliu
Yellow = Planning. Red = Postop
Red Vector indicates direction of translation

Universiteit Leiden

TUDelft Delft University of Technology

Erasmus ERASMUS UNIVERSITEIT ROTTERDAM
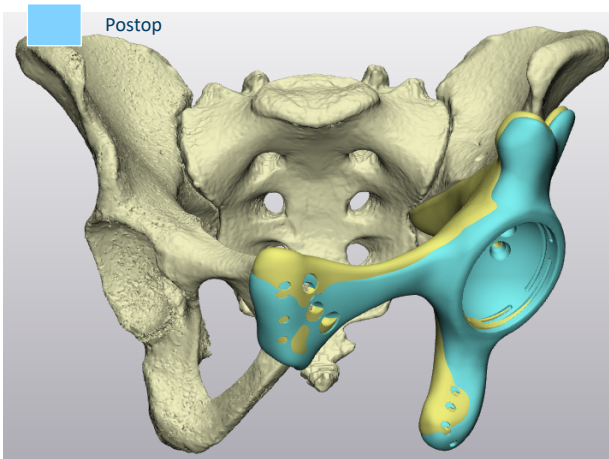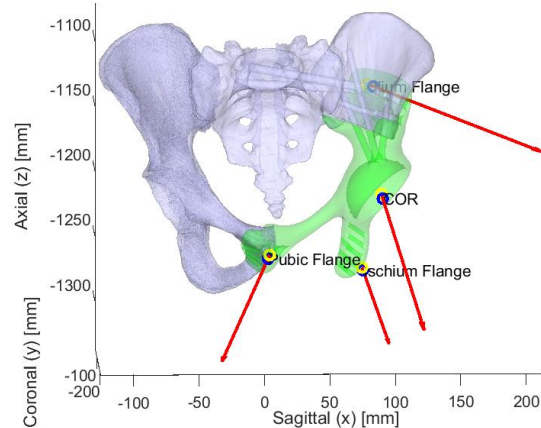
Case 16

Angle	Planning	Postop	Δ (°)
AV	16,6	20,3	3,6
INCL	40,1	48,8	8,7

	Rotation (°)	Direction
Acetabular Cup	0,9	Dorsal

Flange position	Sagittal [mm]	Coronal [mm]	Axial [mm]
COR	3,6	1,0	-0,3
Pubis Flange	4,2	0,6	0,2
Ischial Flange	8,3	-2,0	-2,1
Ilium Flange	-4,8	7,2	-4,1

Legend
Sagittal (x): Medial +, Lateral -
Coronal (y): Dorsal +, Frontal -
Axial (z): Cranial +, Caudal -

Legend
Vectors are factor 30 for visualisation of direction

🟨 Planning

🟦 Postop

PointCloud of Postoperative Implant + COR, Pubis Flangle,Ischium Flang
Yellow = Planning. Red = Postop
Red Vector indicates direction of translation
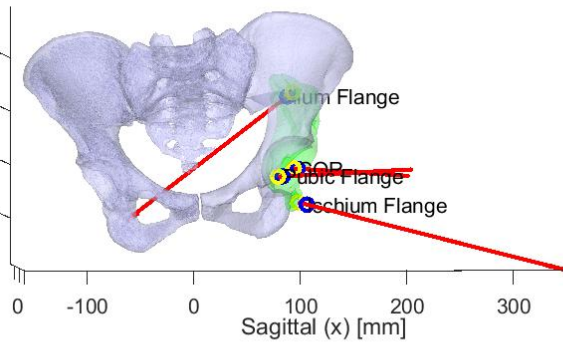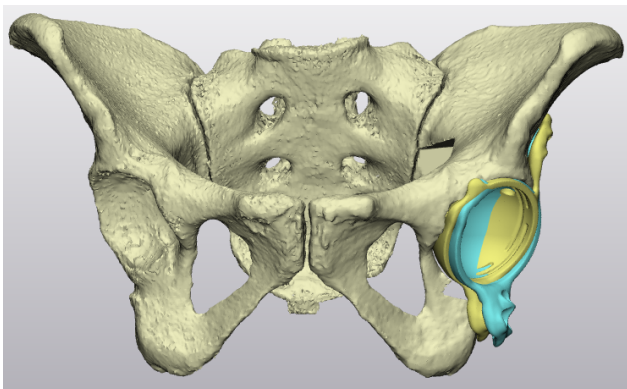
Case 17

Angle	Planning	Postop	Δ (°)
AV	19,0	26,0	7,1
INCL	41,5	42,4	0,9

	Rotation (°)	Direction
Acetabular Cup	1,3	Frontal

Flange position	Sagittal [mm]	Coronal [mm]	Axial [mm]
COR	-0,4	-8,0	-2,0
Pubis Flange	1,9	-6,7	-0,2
Ischial Flange	-3,0	-9,3	-4,1
Ilium Flange	-4,1	1,8	-6,9

Legend
Sagittal (x): Medial +, Lateral -
Coronal (y): Dorsal +, Frontal -
Axial (z): Cranial +, Caudal -

Legend
Vectors are factor 30 for visualisation of direction

🟨 Planning

🟦 Postop

PointCloud of Postoperative Implant + COR, Pubis Flangle,Ischium Flangle,I
Yellow = Planning. Red = Postop
Red Vector indicates direction of translation

Universiteit Leiden

TU Delft
Delft University of Technology

Erasmus
ERASMUS UNIVERSITEIT ROTTERDAM
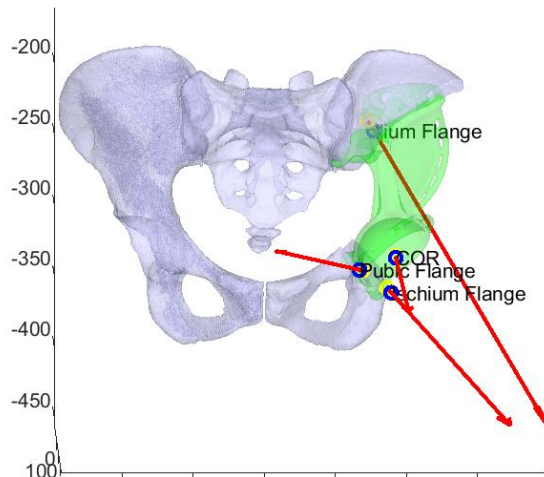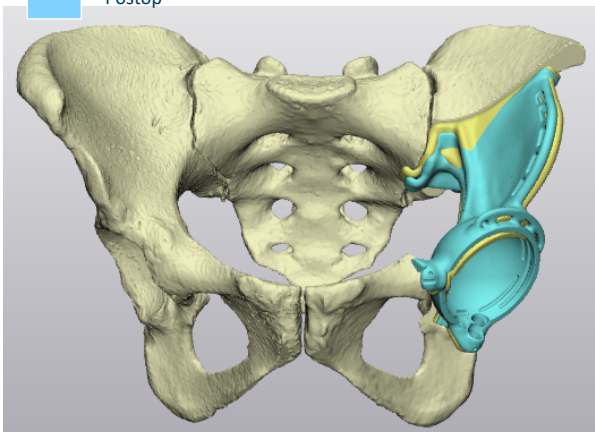
Case 18

Angle	Planning	Postop	Δ (°)
AV	23,2	11,0	-12,2
INCL	47,6	56,1	8,5

	Rotation (°)	Direction
Acetabular Cup	10,7	Frontal

Flange position	Sagittal [mm]	Coronal [mm]	Axial [mm]
COR	-6,0	10,1	2,0
Pubis Flange	-9,3	12,4	-5,2
Ischial Flange	-8,7	14,6	11,2
Ilium Flange	2,0	2,6	7,8

Legend
Sagittal (x): Medial +, Lateral -
Coronal (y): Dorsal +, Frontal -
Axial (z): Cranial +, Caudal -

Legend
Vectors are factor 30 for visualisation of direction
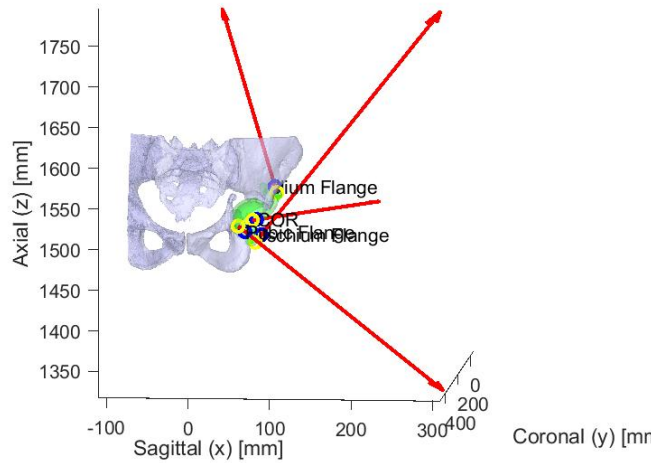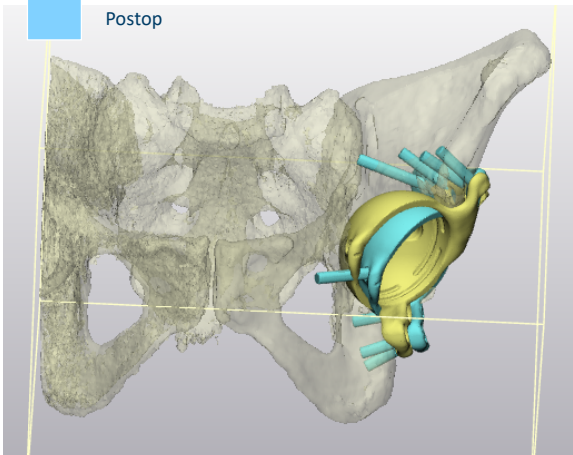
■ Planning
■ Postop

Case 19

Angle	Planning	Postop	Δ (°)
AV	22,1	24,9	2,8
INCL	40,8	38,2	-2,6

	Rotation (°)	Direction
Acetabular Cup	0,1	Frontal

Flange position	Sagittal [mm]	Coronal [mm]	Axial [mm]
COR	6,4	-2,4	-0,7
Pubis Flange	9,0	1,0	4,4
Ischial Flange	-	-	-
Ilium Flange	-0,7	0,2	-1,8

Legend
Sagittal (x): Medial +, Lateral -
Coronal (y): Dorsal +, Frontal -
Axial (z): Cranial +, Caudal -

Legend
Vectors are factor 30 for visualisation of direction
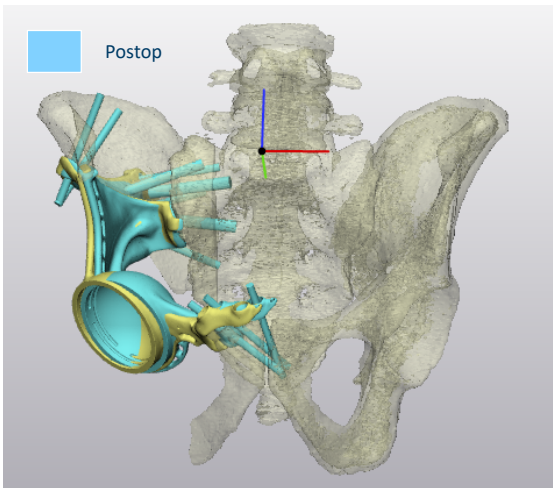
■ Planning
■ Postop

ud of Postoperative Implant + COR, Pubis Flangle,Ischium Flangle
Yellow = Planning. Red = Postop
Red Vector indicates direction of translation
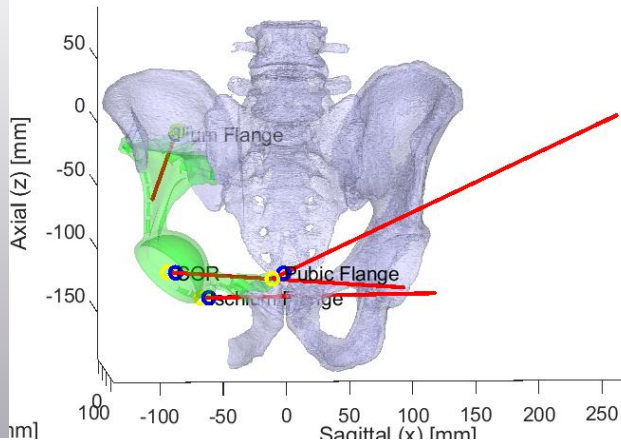
Case 20

Angle	Planning	Postop	Δ (°)
AV	23,3	21,4	-1,9
INCL	44,5	43,3	-1,2

	Rotation (°)	Direction
Acetabular Cup	0,2	Dorsal

Flange position	Sagittal [mm]	Coronal [mm]	Axial [mm]
COR	-0,2	-0,6	-1,8
Pubis Flange	-1,1	-2,1	-1,5
Ischial Flange	1,0	0,2	-1,2
Ilium Flange	-1,0	-2,3	-1,3

Legend
Sagittal (x): Medial +, Lateral -
Coronal (y): Dorsal +, Frontal -
Axial (z): Cranial +, Caudal -

Legend
Vectors are factor 30 for visualisation of direction

Planning

Postop

PointCloud of Postoperative Implant + COR, Pubis Flangle,Ischium Flangle,Iliu
Yellow = Planning. Red = Postop
Red Vector indicates direction of translation

Case 21

Angle	Planning	Postop	Δ (°)
AV	24,4	25,2	0,8
INCL	40,1	39,9	-0,2

	Rotation (°)	Direction
Acetabular Cup	0,1	Dorsal
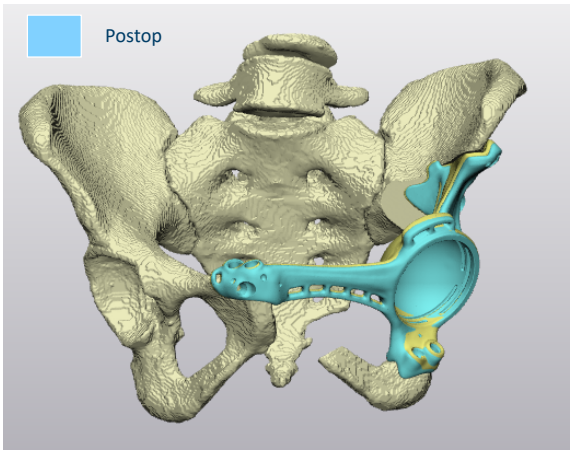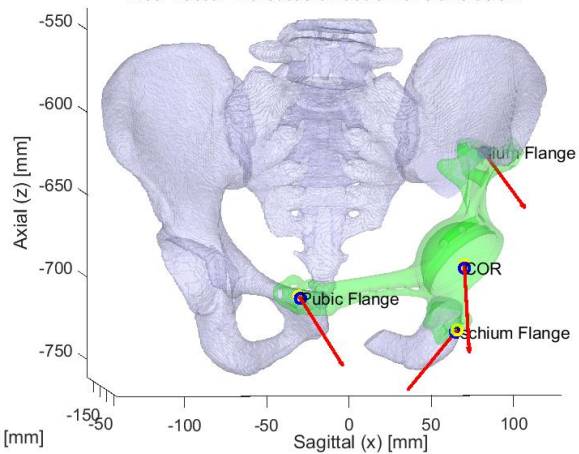
Flange position	Sagittal [mm]	Coronal [mm]	Axial [mm]
COR	-0,5	-3,4	1,6
Pubis Flange	-0,2	-3,4	2,1
Ischial Flange	-0,7	-3,6	1,4
Ilium Flange	-0,8	-3,0	1,5

Legend
Sagittal (x): Medial +, Lateral -
Coronal (y): Dorsal +, Frontal -
Axial (z): Cranial +, Caudal -

Legend
Vectors are factor 30 for visualisation of direction

Planning

Postop

Cloud of Postoperative Implant + COR, Pubis Flangle,Ischium Flangle,Ilium Fl
Yellow = Planning. Red = Postop
Red Vector indicates direction of translation

Universiteit Leiden

TUDelft Delft University of Technology

Erasmus UNIVERSITEIT ROTTERDAM
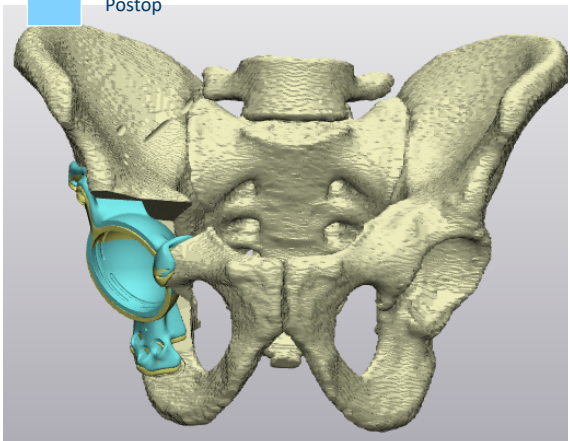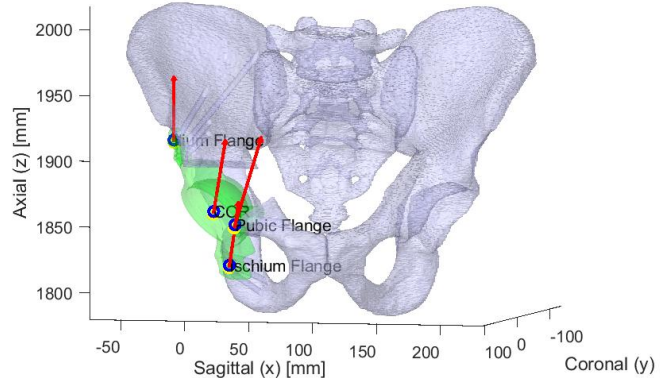
Case 22

Angle	Planning	Postop	Δ (°)
AV	32,6	35,5	2,9
INCL	47,9	46,0	-1,8

	Rotation (°)	Direction
Acetabular Cup	4,7	Dorsal

Flange position	Sagittal [mm]	Coronal [mm]	Axial [mm]
COR	-1,3	5,4	-2,6
Pubis Flange	0,4	3,0	1,2
Ischial Flange	0,8	2,7	-5,3
Ilium Flange	-3,3	8,3	-6,4

Legend
Sagittal (x): Medial +, Lateral -
Coronal (y): Dorsal +, Frontal -
Axial (z): Cranial +, Caudal -

Legend
Vectors are factor 30 for visualisation of direction

■ Planning

■ Postop

PointCloud of Postoperative Implant + COR, Pubis Flangle, Ischium Flangle
Yellow = Planning. Red = Postop
Red Vector indicates direction of translation
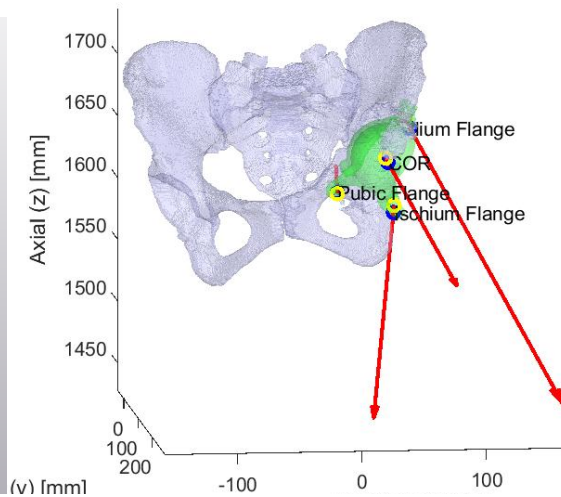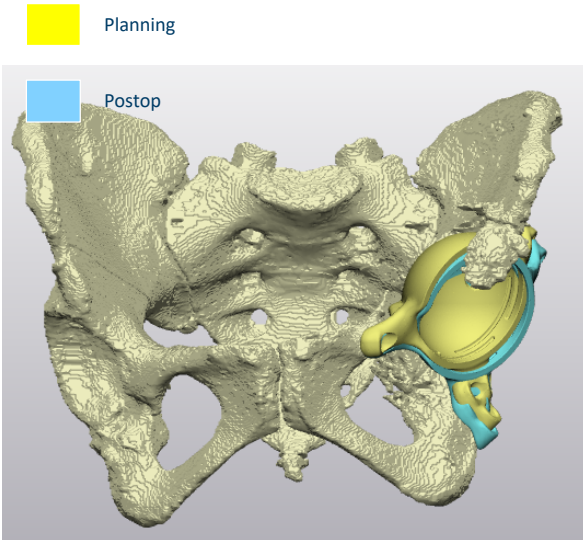
Case 23

Angle	Planning	Postop	Δ (°)
AV	24,3	28,6	4,3
INCL	39,1	36,2	-2,8

	Rotation (°)	Direction
Acetabular Cup	1,5	Dorsal

Flange position	Sagittal [mm]	Coronal [mm]	Axial [mm]
COR	-1,8	-0,1	-0,2
Pubis Flange	1,2	2,7	7,7
Ischial Flange	-1,6	-1,8	-1,8
Ilium Flange	-3,1	0,6	-1,6

Legend
Sagittal (x): Medial +, Lateral -
Coronal (y): Dorsal +, Frontal -
Axial (z): Cranial +, Caudal -

Legend
Vectors are factor 30 for visualisation of direction

■ Planning

■ Postop

Universiteit Leiden

TUDelft Delft University of Technology

Erasmus ERASMUS UNIVERSITEIT ROTTERDAM
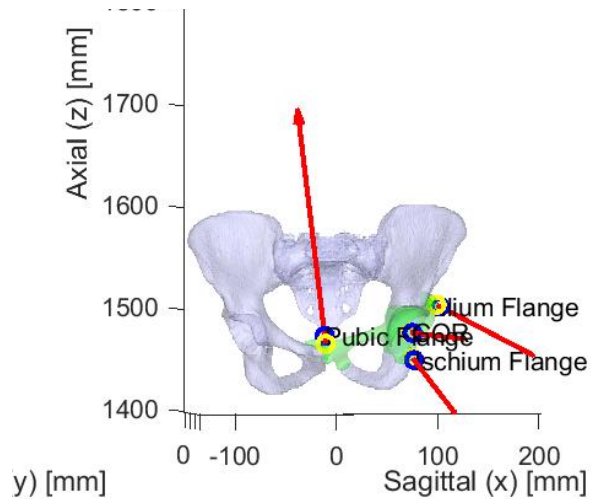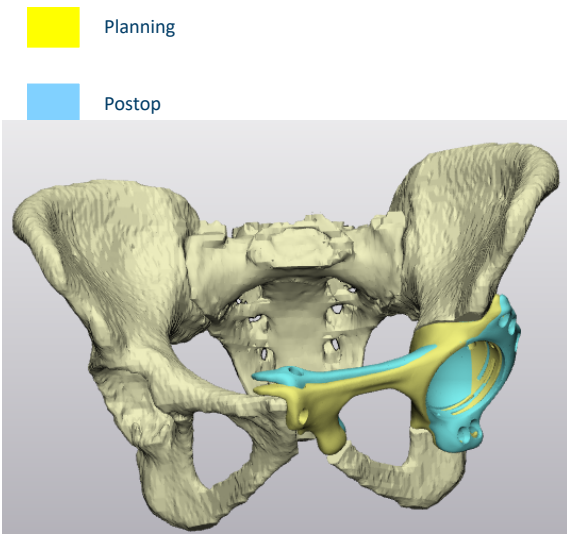
Case 24

Angle	Planning	Postop	Δ (°)
AV	21,6	23,3	1,7
INCL	40,0	44,9	4,8

	Rotation (°)	Direction
Acetabular Cup	1,3	Dorsal

Flange position	Sagittal [mm]	Coronal [mm]	Axial [mm]
COR	0,8	0,9	0,0
Pubis Flange	-0,6	-0,1	0,0
Ischial Flange	-1,1	-0,7	-1,2
Ilium Flange	4,4	3,6	0,5

Legend
Sagittal (x):   Medial +, Lateral -
Coronal (y):   Dorsal +, Frontal -
Axial (z):   Cranial +, Caudal -

Legend
Vectors are factor 30 for visualisation of direction

- Yellow: Planning
- Blue: Postop

PointCloud of Postoperative Implant + COR, Pubis Flangle,Ischium Flangl
Yellow = Planning. Red = Postop
Red Vector indicates direction of translation
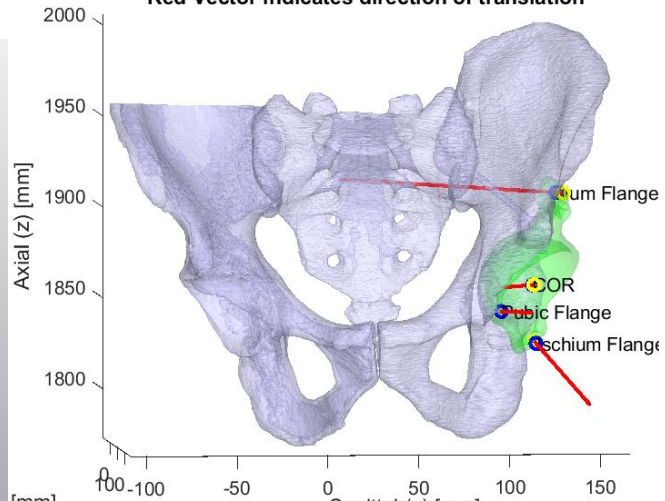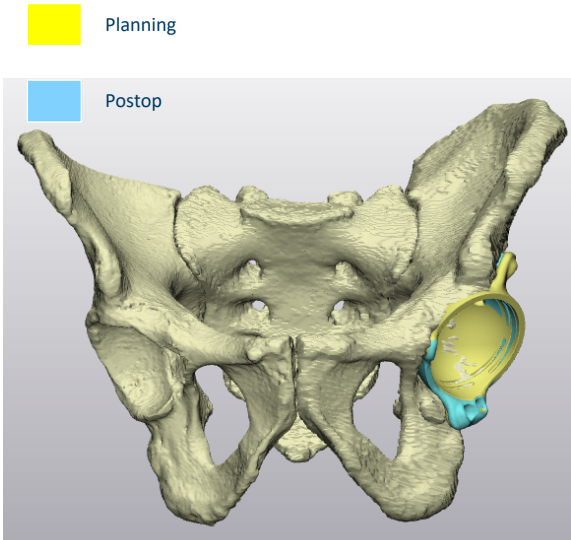
Case 25

Angle	Planning	Postop	Δ (°)
AV	16,9	14,9	-2,0
INCL	40,8	38,9	-1,9

	Rotation (°)	Direction
Acetabular Cup	1,5	Frontal

Flange position	Sagittal [mm]	Coronal [mm]	Axial [mm]
COR	1,2	2,0	-0,8
Pubis Flange	1,5	2,5	-1,5
Ischial Flange	1,7	3,6	1,0
Ilium Flange	-0,2	-1,5	0,6

Legend
Sagittal (x):   Medial +, Lateral -
Coronal (y):   Dorsal +, Frontal -
Axial (z):   Cranial +, Caudal -

Legend
Vectors are factor 30 for visualisation of direction

- Yellow: Planning
- Blue: Postop

Cloud of Postoperative Implant + COR, Pubis Flangle,Ischium Flangle,Ili
Yellow = Planning. Red = Postop
Red Vector indicates direction of translation

Universiteit Leiden

TUDelft Delft University of Technology

Erasmus UNIVERSITEIT ROTTERDAM
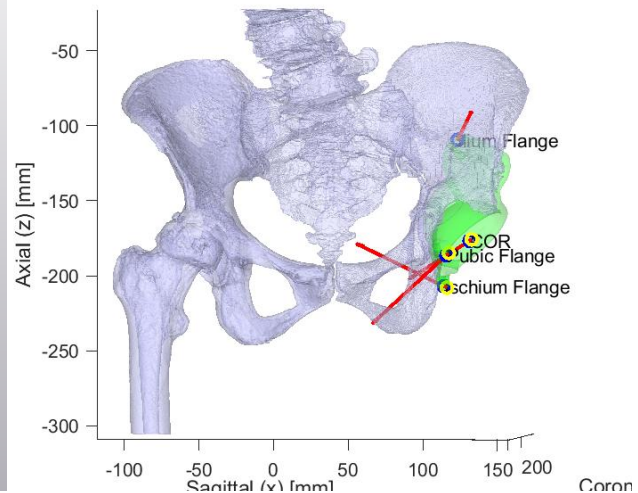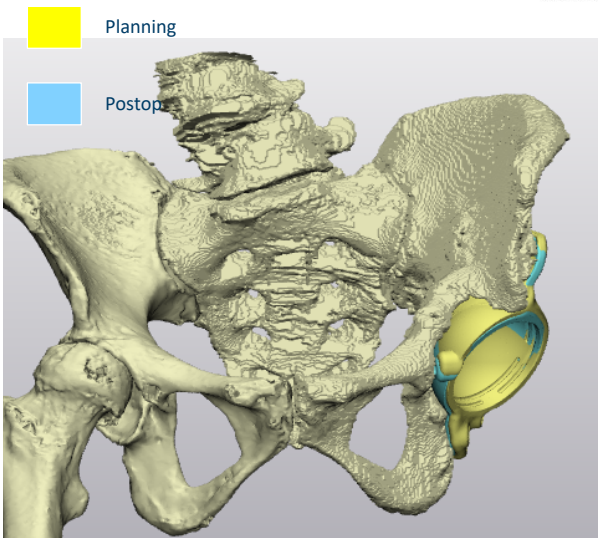
Case 26

Angle	Planning	Postop	Δ (°)
AV	16,3	11,7	-4,6
INCL	27,6	41,8	14,2

	Rotation (°)	Direction
Acetabular Cup	2,5	Dorsal

Flange position	Sagittal [mm]	Coronal [mm]	Axial [mm]
COR	-4,1	3,4	1,9
Pubis Flange	-9,1	0,4	-3,4
Ischial Flange	-3,3	3,7	2,4
Ilium Flange	4,5	6,7	8,4

Legend
Sagittal (x): Medial +, Lateral -
Coronal (y): Dorsal +, Frontal -
Axial (z): Cranial +, Caudal -

Legend
Vectors are factor 30 for visualisation of direction

■ (yellow) Planning
■ (blue) Postop
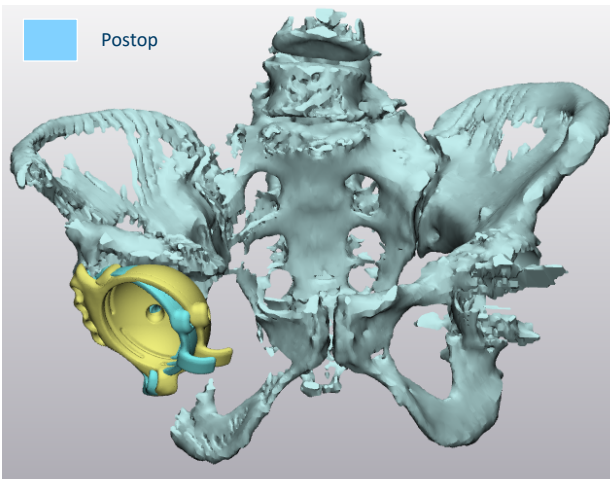
PointCloud of Postoperative Implant + COR, Pubis Flangle, Ischium Flangle
Yellow = Planning. Red = Postop
Red Vector indicates direction of translation
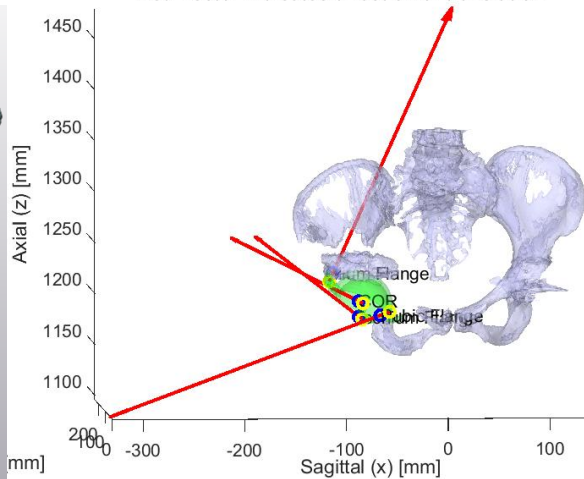
Case 27

Angle	Planning	Postop	Δ (°)
AV	11,7	11,8	0,1
INCL	44,5	44,7	0,2

	Rotation (°)	Direction
Acetabular Cup	0,5	Dorsal

Flange position	Sagittal [mm]	Coronal [mm]	Axial [mm]
COR	1,0	1,7	0,2
Pubis Flange	0,8	1,4	0,3
Ischial Flange	1,1	1,4	0,0
Ilium Flange	1,5	2,2	-0,3

Legend
Sagittal (x): Medial +, Lateral -
Coronal (y): Dorsal +, Frontal -
Axial (z): Cranial +, Caudal -

Legend
Vectors are factor 30 for visualisation of direction

■ (yellow) Planning
■ (blue) Postop

ud of Postoperative Implant + COR, Pubis Flangle, Ischium Flangle, Ilium Flangle
Yellow = Planning. Red = Postop
Red Vector indicates direction of translation

Universiteit Leiden   TUDelft Delft University of Technology   Erasmus ERASMUS UNIVERSITEIT ROTTERDAM
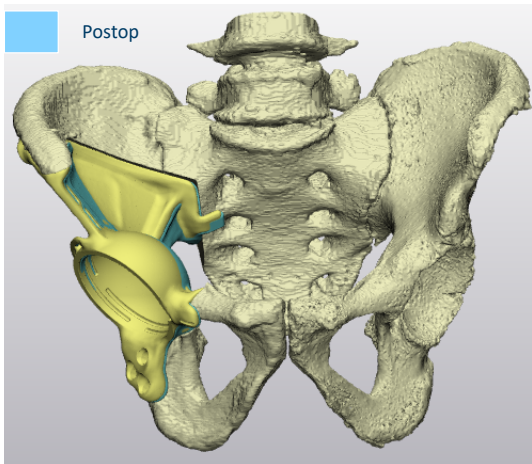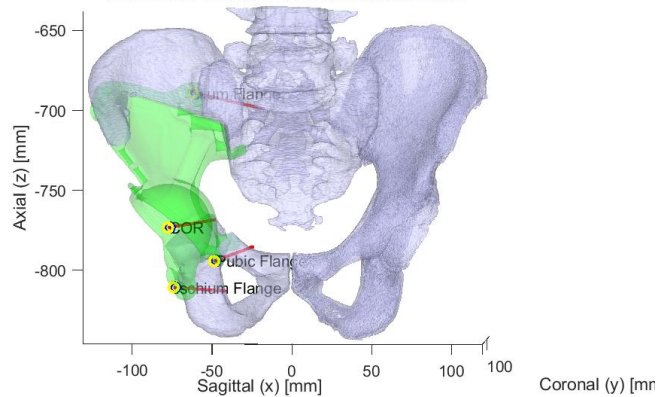
Case 28

Angle	Planning	Postop	Δ (°)
AV	5	14,7	-2,0
INCL	46,7	47,8	1,2

	Rotation (°)	Direction
Acetabular Cup	1,6	Dorsal

Flange position	Sagittal [mm]	Coronal [mm]	Axial [mm]
COR	-2,8	3,2	0,2
Pubis Flange	-5,7	-1,1	-1,1
Ischial Flange	-1,9	3,0	0,2
Ilium Flange	1,4	2,6	0,0

Legend
Sagittal (x):   Medial +, Lateral -
Coronal (y):   Dorsal +, Frontal -
Axial (z):   Cranial +, Caudal -

Legend
Vectors are factor 30 for visualisation of direction
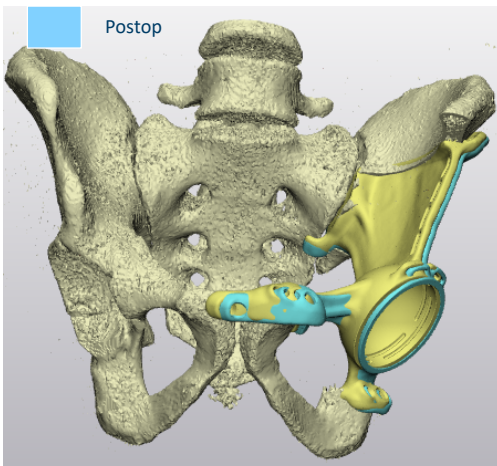
Planning

Postop

d of Postoperative Implant + COR, Pubis Flangle,Ischium Flangle,Ilium Fl
Yellow = Planning. Red = Postop
Red Vector indicates direction of translation
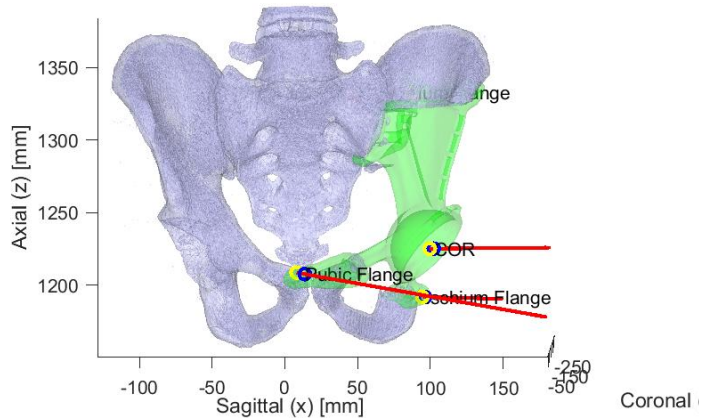
Case 29

Angle	Planning	Postop	Δ (°)
AV	13,6	16,5	2,9
INCL	35,2	36,2	1,0

	Rotation (°)	Direction
Acetabular Cup	1,4	Frontal

Flange position	Sagittal [mm]	Coronal [mm]	Axial [mm]
COR	0,8	-3,1	0,6
Pubis Flange	3,0	1,4	-0,4
Ischial Flange	-	-	-
Ilium Flange	-0,1	-0,2	-1,1

Legend
Sagittal (x):   Medial +, Lateral -
Coronal (y):   Dorsal +, Frontal -
Axial (z):   Cranial +, Caudal -

Legend
Vectors are factor 30 for visualisation of direction
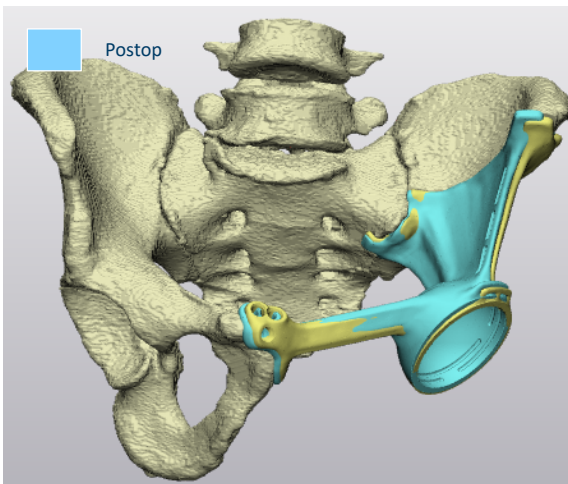
Planning

Postop

PointCloud of Postoperative Implant + COR, Pubis Flangle,Ischium Flangle,
Yellow = Planning. Red = Postop
Red Vector indicates direction of translation
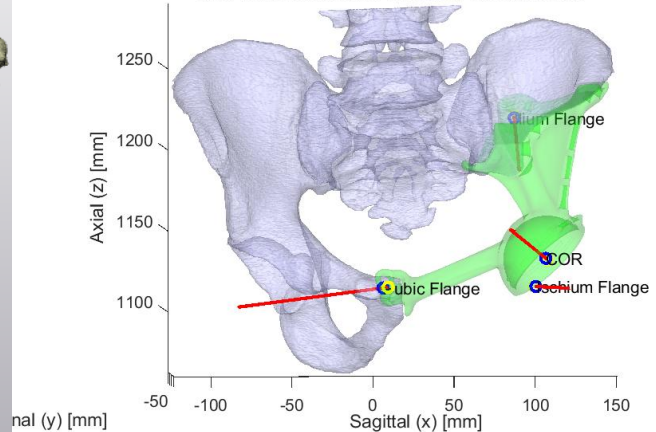
Case 30

Angle	Planning	Postop	Δ (°)
AV	22,1	23,5	1,4
INCL	44,8	45,2	0,4

	Rotation (°)	Direction
Acetabular Cup	0,8	Dorsal

Flange position	Sagittal [mm]	Coronal [mm]	Axial [mm]
COR	2,2	-0,6	-1,9
Pubis Flange	2,5	-0,8	-0,8
Ischial Flange	2,1	-1,4	-2,7
Ilium Flange	1,6	2,3	-2,9

Legend
Sagittal (x): Medial +, Lateral -
Coronal (y): Dorsal +, Frontal -
Axial (z): Cranial +, Caudal -

Legend
Vectors are factor 30 for visualisation of direction
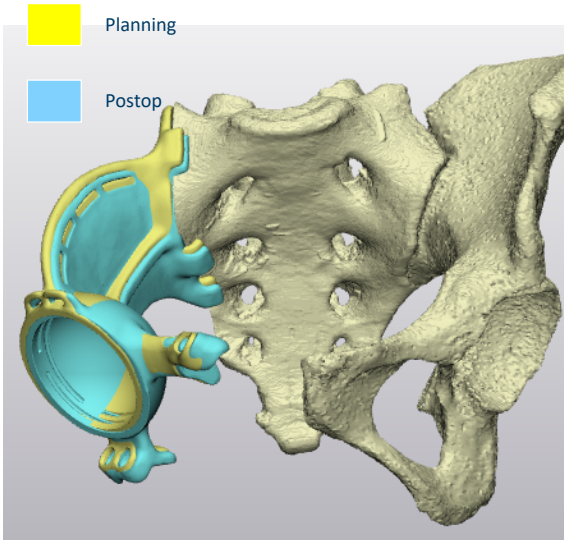
Planning
Postop

d of Postoperative Implant + COR, Pubis Flangle,Ischium Flange,Ilium F
Yellow = Planning. Red = Postop
Red Vector indicates direction of translation
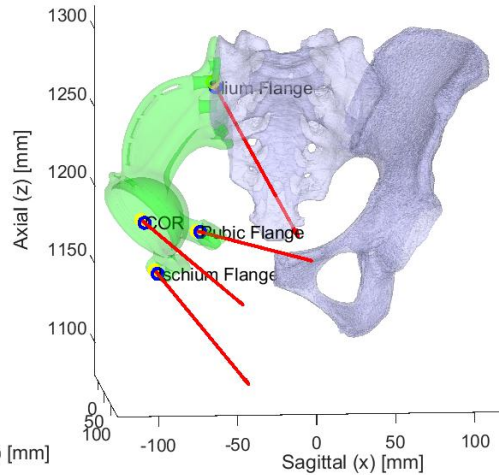
Case 31

Angle	Planning	Postop	Δ (°)
AV	22,7	24,7	2,1
INCL	43,3	43,4	0,1

	Rotation (°)	Direction
Acetabular Cup	1,7	Dorsal

Flange position	Sagittal [mm]	Coronal [mm]	Axial [mm]
COR	-2,6	-3,6	-4,4
Pubis Flange	-2,1	-3,9	-0,8
Ischial Flange	-2,3	-4,7	-5,6
Ilium Flange	-4,4	0,6	-6,2

Legend
Sagittal (x): Medial +, Lateral -
Coronal (y): Dorsal +, Frontal -
Axial (z): Cranial +, Caudal -

Legend
Vectors are factor 30 for visualisation of direction
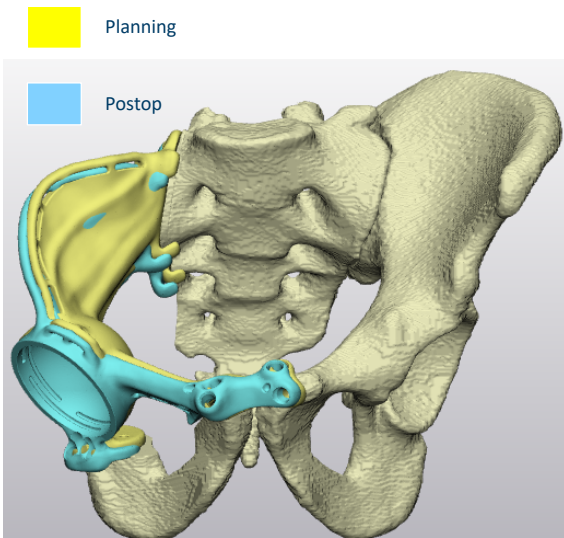
Planning
Postop

ostoperative Implant + COR, Pubis Flangle,Ischium Flangle,Ili
Yellow = Planning. Red = Postop
Red Vector indicates direction of translation
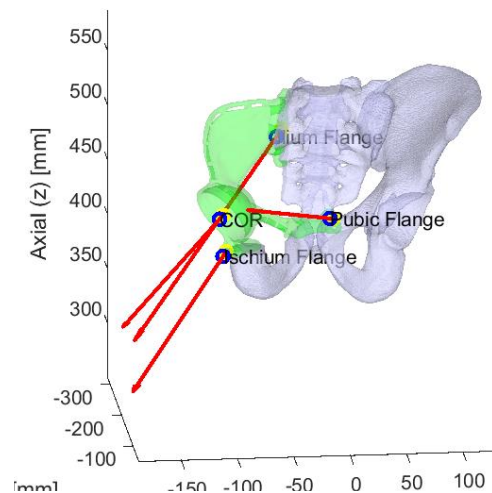
Case 32

Angle	Planning	Postop	Δ (°)
AV	12,9	11,8	-1,1
INCL	49,6	45,9	-3,6

	Rotation (°)	Direction
Acetabular Cup	2,5	Dorsal

Flange position	Sagittal [mm]	Coronal [mm]	Axial [mm]
COR	5,4	-0,5	-2,8
Pubis Flange	5,2	-1,1	-1,8
Ischial Flange	8,1	-1,0	-2,2
Ilium Flange	0,3	-0,4	-2,6

Legend
Sagittal (x): Medial +, Lateral -
Coronal (y): Dorsal +, Frontal -
Axial (z): Cranial +, Caudal -

Legend
Vectors are factor 30 for visualisation of direction

■ Planning
■ Postop

**Postoperative Implant + COR, Pubis Flangle,Ischium Flangle,Ilium Flang
Yellow = Planning. Red = Postop
Red Vector indicates direction of translation**

Case 33

Angle	Planning	Postop	Δ (°)
AV	27,7	30,7	3,1
INCL	45,4	44,6	-0,9

	Rotation (°)	Direction
Acetabular Cup	1,9	Frontal
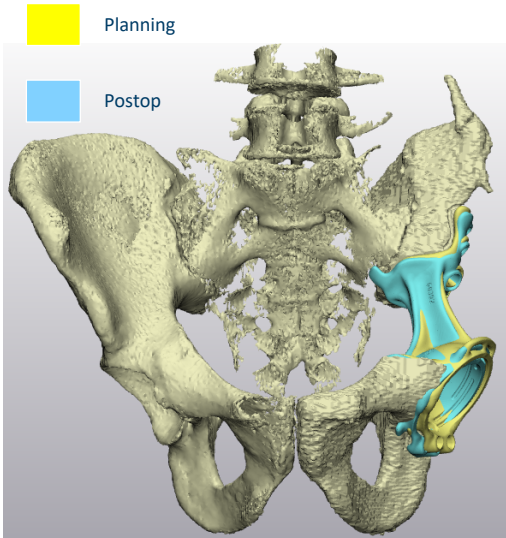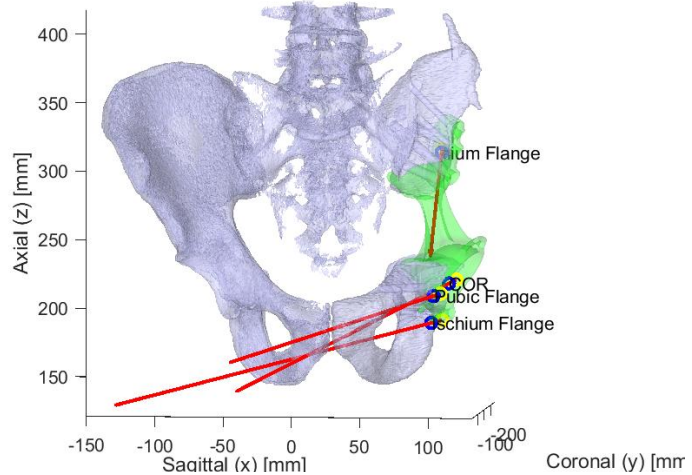
Flange position	Sagittal [mm]	Coronal [mm]	Axial [mm]
COR	-1,8	-1,8	3,1
Pubis Flange	0,1	-1,1	3,4
Ischial Flange	-3,3	-1,2	3,0
Ilium Flange	-5,4	0,1	3,1

Legend
Sagittal (x): Medial +, Lateral -
Coronal (y): Dorsal +, Frontal -
Axial (z): Cranial +, Caudal -

Legend
Vectors are factor 30 for visualisation of direction

■ Planning
■ Postop

**intCloud of Postoperative Implant + COR, Pubis Flangle,Ischium Flangle,Ili
Yellow = Planning. Red = Postop
Red Vector indicates direction of translation**

Universiteit Leiden

TUDelft Delft University of Technology

Erasmus ERASMUS UNIVERSITEIT ROTTERDAM
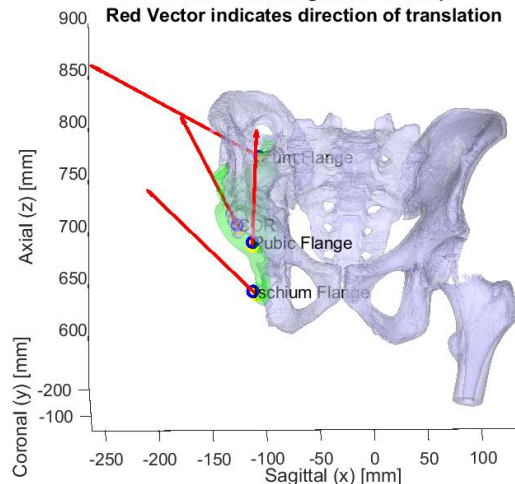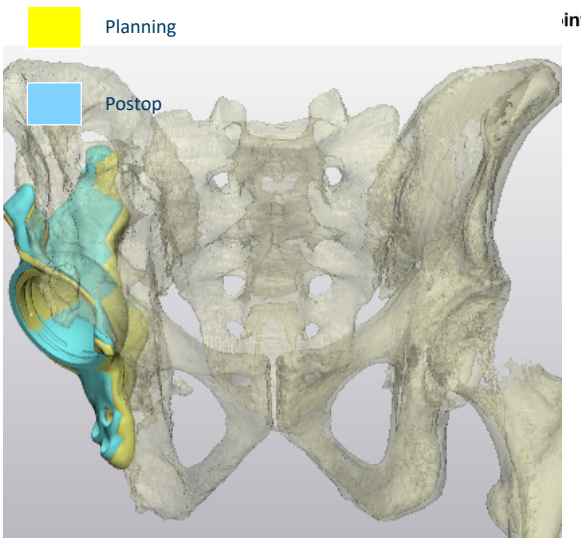
Case 34

Angle	Planning	Postop	Δ (°)
AV	15,3	13,8	-1,5
INCL	36,5	37,9	1,4

	Rotation (°)	Direction
Acetabular Cup	6,1	Dorsal

Flange position	Sagittal [mm]	Coronal [mm]	Axial [mm]
COR	-6,2	12,0	5,3
Pubis Flange	-	-	-
Ischial Flange	-	-	-
Ilium Flange	-1,1	2,8	6,5

Legend
Sagittal (x): Medial +, Lateral -
Coronal (y): Dorsal +, Frontal -
Axial (z): Cranial +, Caudal -

Legend
Vectors are factor 30 for visualisation of direction
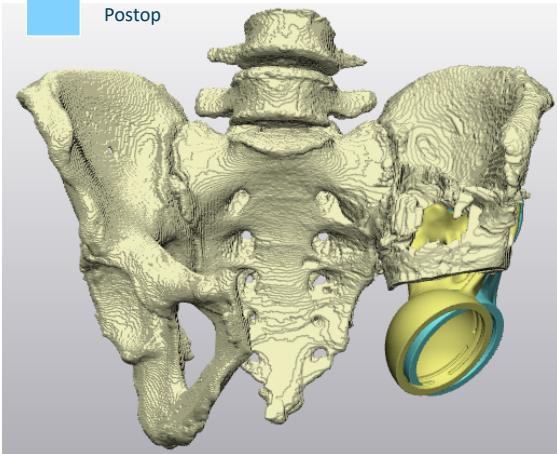
Planning

Postop

Cloud of Postoperative Implant + COR, Pubis Flangle,Ischium Flangle,Ilium F
Yellow = Planning. Red = Postop
Red Vector indicates direction of translation
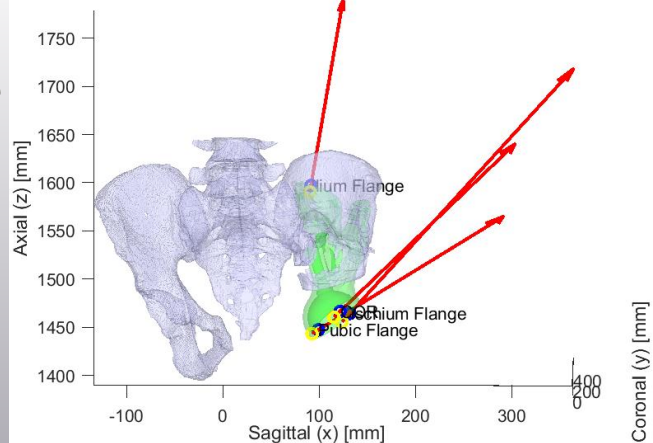
Case 35

Angle	Planning	Postop	Δ (°)
AV	9,8	6,2	-3,7
INCL	38,6	40,0	1,3

	Rotation (°)	Direction
Acetabular Cup	0,9	Frontal

Flange position	Sagittal [mm]	Coronal [mm]	Axial [mm]
COR	-3,0	3,3	-1,8
Pubis Flange	-4,2	3,6	-3,3
Ischial Flange	-2,8	5,8	0,5
Ilium Flange	-0,6	1,5	0,2

Legend
Sagittal (x): Medial +, Lateral -
Coronal (y): Dorsal +, Frontal -
Axial (z): Cranial +, Caudal -

Legend
Vectors are factor 30 for visualisation of direction

Planning

Postop

Cloud of Postoperative Implant + COR, Pubis Flangle,Ischium Flangle
Yellow = Planning. Red = Postop
Red Vector indicates direction of translation

Universiteit Leiden

TUDelft Delft University of Technology

Erasmus Universiteit Rotterdam